Degradation Mechanisms in PEM Water Electrolysis: Diagnosis and Impact

Authors

Annik Bernhardt*[x 1,2,3]; Katja Lange[x 1,2]; Robert Göckeritz[1,2]; Erik Grunwald[1,2]; Angelika Hähnel[1,2]; Alexander Müller[1,2]; Volker Naumann[1,2]; Sistan Rasuli[1,2,4]; Wolfram Münchgesang[5]; Bruno G. Pollet[6]; Kerstin Witte-Bodnar[1,2,4]; Klemens Ilse[1,2]

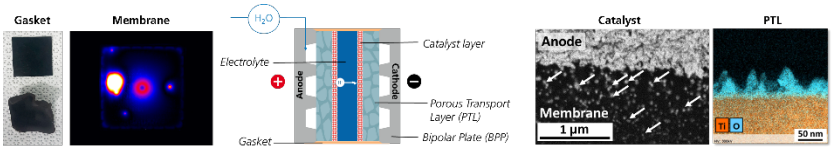
*Corresponding Author
[x] These authors contributed equally
[1] Fraunhofer IMWS, 06120 Halle, Germany; annik.bernhardt@fraunhofer.imws.de, katja.lange2@imws.fraunhofer.de, robert.goeckeritz@csp.fraunhofer.de, erik.grunwald@csp.fraunhofer.de, angelika.haehnel@csp.fraunhofer.de, alexander.mueller@csp.fraunhofer.de, volker.naumann@csp.fraunhofer.de, sistan.rasuli@csp.fraunhofer.de, klemens.ilse@csp.fraunhofer.de, kerstin.witte-bodnar@imws.fraunhofer.de
[2] Fraunhofer CSP, 06120 Halle, Germany
[3] Martin-Luther-Universität Halle-Wittenberg, 06120 Halle, Germany
[4] Anhalt University of Applied Science, 06366 Köthen, Germany
[5] Fraunhofer IWES, 06237 Leuna, Germany; wolfram.muenchgesang@iwes.fraunhofer.de
[6] Université du Québec à Trois-Rivières, G8Z 4M3 Trois-Rivières, Canada; Bruno.Pollet@uqtr.ca

Keywords

PEMWE; PEMWE components; Degradation mechanisms; Diagnostics

Table of Contents

This review provides an analysis on degradation mechanisms in proton electrolyte membrane water electrolyzers (PEMWE), focusing on all key components. It discusses diagnostic and measurement techniques for evaluating degradation, less-studied mechanisms, as well as an expert survey. The aim is to provide a comprehensive understanding of how degradation affects PEMWE performance and to highlight suitable diagnostic approaches.



Abstract

Proton electrolyte membrane (PEM) water electrolyzers (WE) represent a pivotal technology for the electrochemical production of hydrogen. However, a persistent challenge is the loss of efficiency and performance, along with a shortened lifetime caused by degradation of the materials in PEMWE. This review examines the degradation mechanisms of PEMWE components, including the electrolyte membrane, catalyst layers, porous transport layers, bipolar plates and gaskets. Furthermore, it places particular emphasis on measurement techniques used to examine and differentiate the degradation mechanisms, including a discussion of less-studied mechanisms and measurement methods. A survey was conducted among PEMWE experts to analyse prevailing opinions on the severity and frequency of

different degradation mechanisms. It supplements the literature review and allows for a comprehensive understanding of the impacts of degradation.

Abbreviations

Abbreviation	Term
AAS	Atomic Absorption Spectroscopy
AFM	Atomic Force Microscopy
BoP	Balance of Plant
BPP	Bipolar Plate
CCM	Catalyst-coated Membrane
CT	Computed Tomography
DC	Direct Current
DOE	Department of Energy
DSC	Differential Scanning Calorimetry
ECSA	Electrochemical Surface Area
ECT	Eddy Current Testing
EDX	Energy-dispersive X-ray Spectroscopy
EoT	End of Test
EPDM	Ethylene Propylene Diene Monomer Rubber
EPMA	Electron Probe Microanalysis
ESR	Electron Spin Resonance
FC	Fuel Cells
FER	Fluoride Emission Rate
FKM	Fluorine Kautschuk Material
FT-IR	Fourier Transformed Infrared Spectroscopy
GC-MS	Gas Chromatography Mass Spectroscopy
GDL	Gas Diffusion Layer
GHG	Greenhouse Gas
HER	Hydrogen Evolution Reaction
ICP-MS	Inductively Coupled Plasma Mass Spectroscopy
ICP-OES	Inductively Coupled Plasma Optical Emission Spectroscopy
IEC	Ion Exchange Capacity
IQR	Interquartile Range

IR	Infrared
ICR	Interfacial Contact Resistance
KPI	Key Performance Indicator
LIBS	Laser-induced Breakdown Spectroscopy
LIT	Lock-In Thermography
MEA	Membrane Electrode Assembly
MFI	Magnetic Field Imaging
MMO	Mixed Metal Oxide
NMR	Nuclear Magnetic Resonance
OCV	Open Circuit Voltage
OER	Oxygen Evolution Reaction
PEM	Proton Electrolyte Membrane
PFSA	Perfluorosulfonic Acid
PTFE	Polytetrafluoroethylene
PTL	Porous Transport Layer
R&D	Research and Development
RDE	Rotating Disc Electrode
SAXS	Small Angle X-ray Scattering
SEM	Scanning Electron Microscopy
SHE	Standard Hydrogen Electrode
SRR	Sulphur Release Rate
(S)TEM	(Scanning) Transmission Electron Microscopy
TGA	Thermogravimetric Analysis
ToF-SIMS	Time of Flight Secondary Ion Mass Spectroscopy
TPB	Triple-Phase Boundary
WE	Water Electrolyzer
XANES	X-ray Absorption Near Edge Structure
XAS	X-Ray Absorption Spectroscopy
XPS	X-ray Photoelectron Spectroscopy
XRD	X-ray Diffraction
XRF	X-ray Fluorescence

1. Introduction

Hydrogen and its production by water electrolysis will play an important role in the future energy system. According to the IRENA, up to 5.5 TW of electrolysis capacity will be needed by 2050 to meet the demand for hydrogen [1]. To improve electrolyzer operation reliably and cost-effectively, expensive state-of-the-art materials need to be optimized. New materials are being tested and used to keep electrolyzer costs down. At the same time, greenhouse gas (GHG) emissions from electrolysis must be minimized, so the energy supply is provided by volatile renewable energy sources. In addition, electrolyzer stacks must be able to operate for at least 10 years while maintaining a high level of efficiency and performance. Therefore, understanding the degradation of electrolyzers is extremely important in order to improve their lifetime. The combination of new materials, flexible operation and long lifetime needs to be optimized. However, this is not yet supported by sufficient long-term operation under realistic conditions. Many defects contributing to degradation have been discussed and analyzed in the relevant literature. Previous reviews of polymer electrolyte membrane water electrolyzers (PEMWE) degradation have focused, for example, on specific components [2–4] or even single components such as the membrane [5, 6] or catalyst layer [7–9]. Strategies to alleviate and mitigate degradation mechanisms have been discussed [2], along with testing procedures for individual PEMWE components [10] and the effect of degradation on system performance [3, 11]. The potential role of artificial intelligence in materials research for electrolyzers has also been discussed recently [12]. Among others, the Joint Research Centre of the European Commission has published stress tests and protocols for water electrolyzers [13]. However, the level of practical experience on PEM electrolyzers still lags behind that of PEM fuel cells (PEMFC). For example, standardized tests and protocols are not yet widely established and research into lesser-known degradation mechanisms, some of which are only referenced for PEMFC, is still lacking. In addition, quantifying the contribution of various degradation mechanisms is difficult, hindering a complete understanding of which mechanisms are the most significant for long-term operation.

The objective of this review is to provide a clear summary of degradation mechanisms of PEM water electrolyzers with a focus on ex-situ measurements. The analysis is structured by component (see Figure 1), with the scope of consideration extending to the cell level and taking interactions between mechanisms into account. The balance of plant, another source of degradation, is not covered in this review. In general, impurities generated in these systems, as well as uncontrolled operating instabilities (e.g. pressure drops, temperature fluctuations, electric spikes) can influence degradations by facilitating the mechanisms discussed here. To gain further insight into mechanisms that have been studied in literature and research to date, we conducted an expert survey assessing the relevance of various degradation mechanisms. In this way, the focus of previous considerations will be critically examined and evaluated as to whether areas of discussion have been over- or underestimated to date. Another emphasis of this work is examining how degradation effects can be detected diagnostically, considering both established measurement methods as well as those we consider to be promising. In some cases, the discussion of degradation mechanisms and corresponding measurement methods is supported by our own measurement results. In the end, gaps in the research are highlighted and elucidated.

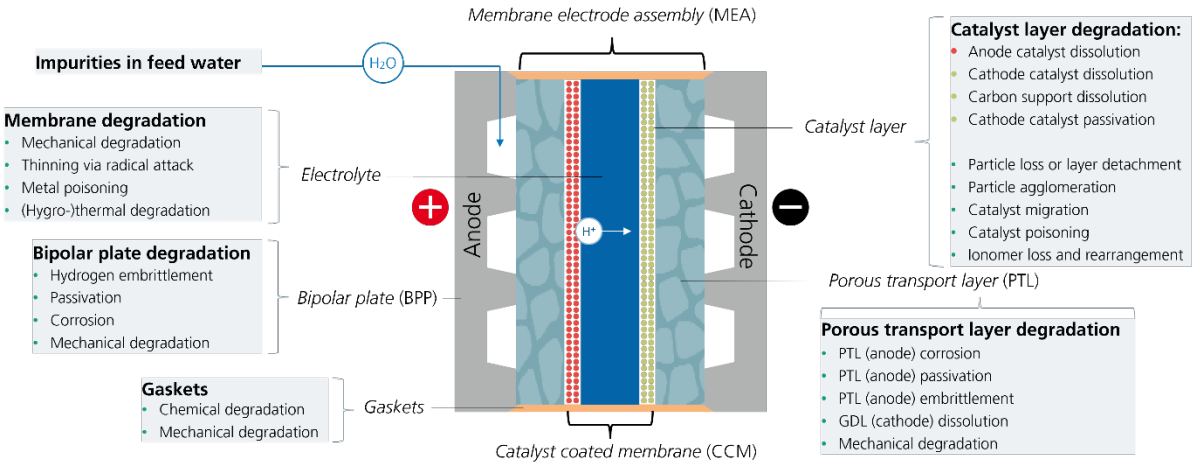


Figure 1: Overview of the degradation mechanisms that may occur in PEM electrolysis.

2. PEMWE Electrochemistry

Water electrolysis for hydrogen production at acidic pH generally proceeds by the oxidation of water on the anode-side forming oxygen and the reduction of the resulting protons on the cathode-side to form hydrogen. The two reactions are also designated as oxygen evolution reaction (OER) and hydrogen evolution reaction (HER). In Equations 1 and 2, the reactions are shown.

$$H_2O \rightleftharpoons {}^1/_2\, O_2 + 2H^+ + 2e^- \quad (1)$$

$$2H^+ + 2e^- \rightleftharpoons H_2 \quad (2)$$

The necessary theoretical potentials vs. SHE (standard hydrogen electrode) for the two half-reactions are at 1.229 V (OER) and 0.000 V (HER), resulting in the theoretical potential of the full water splitting reaction of 1.229 V under standard conditions. In practice, the required potential is higher due to the existence of overpotentials originating from activation, ohmic and mass transport limitations. The reactions are carried out at the anode and cathode catalyst layers in the PEMWE respectively, which are indicated as red and green dotted areas in Figure 1. Also necessary for the reaction is the electrolyte in-between the catalyst layers, which in PEMWE is a proton-conducting polymer membrane. The same or similar polymers also are mixed into the catalyst layers to ensure the proton transport there. Both produced gases need to be transported out of the electrolyzer. In addition, water needs to be supplied to the anode-side catalyst layer and drag water that arrives at the cathode needs to be transported out, which necessitates suitable porosity for an effectively operating cell. At the same time, the catalyst layers have to be contacted electrically, in order to ensure electron transport. Responsible for all of these tasks beyond the catalyst layers are the porous transport layers. Within this review, we use the term porous transport layer (PTL) for the anode-side exclusively and gas diffusion layer (GDL) for the cathode-side. The outermost layer of the main electrolyzer cell are the bipolar plates (BPP). They ensure mechanical stability, further electrical contact and optionally medium transport into and out of the cell via flow channels. Lastly, electrolyzer cells need to be outfitted with gaskets, which seal the cell, support contacting of components and preserve a consistent size of the stack. More details on the components and the materials used for them are given in each specific chapter.

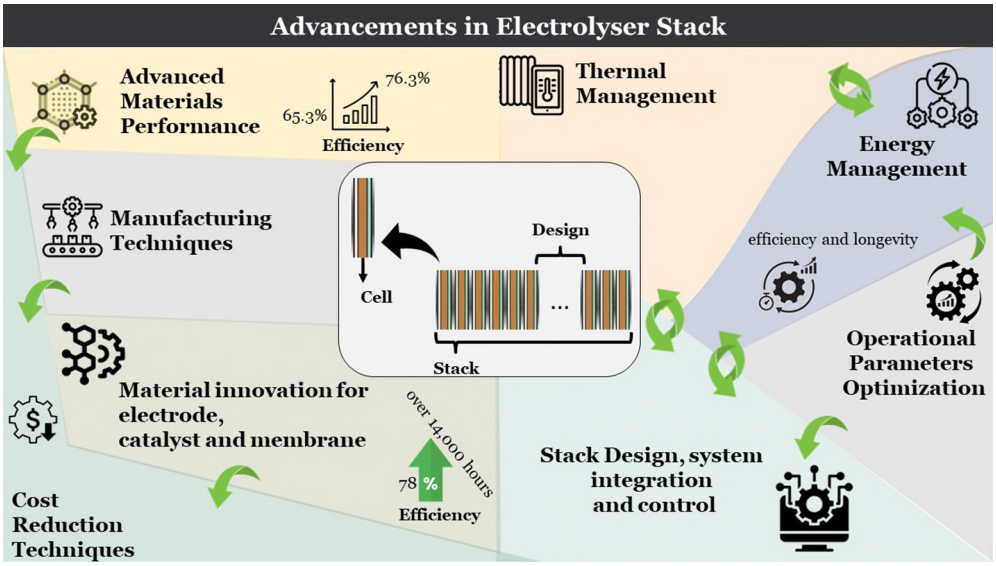


Figure 2: R&D areas for improving performance, efficiency, durability and integration, reprinted from [14] with permission from Elsevier.

Of the degradation mechanisms discussed in the following chapters, three interrelated factors are most often discussed as targets for long-term performance preservation: reducing or preventing membrane thinning, catalyst dissolution and general component corrosion. These issues collectively compromise a large section of system durability and efficiency. To address these challenges, a variety of material and design innovations have been proposed: Reinforced membranes, incorporating inert or mechanically robust materials, enhance resistance to thinning, cracking and chemical attack. These membranes are designed to maintain structural stability under high-pressures (<100 bar) and temperatures <100 °C. Protective coatings are applied to metallic components to mitigate dissolution and corrosion. For example, coatings on PTLs and bipolar plates help maintain conductivity while resisting chemical degradation. In particular, Ti-based PTLs exhibit excellent corrosion resistance and have demonstrated potential for enhancing overall electrolyzer performance. Advanced component designs, such as ionomer-free catalyst layers, can also reduce the risk of degradation and simplify material recovery during recycling processes. Despite these promising developments, long-term durability testing remains essential to evaluate their real-world applicability. Materials must be validated under operational conditions that include acidic environments, thermal fluctuations and sustained electrochemical stress to ensure they deliver the intended performance improvements over extended lifetimes.

The strategies for achieving key performance and cost targets in PEMWE center on the simultaneous advancement of critical parameters to enable efficient, durable and economically viable hydrogen production by 2030. An overview of the Research and Development (R&D) areas that are targeted can be seen in Figure 2 and is more deeply discussed in Madila et al. [14]. These efforts prioritize evolutionary technological improvements over disruptive changes, aiming to enhance energy efficiency, reduce capital and operational expenses, extend system durability and improve responsiveness. Central to these goals is the reduction in the use of scarce and expensive materials especially precious metals by innovating in electrode design, employing thinner membranes and developing advanced coatings and recombination catalysts. Significant focus is also placed on optimizing cost-intensive components such as bipolar plates and porous transport layers, all while maintaining high operational standards. European [15] and U.S. [16] roadmaps align on the need for integrated progress across cell performance, system-level efficiency and material innovation, supported by government funding for R&D, scale-up of manufacturing and design standardization. This comprehensive and balanced approach is essential for overcoming material and cost barriers,

supporting large-scale commercialization and ensuring the sustainable growth of green hydrogen production in response to evolving regulatory and market demands. The summarized European Strategic Research and Innovation Agenda and the U.S. Department of Energy (DOE) technical targets for PEM water electrolysis are given in Table 1.

Apart from efficiency and cost, other key performance indicators (KPI) include durability (targeting 80 000–100 000 hours stack life for low-temperature and >20 000 hours for high-temperature), current density (to increase hydrogen output per cell area; targets of 2–4 A/cm² for PEMWE to balance life) and capital cost reduction (through increased cell size, automation and cheaper materials). For example, the U.S. DOE has set technical targets for PEM water electrolyzers to reduce iridium usage by 90% and increase membrane lifetime fourfold.

Table 1: Targets in comparison: State-of-the-art and future KPIs for all electrolyzer technologies. Adapted from IRENA [17], EU Targets from the Clean Hydrogen Joint Undertaking [18] and US Water Electrolyzer Technical Targets from the Hydrogen and Fuel Cell Technologies Office [19]

Characteristics	Unit	SoA 2022 (IRENA)	Target IRENA (2050)	Target EU (2030)	Target USA DOE (ultimate)	R&D Focus (IRENA)
Electrical efficiency (stack)	kWh/kgH_2	47-66	<42	-	43	Catalysts/membrane
Electrical efficiency (system)	kWh/kgH_2	50-83	<45	48	46	BoP
Capital cost (system)	USD/kW	700-1400	<200	570 [1]	150	Rectifier, water purification
Degradation	%/1,000h	0.25 [2]	-	0.12	0.13	Membrane, catalysts, PTLs
Lifetime	h	50 000-80 000	100 000-120 000	-	-	Membrane, catalysts, PTLs
Nominal current density	A/cm^2	1-3	4-6	3.0	3.0	Design, membrane
Cell voltage	V	1.4-2.3	<1.7	-	1.6	Catalyst, membrane
Critical raw materials use	g/kW	0.8 [2]	-	0.25	0.03	

[1] Capital Cost EU: 500 €/kW (exchange rate 1€ = 1.142USD) [2] Value from US American targets, as IRENA does not state values for these characteristics. **BoP** – Balance of Plant

3. Degradation Processes

In the following, degradation processes for each component are discussed separately including their effects, influencing factors, mitigation strategies and measurement. Some components have the umbrella term mechanical degradation listed as one of the mechanisms. This includes functional losses from tearing, stabbing and excess pressure. These are a result of initial quality defects (e.g. stray fibers that can stab through other components), assembly errors or operational mistakes. Other degradation mechanisms (e.g. radical attack leading to thinning, which makes appearance of a hole more likely) can enhance them. Since the final failure is due to weakness in mechanical integrity and properties, this degradation is called mechanical within this review.

3.1. Membrane

The solid polymer electrolyte membrane in a PEMWE separates the anode and cathode side reactions and the resulting gases and ensures the transport of protons while being electrically isolating. For these reasons protonic conductivity along with mechanical stability are the most important attributes of such membranes. The use of membranes based on perfluorosulfonic acid (PFSA), such as Nafion™, Fumion™ or Aquavion™, are considered state-of-the-art. These consist of a polytetrafluoroethylene backbone and perfluorovinylether sidechains terminated by sulfonate groups. Several alternative classes of materials [20] such as polybenzimidazoles [21–23], polyether sulfones [24, 25], sulfonated polyether ether ketones [25–27], polyoxadiazole [28–30] and polysulfone [27, 31] are explored in research but not used commercially. For this reason, the degradation mechanisms reviewed here will be focused on PFSA-membranes. Among the type of sidechain used and the ionic exchange capacity, the thickness of such membranes and the use of reinforcement are important to consider for the initial performance and long-term degradation of a PEMWE. Due to various effects, such as gas crossover and low mechanical stability, thinner membranes degrade faster. This also leads to increased safety risks. At the same time, thin membranes have a lower transport resistance than thick ones and thus enable higher initial performance due to an increased overall cell efficiency [32].

Despite a low impact on the overpotential, the most detrimental overall defect that can occur in membranes is the formation of pinholes, since these lead to an increased gas crossover that poses a safety risk necessitating the shut-down of the cell. Both membrane thinning (3.1.1.) and mechanical degradation (3.1.2) can lead to pinhole formation, either due to occurrence at preferential sites or by increasing initial thin spots or mechanical weaknesses.

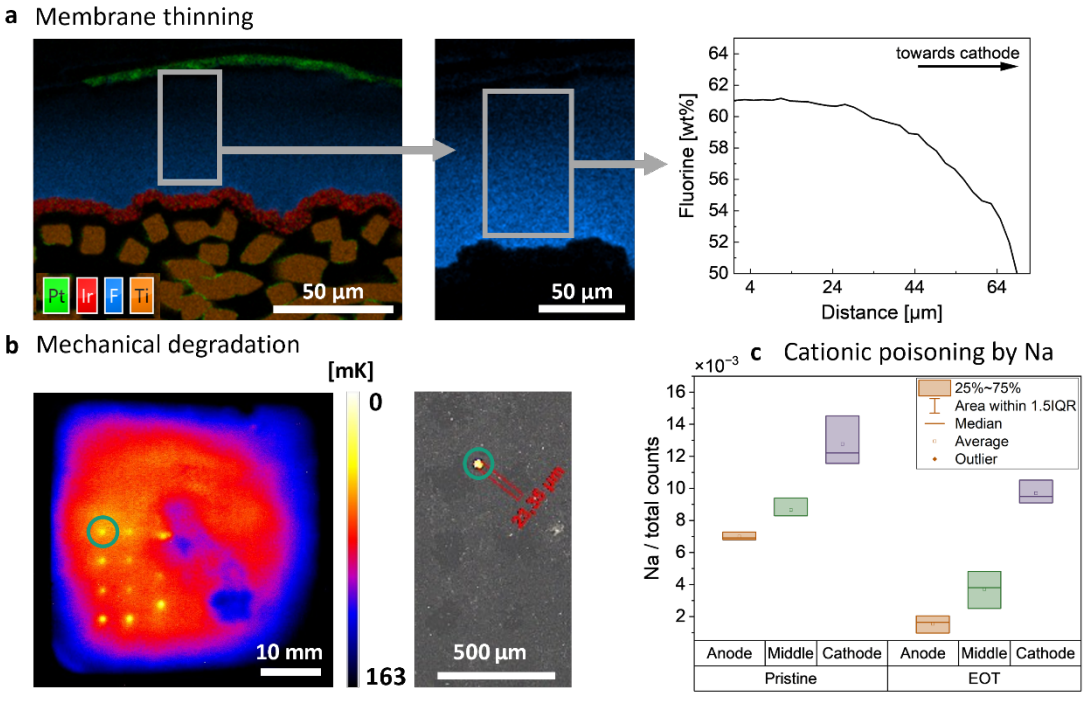


Figure 3: Measurement of membrane degradation pathways: a) Radical attack in a used Membrane Electrode Assembly (MEA) diagnosed from the fluorine gradient imaged by energy-dispersive x-ray spectroscopy (EDX) mapping and extracted fluorine mass fraction profile (summed signal over width of acquisition area) showing a gradient with lower mass fraction towards the cathode; b) Artificially created holes with diameters 20 - 100 µm as seen from light microscopy (right) are identified from the heat generation in lock-in-thermography (LIT); c) Cationic poisoning by Na is reduced over the runtime of the electrolyzer as can be seen from Time of Flight Secondary Ion Mass Spectroscopy (ToF-SIMS) signal of the anode-side, middle (middle of membrane) and cathode-side of the membrane. ***IQR*** *- Interquartile range,* ***EOT*** *– End of Test*

3.1.1. Thinning via Radical Attack

The formation of radical species is a well-known phenomenon in both PEMWE and PEMFC [33]. In PEMWE this process occurs predominantly at the cathode [11, 33–36], where crossed-over molecular oxygen gas is reduced to hydrogen peroxide (H_2O_2), which further reacts to hydroxyl radicals (OH•) and other radical species. This reaction is sped up in the presence of multivalent cations, especially Fe^{2+} due to Fenton's reaction [33, 35, 37].

The radicals resulting from this process can degrade the polymer membrane through side-chain unzipping and main chain scission in a self-accelerating mechanism that are partially shown in Figure 4 [11, 37, 38]. Due to these mechanisms, both fluorine (F) and sulphur (S) are released. In order to track the degradation the Fluoride Emission Rate (FER) and Sulphur Release Rate (SRR) as measured for example via selective electrodes [33, 35, 39–41], Inductively Coupled Plasma Mass Spectroscopy (ICP-MS) [42, 43], photometric detection [44, 45], conductivity of effluent water [46], or ion chromatography [47–50] can be used. Fourier-Transformed Infrared Spectroscopy (FT-IR) [51], Raman spectroscopy [52] and Nuclear Magnetic Resonance (NMR) [51, 53, 54] can be used to track the degradation via functional groups of the membrane in-situ. Additionally, when the degradation is strong enough, the thinning of the membrane can be seen post-mortem via Scanning Electron Microscopy with energy-dispersive x-ray spectroscopy (SEM-EDX) [39–41, 44, 47, 50, 55–57] and Transmission Electron Microscopy (TEM) [36]. These techniques also allow for the appearance of a gradient of i.e. fluoride as can be seen in Figure 3 a), where the color gradient from SEM-EDX can be quantified to a loss of fluorine from 61% to 53% from anode to cathode within the membrane. The degradation results not only in a thinner membrane, but can also increase the likelihood of pinholes or cause brittleness which increases mechanical degradation and reduced adhesion of catalyst layers [11, 58]. Ex-situ, the thinning by radicals is often simulated using a Fenton test, meaning immersion of the membrane into a solution containing H_2O_2 and Fe^{2+}.

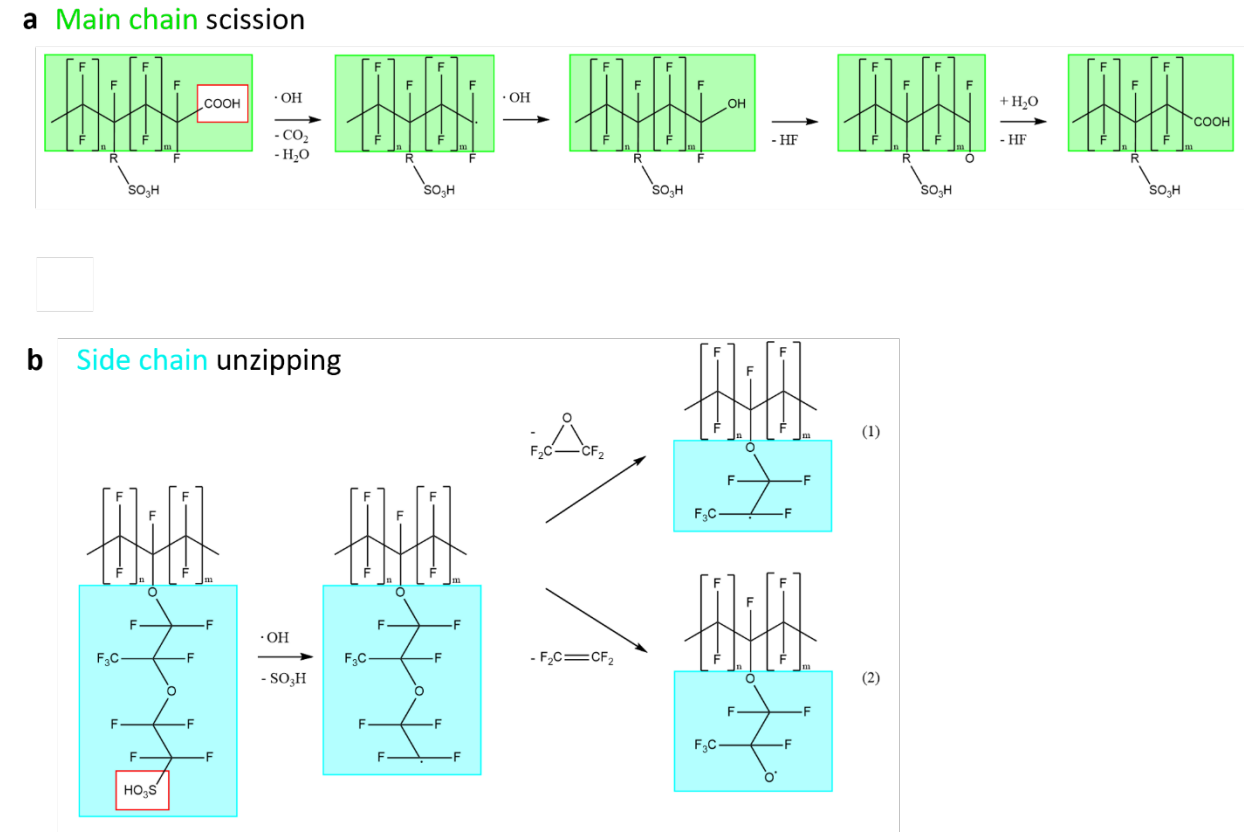


Figure 4: Membrane thinning by a) main chain scission and b) side chain unzipping based on [38, 54, 59, 60].

To mitigate this effect, various strategies can be used: the use of different membranes, which are less sensitive to radical attack, the incorporation of antioxidative additives or radical scavengers, such as cerium (Ce) ions [61], or the reduction of gas crossover e.g. via thicker membranes [2]. In addition, lowering the overall temperature or avoiding the creation of hotspots can slow the thinning process [35, 62]. Avoiding especially low or high current densities and variability in operating conditions can also lower membrane degradation [11, 41]. It should be noted that the membrane thinning can initially lead to a lower voltage due to a lower ohmic resistance, which masks degradation in electrochemical measurements.

3.1.2. Mechanical Degradation

Mechanical degradation of the membrane includes all mechanisms resulting from its physical weakness and can stem from mechanical stresses e.g. due to uneven pressurization, inadequate humidification and reactant pressure [51, 63, 64] and may be worsened by previous chemical degradation. It can lead to pin holes, tearing and cracking of the membrane, as well as deformation due to creep. [65] Propagating cracks can be initiated by pinholes and foreign materials, introduced during manufacturing. The stress due to (inhomogeneous) compression between the bipolar plates can lead to micro-crack fractures along the edges of the flow channels and membrane deformation [66]. Roughness of the GDL or PTL affects membrane durability and amplifies molecular hydrogen crossover rate, probably due to puncture of the membrane by the current collector [67]. If the water feed is non-uniform, operates with too much pressure or an excessive flow rate, the membrane can suffer water starvation [63], pressure damage, or inhomogeneous water distribution [64]. Uneven membrane swelling which is also influenced by the cell design, can consequently lead to buckling [68, 69]. An overview over the factors causing or enhancing mechanical damage to the membrane is shown in Figure 5. The mechanical degradation can be mitigated by careful design of the cell assembly and clamping, as well as care during pressurization. Membrane reinforcement [70], modification of its chemistry [71] and edge protection in the seal area [72] can all play a role. Higher operating temperatures, as well as transient operation and start-up and shut-down procedures can all worsen mechanical degradation [11].

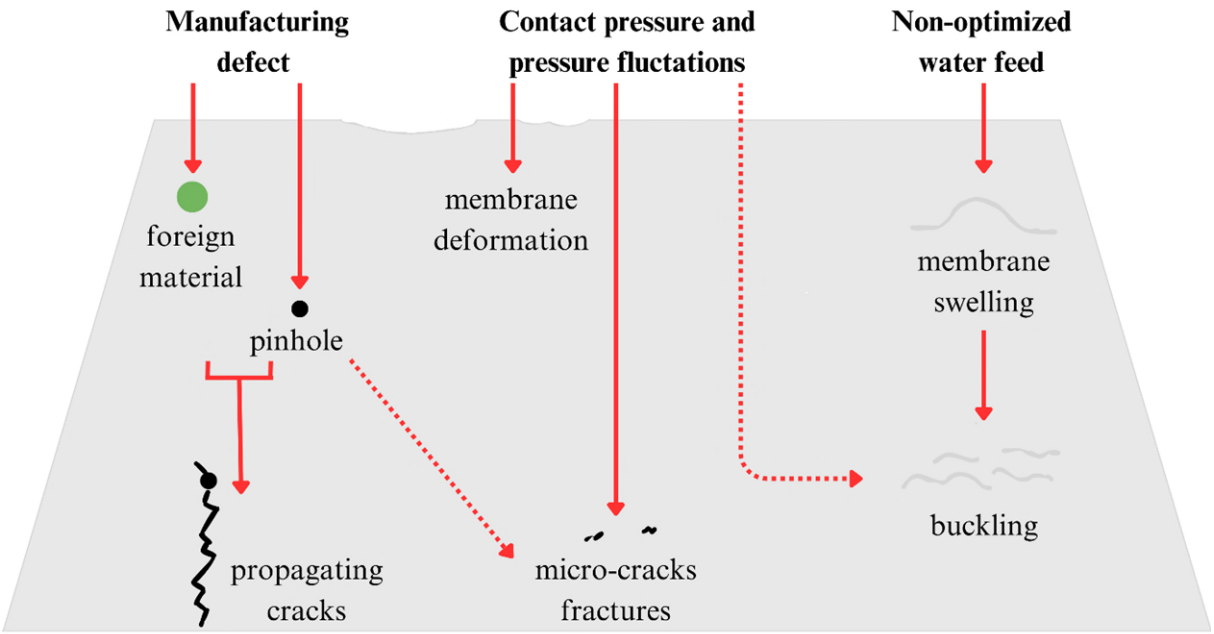


Figure 5: Overview of factors, such as manufacturing defects, contact pressure and water feed influencing the membrane mechanical degradation, which results in pinholes, cracks and buckling.

A wide variety of methods can detect pinholes, cracks and deformations resulting from the mechanical degradation, although the interplay with thinning necessitates additional methods to correctly assign which mechanism plays the bigger role. Among the methods used are Infra-Red (IR)-thermography [35, 47, 73–76], detection via pressure drop tests [73, 74, 77], bubble tests [74], reactive [47, 73, 75, 77–79] or non-reactive [47, 73, 80] gas crossover and microscopy methods such as Scanning Electron Microscope (SEM) [35, 78, 81], optical microscopy [35, 73, 74, 82] and Computed Tomography (CT) [83]. The susceptibility to mechanical failure can also be assessed ex situ via typical mechanical measurements, such as static and dynamic stress testing [51, 65, 68, 82]. An example for the detection of a pinhole by combining reactive gas crossover with IR-thermography can be seen in Figure 3 b).

3.1.3. Metal Poisoning

Membrane poisons include metallic cations and dissolved catalyst ions (see 3.2.7) which contaminate the membrane and lead to an increase in ohmic losses and activation overpotential as well as a decrease in proton (H^+) concentration and conductivity. The most relevant membrane poisoners are metallic cations (e.g. Na^+, Li^+, Ca^{2+}, Cu^{2+}, Ni^{2+}, Fe^{3+}) which can be introduced through the feed water, Balance-of-Plant (BoP) components, sealants and degradation of cell components [84, 85]. They already have a negative impact in trace amounts [86, 87]. The ions dissolve into the membrane via diffusion and permeation and occupy the ion exchange sites of the membrane, thus lowering its proton conductivity [88] . Higher valency cations have a higher impact than those of lower valency [88, 89]. In addition, some cations can accelerate radical degradation (see 3.1.1). This poisoning is partially reversible by bathing the membrane in sulfuric acid (H_2SO_4) or nitric acid (HNO_3) solution [63, 90] or by a current-driven process [91]. An example for the detection of metal cations via ToF-SIMS is shown in Figure 3 c).

Dissolved catalyst particles can also precipitate into the membrane due to the electric field and poison it by the same mechanism or react with dissolved molecular hydrogen, chemically reducing into insoluble particles (see 3.2.7) [36]. Besides performance tests with intentionally contaminated feed water [86–88, 90–94], SEM-EDX [36, 43, 57, 58, 89, 95], ICP-MS [63, 87, 96], Electron Probe Microanalysis (EPMA) [63, 87, 88, 96, 97], X-Ray Fluorescence (XRF) [98] and X-ray Photoelectron Spectroscopy (XPS) [96] have also been used to examine the impact of contaminants on membranes. Ex-situ, these tests can be simulated by soaking the membrane in solutions containing a defined amount of the poisoning cations.

Main mitigation strategies include adequate feed water filtration and using polymer materials instead of metals for components such as fittings, tanks and pipes. It should be noted that polymeric materials used in e.g. sealings can also introduce cationic impurities such as Ca^{2+} [99–102]. In addition, such materials are less feasible for use under higher pressures.

3.1.4. Thermal Degradation

Purely thermal decomposition does not play a role under typical PEMWE conditions, as operating temperatures (60-80 °C) remain below glass transition (<120 °C) and degradation (<250 °C) temperatures [103–105]. Nevertheless, temperature increases can amplify the impact of other degradation mechanisms, such as the increase of radical attack [33] and local hotspots, i.e. due to water starvation [63]. The cell edges are more prone to hot spots due to temperature maldistribution from gas bubble accumulation [106]. In addition, hygrothermal degradation can decrease the availability of sulfonic acid groups ($-SO_3H$) [35, 107, 108]. The degradation of $R\text{-}SO_3H$ groups by formation of cross-linking anhydrides $R\text{-}SO_2\text{-}O\text{-}SO_2\text{-}R$ has been observed ex-situ and in PEMFC [109, 110], but to our knowledge has not been studied in PEMWE yet. It seems reasonable that the mechanism exists in PEMWE as well, but it might be less pronounced than other mechanisms. In addition to the lower Ion-Exchange Capacity (IEC), the hygrothermal degradation also worsens mechanical properties [109] and

influences gas and water transport [111]. The anhydride formation can be reversed by boiling the membrane in concentrated acid. It has been studied using FT-IR spectroscopy [109, 111, 112] and NMR spectroscopy [107].

3.2. Catalyst Layers

The catalyst layers are the locations where the electrochemical reactions of the cell take place: oxidation of water to molecular oxygen at the anode and the reduction of protons to molecular hydrogen gas at the cathode. They need to be catalytically active, conductive for both protons and electrons, show low contact resistances and be mechanically and chemically stable. In addition, water needs to reach the active sides and produced gases need to be transported out of the layers. To bring together these demands, porous composite materials consisting of the catalytically active material (catalytic activity and often electrical conductivity), ionomer (proton conductivity) and sometimes an additional support material (dispersion to increase specific activity, often electrical conductivity and mechanical stability) are used. Ionomers for both catalyst layers are overwhelmingly chemically identical to the base polymer of the membrane.

During the last fifty years, iridium (Ir)-based or coated anodes have been established as the benchmark due to comparatively high stability combined with high mass specific catalytic activity. While there are more active metal catalyst materials (e.g. ruthenium, Ru), these tend to suffer from lower stability [113]. Underlying degradation mechanisms of Ru-based catalysts are largely similar to Ir-based catalysts [114]. Generally, IrO_2 (iridium oxide) is more stable against dissolution than Ir metal catalyst [115] and amorphous mixed oxides [116]. When a support material is used for the anode, these are mostly transition metal oxides and ceramics [117–122]. The possibility of ionomer-free anodes with high stability has also been shown [123].

On the cathode side, nanostructured or nanodispersed platinum (Pt) is used, ensuring the lowest overpotential for the cathodic reduction of protons. The less harsh environment of the cathode allows for the use of carbon supports and thus well-established Pt/C catalyst powders [124]. The type of carbon support used and Pt/C ration can influence the degradation [125, 126].

An overview of degradations mechanisms that affect the catalyst layers is shown in Figure 6. While testing catalyst layers in a MEA setup is preferred, most degradation mechanisms can also be observed using rotating disc electrodes (RDE). Consequently, RDEs are often used for initial benchmarking and degradation observation of catalysts, although the experiment design must be carefully considered to ensure reproducibility and transferability to MEA setups [127–129]. Not observable with this method are generally the catalyst migration into the membrane and any poisoning that originates from components of the MEA that are not present in an RDE experiment, as well as any effects from extended catalyst layers.

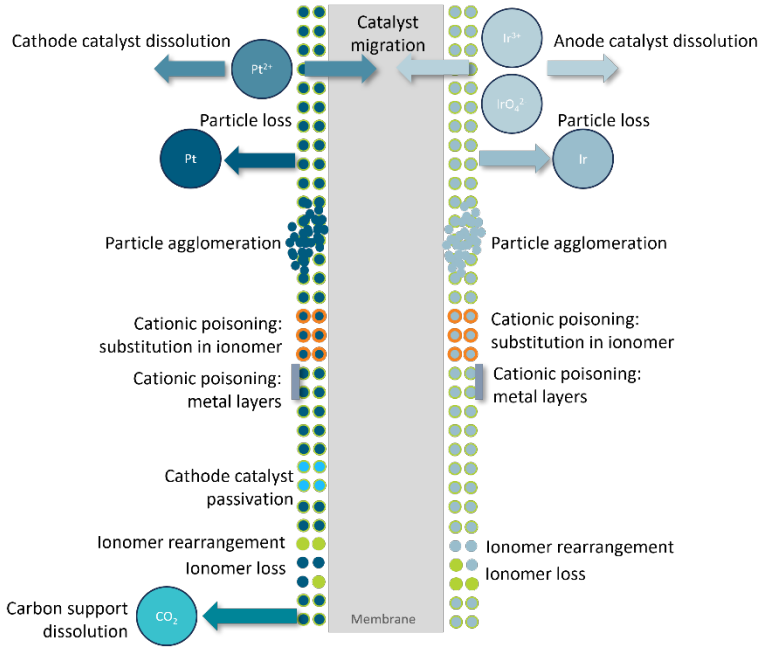


Figure 6: Degradation mechanisms affecting the catalyst layers shown on a schematic catalyst-coated membrane (CCM). Catalyst dissolution, particle loss, agglomeration, cationic poisoning, ionomer rearrangement and ionomer loss affect both catalyst layers. The cathode layer is additionally affected by the cathode catalyst passivation and carbon support dissolution

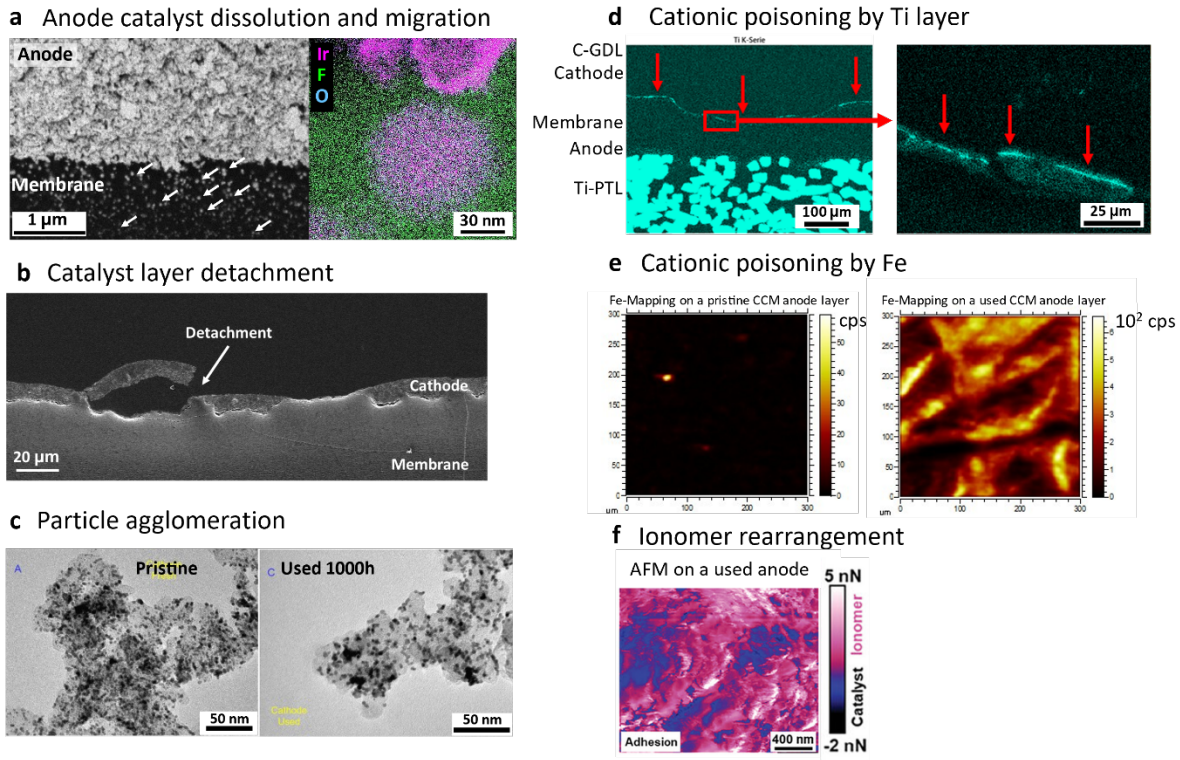


Figure 7: Measurement of catalyst degradation pathways: a) SEM image and STEM-EDX map-overlay of anode catalyst dissolution and migration; b) SEM image of cathode showing the beginning of detachment from the membrane; c) TEM images of pristine and used cathode layer showing particle agglomeration reprinted from [130] with permission from Elsevier, labelling of images and scale bar added by the authors; d) Poisoning Ti layer from dissolved PTL material at the cathode GDL interface imaged by SEM-EDX; e) Mapping of Fe-contaminants derived from ToF-SIMS data of a pristine CCM anode layer (left) and an used CCM (right); and g) Atomic Force Microscopy (AFM) adhesion mapping of aged anode layer structure showing the ionomer arrangement reprinted with from [131] with permission from Wiley, cut to size and label added by the authors.

3.2.1. Anode Catalyst Dissolution

Iridium based electrodes release 4 protons and draw 4 electrons for the oxidation of water to oxygen in a multistep process, which is strongly dependent on the electrode potential, the pH value, the temperature and the pressure [119]. According to Geiger et al. [116] the ratio of the generated oxygen to the released Iridium is an objective measure, independent of loading or surface area, of the stability allowing for the evaluation of different Ir-based catalysts and their comparative stability independent of high initially apparent activity.

Possible pathways depending on the applied potential for the dissolution of Ir and IrO_2 involve Ir^{3+} or IrO_3, which can form soluble IrO_4^{2-} or $Ir_2O_7^{2-}$. At pH < 7, the reactions shown in Figure 8 are relevant [116, 132, 133]. Higher loads [41, 134], frequent start-stop cycles [85], higher temperatures and occurrence of impurities [11] have been shown to enhance the dissolution. In addition, the dissolution may be higher locally, where the catalyst particles are in direct contact with PTL's Ti fibers [135]. The formation of more active hydrous oxides on the catalyst surface and the roughening resulting from dissolution can initially lead to a better cell performance, masking the degradation.

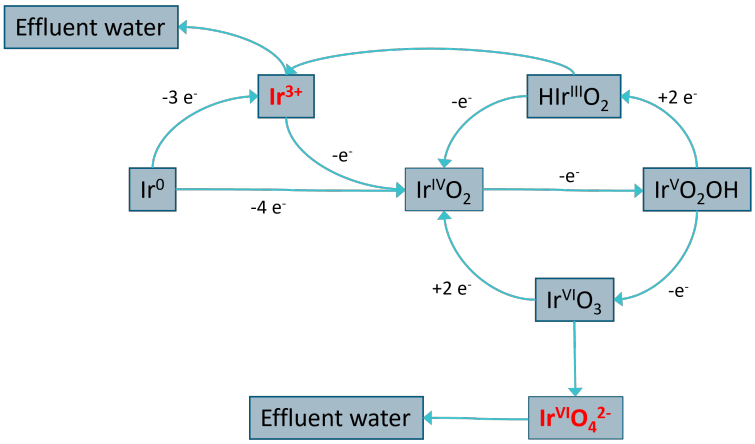


Figure 8: Ir dissolution mechanisms with the dissolving species that may leave the cell with the effluent water marked in red.

To mitigate the dissolution of iridium (oxide), the choice of catalyst support is an important factor. Using inert oxides (e.g. SnO_2, TiO_2, Ta_2O_5, Nb_2O_5, SnO_2/Sb_2O_5 (ATO)) as support increases stability of active IrO_2 and/or RuO_2 against corrosion [117–122, 136]. Although da Silva et al. [137] have shown that supported nanocatalysts are generally less stable than unsupported catalysts with larger particles. Stability enhancement has also been achieved with carbon-supported IrO_x, that was treated with microwaves [138]. The catalyst and support morphology can also play a role, since nanodendritic IrO_2 [139] and a combination of honeycomb IrO_6 and foam-like IrO_x [140] have both shown high activity and stability and nanostructured ATO [122] has been proven more stable than commercial versions. Improvement of in-plane conductivity leading to higher stability has also been achieved with gold layers [141].

The dissolution of iridium oxide has been studied with a variety of methods, such as SEM-EDX [43, 55, 135, 136, 142–145], XPS [55, 139, 146, 147], AFM [143, 148], Scanning TEM (STEM) or TEM-EDX [41, 57, 85, 139, 140, 142, 145, 147, 149–151], X-ray Diffraction (XRD) [152], XRF [152], X-ray Absorption Near Edge Structure (XANES) [85, 115, 140, 147, 150] and ICP-MS or Inductively Coupled Plasma Optical Emission Spectroscopy (ICP-OES) [85, 115, 116, 119, 137, 140, 145, 149, 151–154]. Especially SEM and TEM cannot simply differentiate between material lost due to dissolution and material loss due to mechanical mechanisms (see 3.2.5). Exemplary SEM and TEM measurements in Figure 7 a) show degradation-induced particles in the membrane next to the anode layer. These particles are embedded in the membrane and thus not connected electrically anymore. Methods such as XPS are helpful in identifying surface species that can be the nexus of degradation. Especially ICP-MS of effluent water is

attractive to study the dissolution mechanism in-situ and thus enables differentiation from other mechanisms.

3.2.2. Cathode Catalyst Dissolution

Under normal conditions of water electrolysis, the oxidative degradation of Pt is often considered suppressed at the cathode. However, under open-circuit voltage (OCV) conditions, the electrolysis cell can change into the fuel cell mode, in which the anodic dissolution of Pt to Pt^{2+} becomes possible [155]. This is mostly prevented by avoiding operation under OCV, such as shut-downs. There is also evidence, that smaller Pt nanoparticles are unstable under operating conditions that correspond to the local potential at the cathode-membrane-interface, especially during voltage cycling [41]. In addition, the presence of chloride ions can lead to the formation of chloroplatinic complexes, resulting in enhanced loss of cathode catalyst and its agglomeration [156]. Pt dissolution has been studied via XRF [128, 145, 157, 158], (S)TEM-EDX [41, 58, 142, 145, 159, 160], ICP-MS [43, 145, 153, 155, 161], EPMA [161], SEM-EDX [43, 44, 128, 130, 162] and mass measurements [128].

3.2.3. Carbon Support Dissolution

Similar to the Pt dissolution, carbon degradation is not common during electrolysis, although it has been theorized to contribute to degradation of the cathode catalyst layer [163]. Degradation of the support lowers the attachment of the Pt, thus lowering activity. The reaction with water to carbon dioxide (CO_2) requires a standard potential of +0.21 V vs. SHE and is kinetically hindered but under fuel cell conditions it becomes possible, especially during start-up and shut-down procedures [160, 162, 164–167]. In addition, this can be promoted by higher Pt loadings [125, 126] and the accumulation of cations leading to proton depletion [168]. Carbon is less stable with a higher surface area and with lower degree of graphitization [125, 126, 166]. The reaction with H_2O_2 can also degrade carbon supports, although the relevance of this mechanism at typical concentrations in electrolyzers is limited [164, 169]. Carbon corrosion has been mainly observed using CO_2 measurements with Infrared (IR)-sensors [166, 170, 171], Electron Spin Resonance (ESR) [169], Raman spectroscopy [166, 167] and TEM [166, 171].

3.2.4. Cathode Catalyst Passivation

The passivation of Pt by the reaction to oxides has not been observed under PEMWE conditions but is theoretically possible and has been observed in fuel cells [160]. One possibility is the reaction with hydroxyl radicals and dissolved molecular oxygen (standard potential +0.34 V vs. SHE) [172] to PtO (platinum oxide), another is the reaction with water at high electrode potentials [173]. The passivation is a problem due to the reduced electrical conductivity and availability of catalytically active sites. In addition, the PtO layers can be an intermediate to catalyst dissolution as Pt^{2+} [142, 173]. The formation of PtO can possibly be seen by XPS, but differentiation is necessary [142, 158].

3.2.5. Particle Loss and Layer Detachment

Catalyst particles can be lost not only due to dissolution but also by mechanical separation from single particles up to whole layers from the structures the layer adheres to. Reasons for this can be uneven contact pressure, improper membrane swelling or mechanical damage during the initial assembly, as well as the mechanical instability caused by the formation of bubbles, the dissolution of catalyst, the previous degradation of support materials like carbon and oxidation of titanium and the decreased attachment to carbon support at high current densities [11, 81, 85, 160, 174]. During assembly, even pressurization of the MEA can mitigate this. During operation, the suppression of bubble formation and reduction of their size, e.g. by the use of microporous PTLs [175] and the optimization of stress distribution [176] are beneficial. Although particle loss can be analyzed by SEM or (S)TEM-EDX [43, 44, 56, 81, 85, 160, 177], CT [178], X-ray radiography [144, 177, 178] and XRF [157], distinguishing it from

catalyst loss by dissolution remains challenging. An example of the beginning detachment of the cathode from the membrane (delamination) imaged by SEM can be seen in Figure 7 b).

3.2.6. Particle Agglomeration

Nanoparticle agglomeration, the tendency of nanoparticles to increase in size over time to reduce their surface energy, can be considered a degradation mechanism even though it does not lead to direct loss of catalyst. The coalescence of particles reduces the electrochemically active surface and thus leads to a drop in cell performance. As illustrated in Figure 9 the agglomeration can proceed through several mechanisms: Coalescence via crystal migration, growth via modified Ostwald ripening and reprecipitation at other nucleation sites [179]. This degradation mechanism is relevant for both catalyst layers and can increase during higher temperatures, higher voltages or stronger variability in the operation conditions [11, 85, 115, 146, 180].

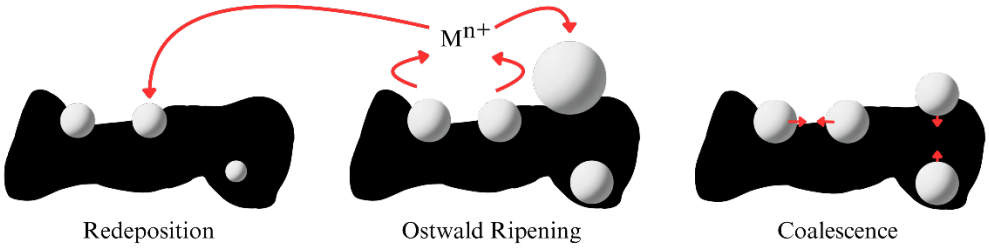


Figure 9: Mechanisms of catalyst particle agglomeration showing the movement of particles during redeposition, Ostwald ripening and coalescence, recreated from [179].

TEM(-EDX) [55, 115, 130, 138, 142, 146, 157–159, 180–184] is especially suited to analyse agglomeration with high spatial resolution. Additionally, CT [185], XRD [130, 157, 158, 183, 184, 186] and Small Angle X-ray Scattering (SAXS) [85, 115, 150] can be used to characterize changes in particle size distribution and surface area. The agglomeration of Pt supported by carbon at the cathode layer is shown in Figure 7 c) investigated by TEM before the beginning and after ending of the test. After 1000 h of usage bigger Pt particles on the carbon support occur [119]. It has been theorized that the presence of oxygen functional groups on Pt/C catalysts anchor Pt particles against their movement towards agglomeration [180]. Stability against agglomeration was also enhanced via the use of TiN (titanium nitride) nanoparticles as redisposition sites as investigated by XPS [158].

3.2.7. Catalyst Migration within the PEMWE Cell

While catalyst dissolution (3.2.1 and 3.2.2) can lead to the resulting metal ions leaving the cell with effluent water, they can also migrate within the cell due to osmotic pressure and the electrical field. This can lead to underestimation of catalyst dissolution from measurements in the effluent water. After migration, the ions can either agglomerate (i.e. at active membrane sites) or be reduced to their metallic form [36, 142]. In addition to the loss of catalyst mass itself, this can present problems by reducing the ion exchange capacity of the membrane and physically blocking electrochemically active surface. The formation of short circuits in the membrane due to precipitating Ir-Clusters has also been described [187]. Curiously, the occurrence of platinum within the membrane can also be advantageous since it functions as a gas recombination layer reducing hydrogen crossover [43, 188] although such layers also increase ohmic resistance and resulting hotspots can increase membrane degradation. Catalyst migration can be mitigated by reducing the catalyst dissolution itself. The migration is mostly studied via SEM or TEM in combination with EDX [36, 41, 43, 57, 85, 115, 142–145, 150, 189–191] of cell cross-sections, but can also be analyzed with synchrotron XRF [98, 192] or gamma ray activation analysis and neutron activation analysis [193]. The beginning of such a migration has been shown by STEM-EDX in Figure 7 a).

3.2.8. Cationic Poisoning

Similarly to the degradation from cation poisoning in the membrane (3.1.3), cations from impurities or degradation of other components like anodic Ti-PTL can substitute H^+ in the ionomer of catalyst layers. This decreases proton transport pathways and thus electrochemically active surface. Additionally, the ions can be reduced to metallic layers deposited on the cathode and thus lower the electrochemical surface area ECSA and introduce additional ohmic resistance [84, 85, 98]. When layers are deposited and removed repeatedly this could also lead to enhancement of catalyst dissolution [194]. The effect of cations can be detected by SEM or (S)TEM-EDX [44, 58, 89, 91, 97, 168, 183, 184, 194], EPMA [63, 195], XRF [98] and neutron scattering with the model compound Gd^{3+} [196, 197]. While the use of ultrapure water and filters can reduce cationic impurities, mitigation of this effect is challenging, since contamination can also stem from BoP and cell components, as well as sealants. In Figure 7 d) an example of the poisoning by a metal layer depositing at the cathode-GDL interface is shown. The Ti creating the layer is theorized to origin from PTL dissolution. In addition, Figure 7 e) demonstrates the contamination of a used CCM anode layer by Fe species as determined by ToF-SIMS. Here it is evident, that much more Fe ions are present in the used sample and that the Fe localization is associated with contact to the Ti-PTL.

3.2.9. Ionomer Loss and Rearrangement

Most degradation mechanisms affecting the membrane can also influence the ionomer but since they are not generally mechanistically different, they are not described separately. Thinning due to radical attack and cationic poisoning effects (as described in 3.1.1 and 3.1.3) is more pronounced for the ionomer due to the smaller feature size. In addition, local heating from the PTL can worsen thermal degradation and thinning of ionomer [198]. An additional ionomer degradation mechanism is the rearrangement within the catalyst layer, which leads to a reduction in triple-phase boundaries (TPB) and mechanical stability [199]. It may be traced to the flow of ionomer at applied potential and temperature [198]. It has been studied by SEM and TEM(-EDX) [115, 147], XPS [147, 198] and AFM [131, 143, 148, 198, 199]. An example for the visualization of ionomer rearrangement via AFM measurements of the adhesion force can be seen in Figure 7 f). There the ionomer and catalyst are differentiated by their different adhesion forces. The mapping of this force over an area enables the determination of a mean size of catalyst and ionomer domains and their intermixing on the surface of a sample [120]. First forays into mitigation by optimizing the interface with the PTL through coating with metallic iridium have been performed [198].

3.3. Cathode-Side Gas Diffusion Layer

On the cathode-side, transport of the produced hydrogen gas and drag water, as well as electrical and thermal conductivity are ensured by carbon materials (e.g. carbon paper or cloth). Often Polytetrafluoroethylene (PTFE) is added to the carbon material to improve the water management. The porous transport layer on the cathode side is called the gas diffusion layer (GDL) to distinguish it from the porous transport layer on the anode side. Most studies on carbon GDLs originate from PEM fuel cell research. The same general principles regarding mechanical damages can be considered to be valid for electrolysis.

3.3.1. Mechanical Degradation

Due to its high porosity the GDL is more susceptible to mechanical damage than other components. Compression of the stack is necessary to lower interfacial resistances and prevent leakages of water and produced gasses. During first compression of a cell, the GDL is compressed thus leading to fiber breakage, delamination and decreasing porosity, which lowers interfacial contact resistances but increases mass transport limitations [200, 201]. Higher local compression during operation, e.g. due to gas production and deterioration of other components, can further damage the GDL. The channels of

the flow field plate (BPP) can also cause mechanical stress as the fibers of the GDL protrude into the channels, which causes non-uniform compression [201, 202].

The mechanical degradation of the GDL has been analyzed using SEM [67, 203–205], CT [205] and light microscopy [203]. The changes in gas permeability, thermal and electrical behavior can also be an indicator of the mechanical changes [201, 204, 206–208]. Impacts on the porosity can be analyzed by i.e. mercury intrusion porosimetry [204, 207]. Ex situ standard mechanical testing (i.e. tensile or compression testing) is preferred to evaluate GDLs susceptibility to these stressors. Mitigation of the mechanical degradation can be carried out by optimizing clamping pressure and reducing pressure inhomogeneities during operation, as well as by fine-tuning porosity and layer thickness and using smoother surfaces [203].

3.3.2. Chemical Degradation

Similar to the carbon support used on the cathode side, the chemical degradation of the GDL is generally not considered a priority, since potentials for chemical degradation are not likely during normal PEMWE operation. In PEMFC, corrosion can occur during startup and shutdown events [207]. Even when these conditions are significantly altered, it is much more likely that the carbon support of the catalyst layer will degrade first, since it is generally exposed to harsher conditions. In PEMFC only 10-20% of CO_2 emission where attributed to GDL carbon corrosion [170, 209]. The possibility of chemical carbon degradation in PEMWE could be observed using similar methods to the ones described in 3.2.3. Ex-situ testing with highly concentrated H_2O_2 does show strong degradation of carbon GDLs as investigated by using mass measurements [210], CO_2 sensors [210], SEM [210] and acidic group titration [211], but the applicability to H_2O_2 amounts usually found in-situ is not clear [32]. Nevertheless, changes in the GDL, e.g. in its hydrophobicity, may lead to changes in water and gas transport [11].

3.4. Anode-Side Porous Transport Layer

A corrosion-resistant material with high electrical conductivity and low mass-transfer, interfacial contact and through-plane resistance is essential for the anode side of PEMWE [212–214], especially because of the harsh conditions close to the membrane. Titanium, in various forms such as meshes, felts, foams and sintered powders, is the most commonly used material for the PTL in PEMWE due to its minimal corrosion at high anodic potentials, high conductivity and mechanical strength [2, 215, 216]. However, Ti can still corrode, become passivated, or experience hydrogen embrittlement, similar to the issues observed with BPPs (see 3.5). In contrast, the less expensive alternative of stainless steel mesh has a high corrosion rate and is the source of significant transport of iron and nickel cations from the anode to the cathode, which contaminates the membrane and catalyst layer [217].

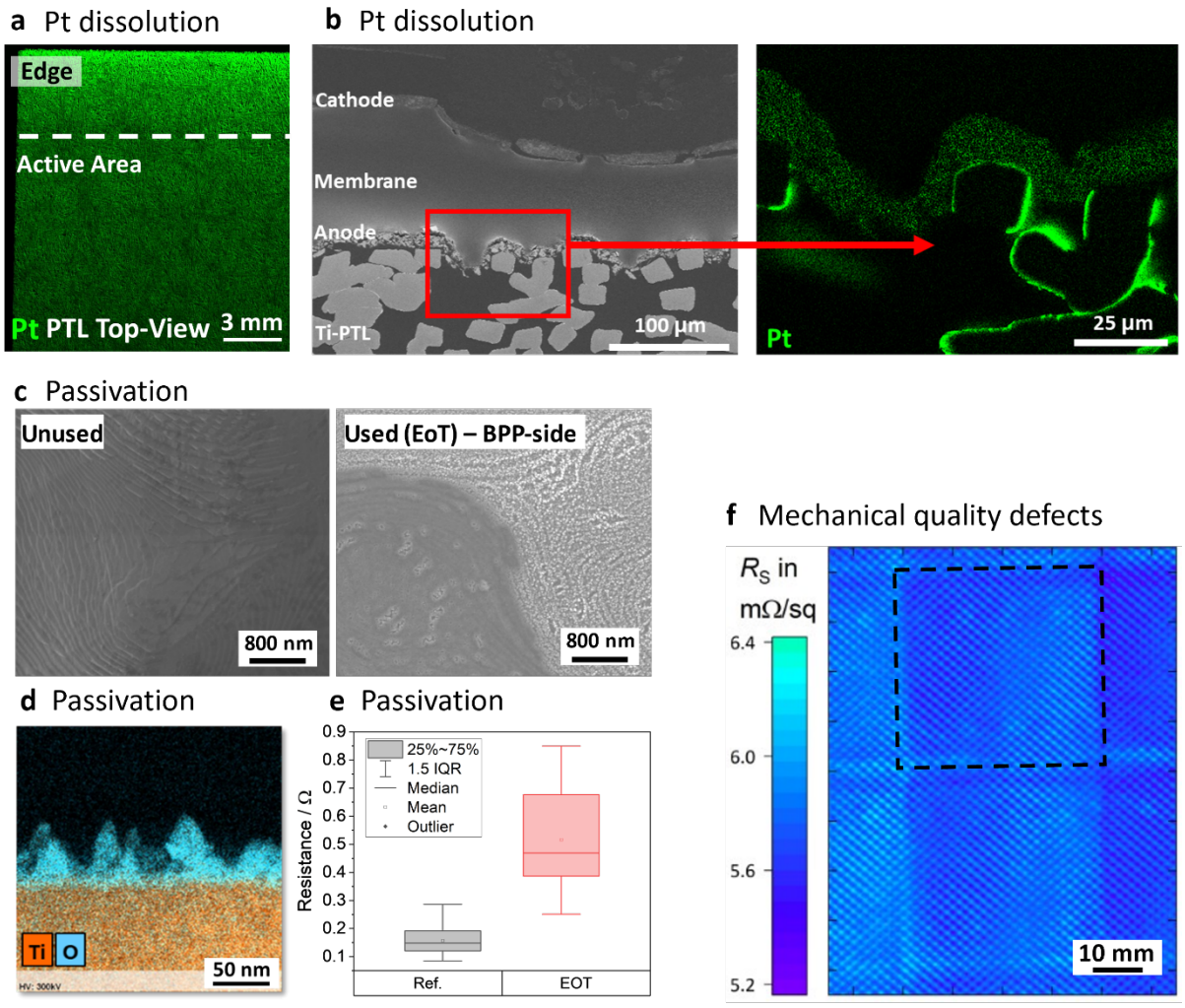


Figure 10: Measurement of degraded PTLs and exemplary observed degradation pathways: a) XRF measurement of a PTL with chemical degradation of the protective Pt layer showing a gradient in the Pt distribution; b) SEM-EDX of an equivalent sample PTL demonstrating Pt migrated into the anode; c) SEM images showing formation of a passivation layer (reference and used) on a PTL; d) STEM-EDX map overlay of passivated PTL showing pyramidic nanostructures at the PTL-BPP interface; e) Increased two-point-measured resistance of the PTL of reference and after passivation process attributed to the contact resistance; and f) Eddy current testing (ECT) of PTL with visible pattern in sheet resistance due to welding processes during production. ***IQR*** *- Interquartile range*

3.4.1. Chemical Degradation

Concerning chemical degradation, the processes, details on effects and measurement of hydrogen embrittlement, passivation and corrosion of Ti and stainless steel, especially on the anode side of PEMWE, are explained in detail in the section on BPPs (see 3.5.1 to 3.5.3). The mechanisms and measurement methods for these aspects are generally the same for BPP and PTL. Hydrogen embrittlement reduces mechanical stability, while passivation and corrosion cause an increase in interfacial contact resistance. Due to PTL corrosion, released cations (e.g. Ti) can enter and poison the catalyst and membrane.

During steady state operation, gas entrapment in the PTL can lead to increased passivation, as has been determined with XPS [41]. In [44], contact angle measurements have been used to measure the oxidation layer on a PTL. In Figure 10 c), d) and e), a combination of SEM, (S)TEM-EDX and resistance measurements show the passivation of a Ti-PTL. It highlights that the effect (increased contact resistance) and the nanostructure (pyramidic structures at the PTL-BPP interface) can be combined to gain a full understanding of the passivation process. Just like with BPPs, coatings are being used to minimize chemical degradation of the PTL. Some possible coatings for the Ti-PTL are Au [218, 219], Ir

[220], Pt [184, 221], Nb [222] and IrO_2/Ta_2O_5 [223]. On stainless steel, Pt, Nb and Ti have been used to increase corrosion resistance [224, 225]. For a low-cost option, carbon has been studied as a potential coating, but it also corrodes under anodic conditions as described in the previous section so that an optimized configuration in combination with Ti is being investigated [226]. Figure 10 a) shows an example of the dissolution of Pt from a Ti-PTL, as measured by XRF mapping. As marked in Figure 10 a), two different areas in contact with the PTL can be identified: the active area and the edge. The green color indicates the amount of Pt present in this area. At the edge, the intensity is higher than in the active area, which means Pt was lost during operation. Some of the Pt from the PTL accumulates in the anode catalyst layer, which can be seen in the SEM-EDX of a similar sample in Figure 10 b).

To test PTL chemical degradation processes and effects ex-situ, a three-electrode method can be used to simulate an artificial PEMWE anode environment. The PTL sample is submerged into an electrolyte and used as the working electrode to perform linear voltammetry scans.

3.4.2. Mechanical Degradation

A high compression pressure in the cell is necessary to prevent leakages and ensure low interfacial contact resistance. Just as the GDL, the PTL can experience mechanical degradation due to this pressure. It is generally less compressible and less prone to breakage than the GDL, but chemical degradation can increase the likelihood of mechanical degradation. Studies have been carried out to determine the ideal thickness, porosity, pore diameter and particle size for optimum mechanical stability, electron conduction, as well as water transport into the cell and product gas transport out of the cell [214, 216, 227–230].

Mechanical damage to the PTL can be observed with SEM [203, 230–232], light microscopy [203] or X-ray CT [232], as well as thermal conductivity or gas permeability tests under compression [201, 202, 233]. Eddy current testing can be used to detect quality defects in the PTL, which could potentially contribute to mechanical degradation. In Figure 10 f), a pattern is visible in the sheet resistance, which stems from welding processes during production.

As with the GDL, ex situ tests to check for changes in mechanical properties due to degradation of PTLs are commonly done using tensile, compression or pressure drop tests.

3.5. Bipolar Plates

Bipolar plates are multifunctional components in PEMWE stacks that connect individual cells in series. They separate molecular hydrogen and molecular oxygen within the stack, facilitate mass transport of reactants and products and ensure heat transfer and electrical conduction. In addition, BPPs provide the structural stability of electrolyzer systems. Around 50% of the cost of a PEMWE stack is attributed to the BPP [234, 235]. This is due to the fact that the challenging conditions in the PEMWE cell (in particular the high anodic potential of 1.6-2.0 V and low pH of 2-4 [236]) result in the use of expensive materials like titanium, coated stainless steel or graphite [2, 237]. Additionally, they have very particular geometric requirements, causing high manufacturing costs [237].

Titanium is considered the state-of-the-art material due to its excellent chemical and mechanical stability [238–240]. However, stainless steel offers a potential lower cost alternative with advantages such as easier machinability and higher resistance to hydrogen embrittlement [239, 241]. Despite these advantages, stainless steel is prone to high rates of corrosion and oxidation in the harsh conditions of PEMWE [148]. The dissolution of metal cations such as Fe^{2+} and Ni^{2+} can subsequently lead to poisoning of the membrane (see 3.1.3) and catalyst (see 3.2.8), compromising system performance and stability [195, 242]. Graphite is often used as a material for the BPP in PEMFC, because it also has very high electrical conductivity. However, its brittleness makes it difficult to manufacture and therefore

expensive [243, 244]. Additionally, its low mechanical stability and a high corrosion rate under the anode conditions in PEMWE make it unsuitable for PEMWE [240, 245].

In order to improve chemical stability, coatings are often applied to the BPP. Ti-BPPs are usually coated with expensive Pt but research has been done to find cost-efficient alternatives such as nitrides [246, 247], but also Au [245, 248], Ag [236, 249] or mixed metal oxides [250] for both Ti and stainless steel BPPs.

BPPs are generally very sturdy. Due to this, the subject of mechanical degradation of BPPs is rarely found in the literature. However, as described in 3.5.2, the mechanical stability can be impaired due to increasingly thinner BPPs being produced, as well as during operation, e.g. by corrosion. In addition, quality defects during production can lead to cracks or defects in the component. A possible way to evaluate these quality defects is via eddy-current-testing.

3.5.1. Passivation

In a PEMWE cell, the combination of high potential, humidity and an oxidizing environment causes the oxidation of titanium [2, 251]. This oxidation effect occurs especially on the anode side [252] and causes the naturally occurring layer of titanium dioxide (TiO_2) on the surface to thicken, which exhibits a low electrical conductivity [248, 250]. As a result, the interfacial contact resistance between the BPP and the porous transport layer increases, leading to a decrease in the overall efficiency of the cell [245, 251] because of a rising electrical power consumption, especially under high current densities [245]. At the same time, the passivation layer acts as a protection barrier against hydrogen embrittlement.

Coatings made of resistant material can help to mitigate passivation, usually noble metals like Au and Pt [241, 253, 254]. Investigated for their use in PEMFC, nitride coatings have been of interest because of their lower cost and low incidence of pin-hole defects [249, 255]. Niobium (Nb) coatings exhibit superior corrosion protection, stable behavior in acid environments and the material is abundantly available [222, 256].

Passivation in the BPP and PTL can be detected and analyzed with XRD [241, 249, 257–259], XPS [41, 56, 241, 257, 258, 260], TEM [81, 220, 241, 249, 258, 259, 261, 262] or via measurement of through-plane direct current (DC) resistance [76, 183, 184, 191, 220, 249], ICR (interfacial contact resistance) [241, 249, 262, 263], AFM [259, 261] and using a BePPel to test for contact resistance [264]. In Figure 10 f) and e), resistance measurements and TEM were used to analyse passivation of a Ti-PTL.

Similarly to the PTL, ex situ testing for passivation can be done in an artificially simulated PEMWE anode environment, using a three-electrode method by submerging BPP samples into an electrolyte (e.g. O_2 saturated H_2SO_4) to perform linear voltammetry scans.

3.5.2. Corrosion

Ti corrosion typically occurs at much lower potentials than those present in PEMWE [252]. However, in the presence of fluoride ions F^-, which may originate from the deterioration of the membrane, Ti can undergo corrosion [11, 265–267], especially on the anode side. These F^- ions attack the titanium dioxide (TiO_2) layer, leading to the formation of titanium-fluoride (Ti-F^-) compounds [265], as described by the following equation:

$$TiO_2 + 4H^+_{aq} + 6F^-_{aq} \rightarrow TiF^{2-}_6 + 2H_2O \qquad 3$$

Additionally, operation at higher temperature (≥80 °C) reduces the enthalpy of the reaction which leads to a lowered potential for the corrosion reaction, while the passivation layer simultaneously gets thicker, providing a certain degree of corrosion protection [11].

Stainless steel BPPs (e.g. SS304, SS316L, SS321 or SS904L) are not as corrosion resistant as Ti-BPPs, especially under anode PEMWE conditions [2, 237, 251, 255]. During long term operation, corrosion can cause cations such as Fe^{3+} and Ni^{2+} to enter the cell and poison catalyst and the membrane by taking over the ion exchange sites [251, 268–271]. Additionally, the corrosion of the BPP leads to an increase of the interfacial contact resistance [240, 272].

Coatings investigated for Ti include combinations of Pt [241, 251, 273], Ag [236, 249], nitride [246, 249, 255, 274], Zr [255, 274], Nb [222] and mixed metal oxides (MMO) [250]. Tested coatings for stainless steel are e.g. Pt [241, 251], Ti [148, 241, 248, 256, 262, 263, 275], Nb [222, 256, 262, 276], nitride [263, 274], Zr [274], Au [244] or a combination of those elements.

Corrosion of the BPP and PTL can be measured via SEM(-EDX) [241, 250, 256, 261, 263, 276], AFM [222, 241, 256, 261, 276], XRD [241] and XPS [241, 256, 261, 276]. To check for released ions, the feed water or degradation testing solution can be investigated with ICP-OES [263] or ICP-MS [43, 242, 277, 278]. Analogous to passivation of BPP, ex situ tests for corrosion can be carried out using electrochemical measurements.

3.5.3. Hydrogen Embrittlement

Just as in the PTL, the titanium BPP is prone to embrittlement in the presence of hydrogen, especially at elevated temperatures (>80 °C) [2, 252, 279]. When the produced hydrogen on the cathode side exceeds the solubility limit in Ti, it is absorbed into the material, especially under high pressure. It is either absorbed as atomic hydrogen, recombining into molecular hydrogen in the Ti metal lattice, building pressure until the metal cracks [280], or it can form hydrides (TiH_x) at grain boundaries [238, 246, 280, 281]. This leads to material embrittlement which can result in mechanical failure of the BPP (e.g. cracking) [282] (see Figure 11). Over the course of 500 h of operation, a Ti-BPP has been found to absorb >1000 ppm hydrogen [280]. At temperatures <80 °C, embrittlement is slow due to the formation of a protective passivation layer (TiO_2) on the titanium component [2, 282]. Unfortunately, this layer is attacked by fluoride ions F^-, which can result from membrane degradation during long-term operation. A layer of resistant carbon coating on Ti has been found to have a positive effect on the hydrogen uptake level while also being low-cost and a good electrical conductor [280].

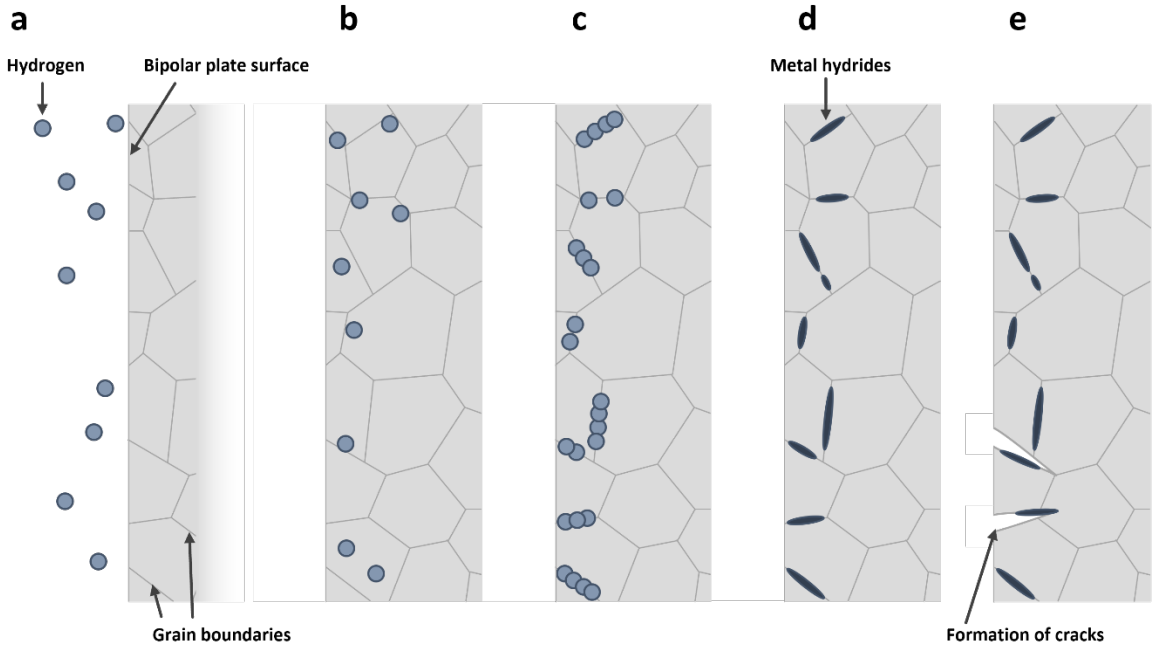


Figure 11: Hydrogen Diffusion into BPP material. Hydrogen rich environment at BPP surface (a) leads to hydrogen being absorbed into BPP (b), forming hydrides (TiH_2) at grain boundaries (c + d). Possible cracking of the metal (e). Recreated from [283]

To analyse hydrogen embrittlement, the hydrogen uptake in the BPP and PTL can be determined by weighing the component before and after operation [246, 262]. Hydrogen concentration can also be measured via gas chromatography [279, 284] or hot vacuum extraction coupled with mass spectroscopy [280] while SEM has been used to check for the formation of hydrides by the changed contrast [262, 279]. To test a material for its susceptibility to hydrogen embrittlement in ex-situ, samples can be exposed to a hydrogen atmosphere under increased pressure and temperature.

3.6. Gaskets

The gaskets in an electrolyzer seal the PEMWE cell, preventing the escape and crossover of educts and products (water, oxygen, hydrogen), which maintains efficiency and safety [285, 286]. They also have to tolerate high temperatures and temperature fluctuations, ensuring that the stack size remains consistent and compensating for other components' tolerances. Additionally, they maintain optimal contact between cell components and reduce ohmic losses [287, 288]. Few studies focus on gasket materials for PEMWE [287], though many exist for FC [100–102, 285, 286, 288–290]. Since similar materials are used for both, the requirements are comparable. Suitable gaskets must have long-term acid stability, durability, mechanical and thermal stability, excellent aging characteristics and cost-effectiveness. Typical materials are PTFE [287, 291], Fluorine Kautschuk Material (FKM) [99, 287, 288], Ethylene Propylene Diene Monomer Rubber (EPDM) [99, 287, 288], silicone [99–102, 285, 289, 290, 292] or nitrile rubber [287, 288].

3.6.1. Chemical Degradation

In PEMWE, sealings undergo chemical degradation due to stressors like the presence of hydrogen and oxygen, as well as acidic environments, with lower pH on the anode side. Gasket failure can lead to gas leakage or crossover, causing cell failure [11]. Electrical short-circuits can occur if components are not properly insulated and gasket material can release ions (e.g. Si, Ca, Zn^{2+}) and negatively impact the membrane or catalyst layer [11, 293].

Analysis of gasket material degradation can be done via FT-IR [99–102, 288–290], XPS [101, 289] to study the surface chemistry, EDX [285], atomic absorption spectrometry (AAS) [99–102, 290], Gas

Chromatography Mass Spectroscopy (GC-MS) [288, 292], ICP-MS [292] and Thermogravimetric Analysis (TGA) [292].

3.6.2. Mechanical Degradation

The gaskets in PEMWE also face mechanical stress from pressure (e.g. clamping), high temperatures (50-80 °C) as well as high humidity and wet conditions during operation [101, 287].

For mechanical evaluation, micro-indentation [100, 101, 289, 290] and tensile tests can be done (see Figure 12 b), as well as light microscopy [99–101, 290, 292] and SEM [102, 285, 292] to analyse mechanical degradation processes. Permeation tests are used to evaluate how leak-proof the sealing materials are (see Figure 12 c)).

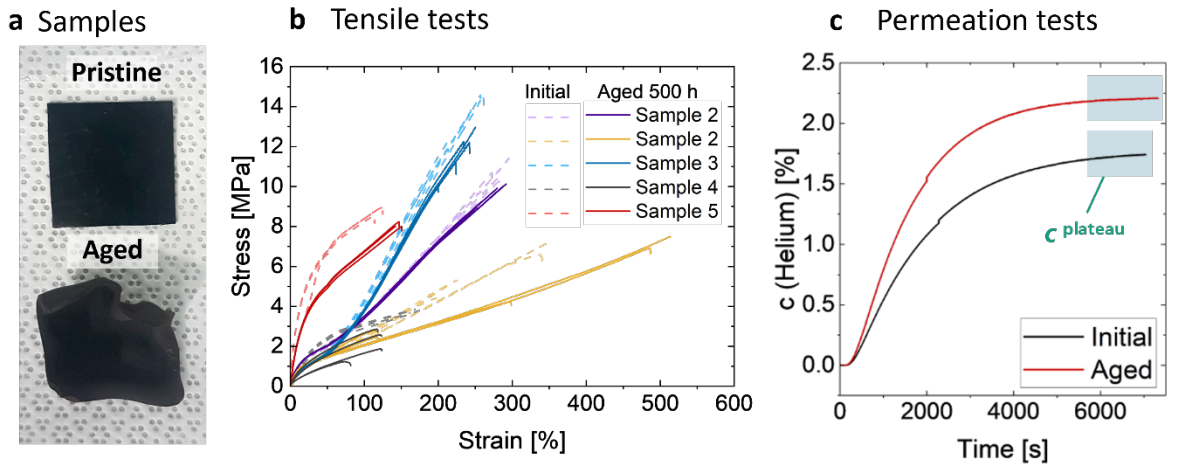


Figure 12: (a) Appearance and shape of samples before and after 500 h aging in O_2 saturated acid, (b)Testing compilation of the tensile test results for five different materials before and after aging for 500 h, (c) Example of He permeation results for gasket material before and after aging, illustrating a decrease in permeability after stress

4. Importance of Different Mechanisms: A Survey

4.1. Design and Evaluation

A survey was created and circulated among experts from industry and academia from April to October 2024 to gain an impression of the relevance of the degradation mechanisms considered in the literature and research. The anonymized data included some biographical information of the respondents in order to be able to assess their level of experience and position in the electrolyzer environment. In a free text field, respondents could first indicate what they considered to be the three worst degradation mechanisms, whereby a diagram of a PEM water electrolyzer with labelled components was shown. To avoid bias, no degradation mechanisms were named yet. The components were then ranked according to how strongly the respective component is affected by degradation. For the component ranked in first place (i.e. the one with the worst degradation), the degradation mechanisms specified had to be assessed and given a score of 1 to 5 (1=slight, 5=severe). All other components could be rated optionally. During these rankings descriptions for the degradation mechanisms as given in Table SI 1 were available. The frequency and severity of occurrence were assessed separately. Mechanisms of additional components could then be rated optionally. A total of 49 fully analyzable data sets resulted from this survey, although the number of responses for each component may vary as some of the questions were answered on an optional basis and could therefore be skipped. It should also be noted that the degradation of gaskets and the carbon support on the cathode side were not yet included in the mechanisms listed in the survey and that instead of hygrothermal membrane degradation only thermal degradation was listed. This is due to the fact that gasket materials are still rarely included in

PEMWE component degradation analysis. The same applies to the carbon support. The term hygrothermal was discussed as more fitting than thermal after the execution of the survey.

The evaluation of the anonymized biographical data revealed that 29% of the respondents came from industry, 30% from universities and 41% from non-university research institutions. Most of them had intermediate experience (1-5 years) in working with PEM water electrolyzers. When asked which components they dealt with most frequently, the answers varied between maximum 53% who worked on topics related to the anode catalyst and minimum 25% working on topics related to the GDL.

In the initial free text answer about the three worst degradation mechanisms, both membrane thinning and anode catalyst dissolution were mentioned the most (17 times), while four mechanisms were not mentioned at all (GDL Mechanical Degradation, PTL Hydrogen Embrittlement, Bipolar Plate Hydrogen Embrittlement and Membrane Thermal Degradation). Overall, the free text answers correspond well with the findings from the rankings later in the survey.

4.2. Susceptibility Ranking of Components

A ranking was conducted in order to determine the susceptibility of the components to degradation, with six components resulting in six distinct ranking positions. A score was then assigned to each position, ranging from 1 (lowest ranking) to 6 (highest ranking). The rankings given by the respondents were added up accordingly and divided by the number of analyzable data sets (49). This resulted in the anode catalyst layer being rated as the most susceptible component (4.8), closely followed by the membrane (4.7) (see Figure 13). The bipolar plates were ranked lowest, with a ranking of only 2.1 and thus appearing to be the least susceptible to degradation.

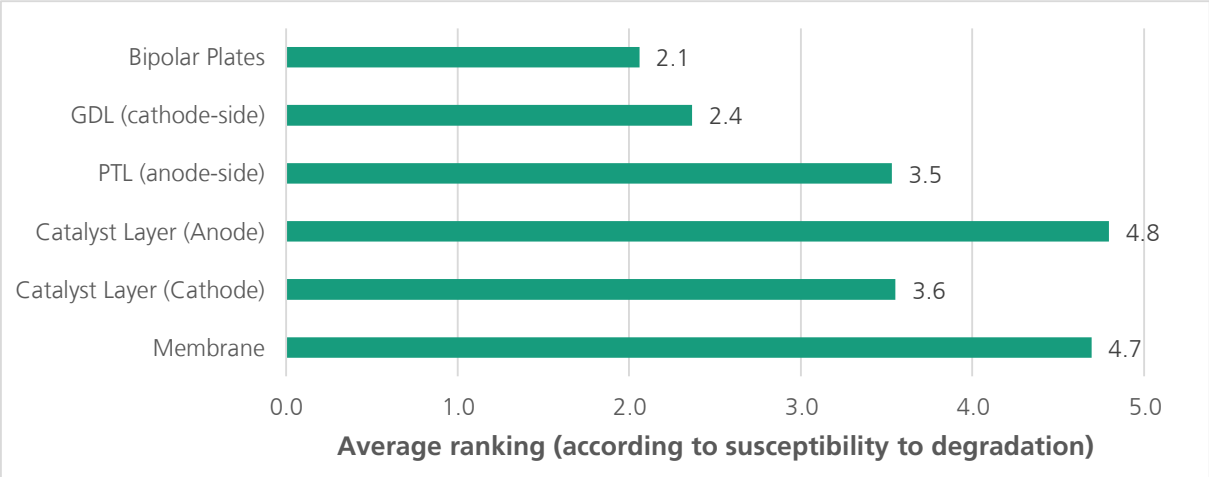


Figure 13: Ranking of components according to their susceptibility to degradation.

It should be noted that the two highest rated components (anode catalyst layer and membrane) were also the ones that the majority of respondents deal the most within their work. This may have influenced the evaluation of the components.

4.3. Ranking of Degradation Mechanisms

To assess the score, the average of all ratings given for each degradation mechanism was calculated. The higher the value, the higher the severity or occurrence of this mechanism. The number of responses from which the values were calculated varies between 20 and 52. This is because the ranking of the other components was optional after the evaluation of the component in first place and was therefore not fully carried out by every participant.

In terms of frequency, the passivation of the PTL was rated by far the highest on average (4.17) (see Figure 14). No other degradation mechanism achieved an average of 4 or higher. Nevertheless, the top 3 also include anode catalyst dissolution (3.90) and membrane thinning by radical attack (3.81). These two mechanisms are also the ones most frequently mentioned in the free text answers. Hydrogen embrittlement in the PTL was found to be the least frequent to occur (2.35).

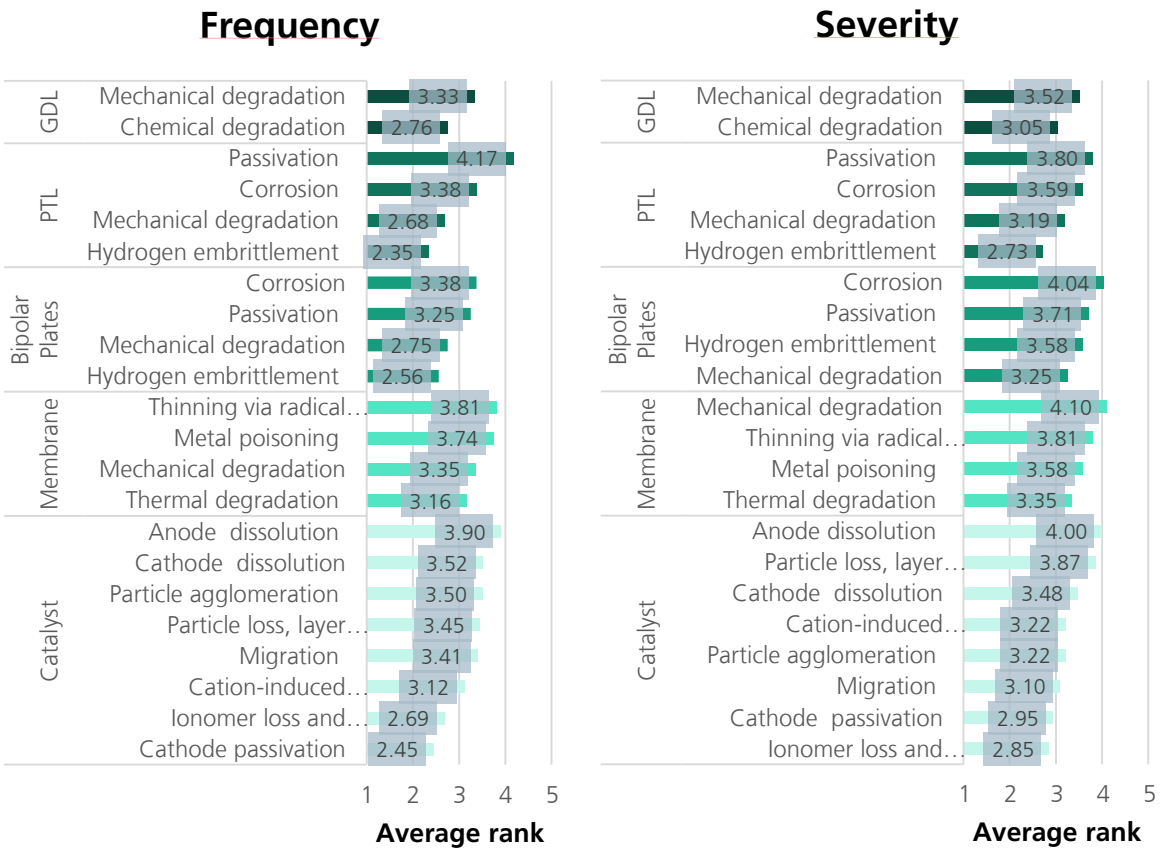
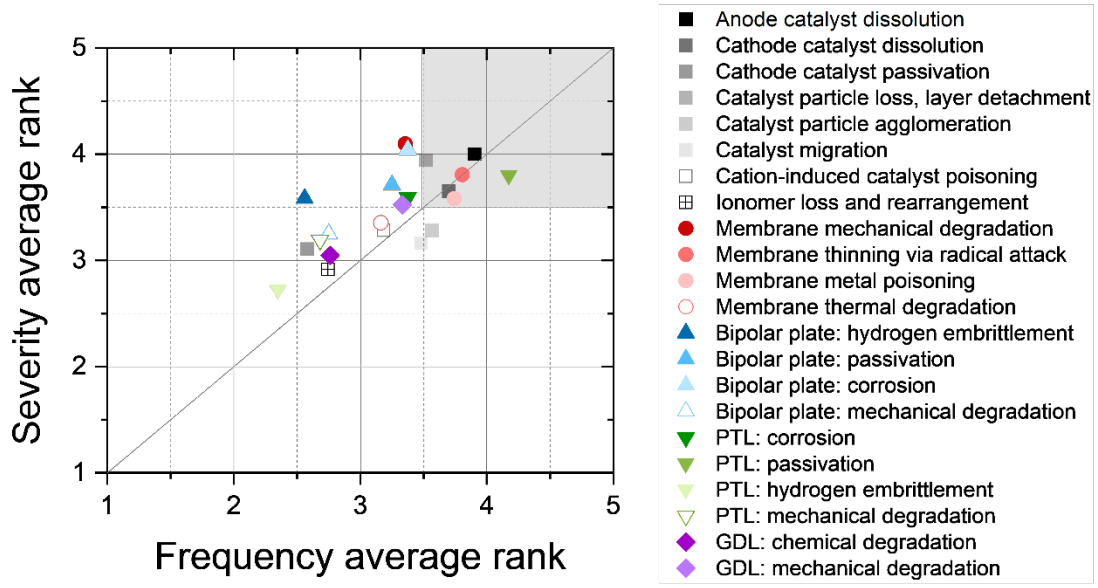


Figure 14: Average rank of degradation mechanisms according to their frequency (left) and severity (right).

The ratings for severity were closer to each other (see Figure 14). Membrane mechanical degradation (4.10), anode catalyst dissolution (4.00) and corrosion of the bipolar plates (4.04) were rated highest. The mechanical degradation of the membrane also includes the formation of pinholes, which in the worst case can lead to the total failure of a cell, just like corrosion of the bipolar plates, which is essential for the stability and cohesion of the cell. Anode catalyst dissolution, on the other hand, tends to lead to a severe decline in cell performance. Hydrogen embrittlement in the PTL, which was also the mechanism ranked as least frequent, was ranked as the least severe (2.73).

The product of both was calculated to form a joint ranking in order to consider the combined evaluation of severity and frequency. The top three degradation mechanisms are PTL passivation, anode catalyst dissolution and membrane thinning (see Figure 15), which corresponds to the same three degradation mechanisms as in the frequency assessment. This leads to the conclusion that the more severe degradation mechanisms are so rare that problems are more likely to be caused by the more frequent degradation mechanisms. In addition, the ratings were plotted against each other as a scatterplot (see Figure 15). The closer the data points are to the diagonal line, the more similar the assessment of severity and frequency. Membrane thinning (Frequency and Severity both 3.81) and cathode catalyst dissolution (3.70 vs. 3.65) are particularly noticeable here, where the scores were the same or very similar.

Overall, all points are arranged approximately along the diagonal, which means that the frequency and severity of most degradation mechanisms were assessed as very similar. However, a slight tilt towards severity can be recognized, which indicates that the mechanisms are attributed a greater influence rather than a high level of occurrence. The hydrogen embrittlement of the bipolar plates is particularly notable here, as it was rated as occurring less frequently (frequency 2.56), but with an all the stronger effect (severity 3.58). Additional note is made of mechanisms for which both frequency and severity ratings are > 3.5 by marking the quadrant in a darker shading. It indicates that research into these mechanisms is of the highest importance. The identified mechanisms are: Anode catalyst dissolution, cathode catalyst dissolution, catalyst particle loss, membrane thinning, membrane metal poisoning and PTL passivation.



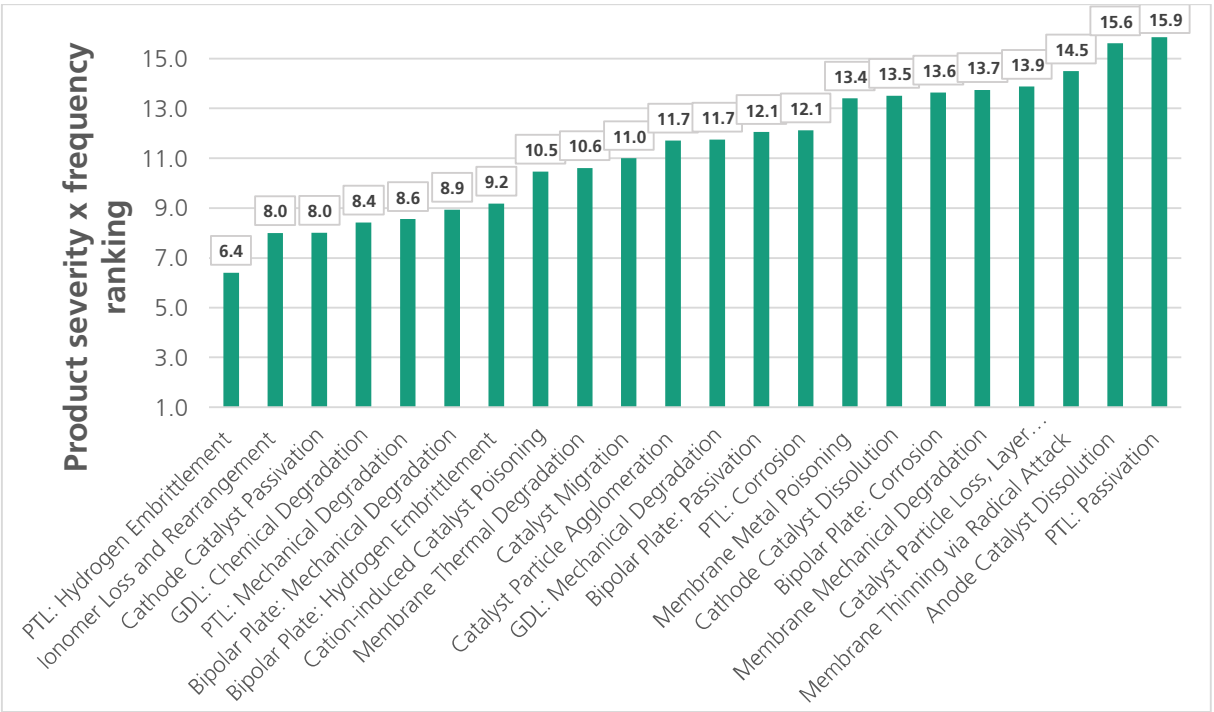


Figure 15: Top: Scatterplot of the average rank of frequency vs. severity with highlighted area for both rankings >3.5 and bottom: product of average rank of severity and frequency for each degradation mechanism.

5. Diagnosis and Measurement of Degradation

In chapter 3 Degradation Processes, the measurement methods that are used to diagnose degradation effects are listed where applicable. Electrochemical methods are generally not considered. A detailed analysis of these can be found in other reviews, e.g. by Wallnöfer-Ogris et al. [11]. They are useful for quantification of overall performance degradation and identifying underlying electrochemical reasons. However, aside from performance tests where parameters are purposefully changed (e.g. contaminations in the feed water), they are often not suited for identifying a concrete degradation mechanism. For this reason, the focus within this review is on measurements that give insight into degradation effects and microstructure by other means. The primary consideration is on post-mortem investigations, meaning after cell tests are finished. As degradation mechanisms are often not directly observable, the inference from their effects is necessary. In Table 2, the previously discussed mechanisms are connected to the observation they cause. It should be noted that many effects result from multiple degradation mechanisms, e.g. a loss of active surface can be caused by both anode and cathode catalyst dissolution as well as catalyst passivation and catalyst particle agglomeration. While the observation can be narrowed done, e.g. to a specific surface or element, a combination of measurement methods is usually necessary to identify the root cause of degradation. In the following paragraphs, different classes of techniques are discussed that can directly or indirectly measure the observed effects. In the supplemental information, Table SI 2 and Table SI 3 show additional characteristics and a full evaluation of which method can demonstrate which degradation mechanism has occurred. Table SI 3 also identifies what has been already described in literature, what has not been used previously but is theoretically possible and which methods are especially well suited to identify a degradation mechanism.

Table 2: Overview of degradation mechanisms and the observation they may cause.

	Ions in water or cell	**Loss of mass or thickness**	**CO_2 release**	**Change of carbon species**	**Loss of active surface**	**Increased contact resistance**	**Delamination**	**Increased particle/crystallite size**	**Lowered IEC**	**Physical blockage**	**Loss of ionomer**	**Lowered mechanical stability**	**Phase separation**	**Cracks and holes**	**Buckling and folding**	**H2/Hydride content**	**Increased permeability**	**Composition change**
Anode cat. dissolution	X	X			X													
Cathode cat. dissolution	X	X			X													
Carbon support dissolution			X	X														
Cathode cat. passivation					X	X												
Catalyst particle loss and layer detachment		X					X					X						
Catalyst particle agglomeration					X			X										
Catalyst migration									X	X								
Catalyst cationic poisoning									X	X								
Ionomer loss and rearrangement											X		X					
Membrane mechanical degradation														X	X			

Membrane thinning via radical attack	X	X							X			X						
Membrane metal poisoning									X	X								
Membrane (hygro-) thermal degradation									X			X						
PTL passivation						X												
PTL hydrogen embrittlement												X				X		
PTL corrosion	X					X						X						
GDL dissolution		X	X	X														
GDL mechanical degradation		X												X				
PTL mechanical degradation		X												X				
BPP hydrogen embrittlement												X				X		
BPP passivation						X												
BPP corrosion																		
BPP mechanical degradation		X												X				
Gasket mechanical degradation												X		X			X	
Gasket chemical degradation	X																X	X

The methods discussed here can be roughly differentiated by measurement principle into electrical, microscopy and tomography, scattering and diffraction, spectroscopy, thermal, mechanical and other or miscellaneous methods.

Electrical methods such as conductivity measurements or eddy current testing are useful for the identification of increased resistances in components. As such they are used to indicate passivation layers on both PTLs and BPPs. While they are not discussed in literature regarding the catalyst layers and membrane, they have potential for identifying loss of catalyst and membrane mass from the change in conductivity. This application needs to be additionally supported by other methods to identify the exact mechanism. Nevertheless, electrical methods have the advantage that the effect influencing the electrical properties of the cell, i.e. increased resistance, is measured directly.

Microscopy methods are well suited to analyse changes in thickness and morphology of components. Thus, mechanical damage and pronounced loss of material can be identified. In addition, the combination of electron microscopy with analytical methods such as EDX and EELS enables determining elemental distributions and contaminations.

Scattering and Diffraction methods are sensitive to distances between features. Depending on the energy of the beam, these distances are on the macro- or microscale or inter-particle and inter-atomic distances at higher energies. Thus, they are well-suited to analyse agglomeration distribution of material and surface roughness across length scales.

Spectroscopy methods are used to analyse chemical compositions and binding states. Due to this, they can elucidate details of how mechanisms proceed and how the chemical environment left behind changes. This can be especially useful for the membrane, which is not accessible for a lot of other methods. In addition, spectroscopic methods are suited for non-destructive and in-operando analysis.

Thermal methods analyse physical and chemical changes with temperature. They are well suited to evaluate components where thermal conductivity is important, i.e. the current collectors. Additionally,

thermal decomposition ex-situ can be used to investigate operating temperature ranges or analyse remaining material mass (such as remaining catalyst after membrane vaporization).

Mechanical methods, as the name suggests, are most useful to probe the susceptibility to mechanical degradation ex-situ. This is especially important for the bipolar plates.

Under miscellaneous methods we group all methods that cannot fit into previous categories. These include various gas crossover analyses, but also those using magnetic fields or different forms of mass measurement. As such, no encompassing conclusions can be drawn in this category.

Overall, it is evident from Table SI 3 that there is a large spread between methods that are used in literature for just one or two degradation mechanisms, e.g. gas crossover test or NMR, and those that are extremely versatile, e.g. SEM and XPS. Some methods, e.g. Magnetic Field Imaging (MFI) or light scattering, have to the best of our knowledge not been used extensively in literature. Still, we evaluate that these have potential to diagnose 12 and 11 different degradation mechanisms, respectively. Other methods that are similarly underutilized are Eddy current testing, thermography and to a lesser extent conductivity measurements, CT and a variety of mechanical testing methods. These could add valuable information to existing diagnosis methods, aid in differentiation and corroboration of mechanisms and allow for greater ease of defect detection. Their novel application has the potential to improve understanding of degradation and its effect on the electrolyzer and warrants further application and development. On the other hand, mechanisms that are already extensively investigated by a variety of methods do not necessarily need additional methods for evaluation. The respective state-of-the-art diagnostic processes for e.g. anode and cathode catalyst layer dissolution already enable an extensive analysis of the degradation mechanisms.

Figure SI 1 shows the number of possible methods that can be used to measure degradation mechanisms that are mentioned in literature and those which are not published but could theoretically be used. Overall, cathode catalyst passivation and membrane hygrothermal degradation are the mechanisms analyzed with the least methods in literature. This could be due to lower interest into their investigation because of perceived low relevance, which is indicated by the survey. For these two mechanisms we also found a comparatively low number of methods that are theoretically suited to analyse them. GDL dissolution, catalyst particle agglomeration and carbon support dissolution also have a low number of techniques associated with them and are not generally discussed as mechanisms of high interest in PEMWE degradation. Anode and cathode catalyst dissolution show the highest numbers of possible analysis methods at 22 and 21 respectively. This reflects the great amount of research into catalyst engineering. Nevertheless, it is also possible that these degradation effects are investigated with a wide array of techniques not because of their importance but instead are so well studied because they are evident with a multitude of postmortem investigation methods and especially with investigation methods that are common within research groups (e.g. SEM). Discussion on less common mechanisms could be increased if their analysis was more accessible. In addition, some degradation mechanisms that are ranked in the higher half of Figure 15 do not have such a high variety of different methods associated with them. For example, membrane metal poisoning, as well as BPP and PTL corrosion were investigated with a below average number of techniques in literature, despite many more being theoretically available. Therefore, methods that are not in use but show potential for the defect analysis of relevant mechanism should be further developed. In addition, method development is also important for the ability to employ a combination of measurements ensuring adequate differentiation between mechanisms.

6. Discussion

Key Results

Overall, literature research and survey results agree that membrane degradation by the attack of radicals and anode catalyst dissolution are impactful degradation mechanisms. PTL passivation is ranked highly in the survey but not discussed as extensively in literature. A reason for this is that passivation is a gradual process that lowers performance over time through decrease in electrical contact. It is therefore expected to garner interest with longer electrolyzer operation times. Another mechanism with a high survey ranking in both severity and frequency as well as reflective broad discussion in literature is membrane poisoning by metals. BPP Corrosion is ranked as severe but not as frequent, which lowers its research prioritization. Membrane mechanical degradation is also low in the frequency rating. Nevertheless, its very high severity accounts for the research focus on the detection and mitigation of mechanical faults, since pinholes and cracks can lead to a whole stack shut down. It also tends to appear suddenly, while most other degradation phenomena build up over time. On the other hand, cathode catalyst dissolution and particle loss have high combined ratings in our survey but are less discussed mechanisms in literature. The dissolution of Pt/C (in electrolysis only present at the cathode) has gained less attention than the anode-side dissolution. This discrepancy is sensible since the anode does present obvious problems in PEMWE conditions. Most considerations for cathode-side catalyst degradation are instead transferred from mechanisms in PEMFC. Nevertheless, Pt dissolution at the cathode should not be assumed to be negligible. The differentiation between catalyst particle loss and dissolution is a great challenge that must be considered for effective mitigation. The chemical state of both catalysts in effluent water and of remaining catalyst in the layers can give some indication as to which mechanisms are present. Such investigations have not been widely carried out yet.

While sorting the PEMWE degradation mechanisms by originating component is a systematic approach, it does not show the whole picture. Several degradation mechanisms, i.e. catalyst migration, can have far-reaching effects in multiple parts of the cell. A broad overview on which degradation mechanisms can trigger each other is given in Table 3. In general, the chemical degradation of membrane, catalysts and PTL, meaning dissolution of material or changes in surfaces or functional groups, can affect other components. It can deteriorate the mechanical properties of the component itself, the contact between components and lead to accumulation of degradation products elsewhere. For example, the corrosion of the PTL will also allow for further mechanical degradation of the PTL and the layer detachment of the catalyst from the PTL. In addition, the process is self-worsening, exposing titanium, which in turn allows for easier corrosion and passivation. Generally, degradation-induced occurrence of further defects is due to the following reasons: the movement of degradation products; the effect on mechanical integrity; the effect on component interfaces; and the exposure of further degradation sites.

Table 3: Degradation mechanisms which can negatively affect each other.

First Mechanism → ***Following Mechanism*** ↓	**Membrane thinning by radicals**	**Membrane mechanical**	**Membrane metal poisoning**	**Hygrothermal membrane degradation**	**Anode catalyst dissolution**	**Cathode catalyst dissolution**	**Cathode catalyst passivation**	**Cathode carbon dissolution**	**Catalyst particle loss/layer detachment**	**Catalyst NP agglomeration**	**Catalyst migration**	**Catalyst cationic poisoning**	**Ionomer rearrangement**	**GDL dissolution**	**GDL mechanical degradation**	**PTL corrosion**	**PTL passivation**	**PTL embrittlement**	**PTL mechanical degradation**	**BPP embrittlement**	**BPP passivation**	**BPP corrosion**	**BPP mechanical degradation**	**Gasket mechanical degradation**	**Gasket chemical degradation**
Membrane thinning by radicals	X		X																			X			
Membrane mechanical	X	X		X																					
Membrane metal poisoning					X	X					X					X						X			
Hygrothermal membrane degradation																									
Anode catalyst dissolution					X				X																
Cathode catalyst dissolution						X			X																
Cathode catalyst passivation																									
Cathode carbon dissolution								X	X																
Catalyst particle loss/layer detachment	X	X		X	X	X		X	X					X	X	X	X		X						
Catalyst NP agglomeration								X																	
Catalyst migration					X	X																			
Catalyst cationic poisoning																X						X			
Ionomer rearrangement																									
GDL dissolution														X	X										
GDL mechanical degradation														X	X										
PTL corrosion	X															X									
PTL passivation																									
PTL embrittlement																X									
PTL mechanical degradation																X		X	X						
BPP embrittlement																									
BPP passivation																									
BPP corrosion	X																					X			
BPP mechanical degradation																				X			X		
Gasket mechanical degradation																								X	X
Gasket chemical degradation																									

It is important to elucidate further on the research overlaps between PEMWE and PEMFC degradation, which has been reviewed in several papers [268, 294–297]. A lot of the degradation mechanisms, e.g. the attack of the membrane by radicals, work by the same fundamental principles. Exceptions to this are the anode side catalyst dissolution and PTL mechanisms, since fuel cells do not use Ir and Ti as state-of-the-art materials due to differing operating conditions. PEMFC also faces additional degradation pathways. Among these are thermal degradation of the membrane (since runaway thermal accumulation is a higher risk), the poisoning of the catalyst by contaminant gases in the incoming gas streams and hydrophobisation of the GDL. In addition, mechanisms like the cathode catalyst dissolution and passivation as well as carbon support dissolution can be more severe in fuel cells. This is due to the use of carbon in both electrodes and thus harsher conditions at the cathode side. Both mechanical and hygrothermal membrane degradation would be expected to be stronger in fuel cells, due to higher fluctuations in water content and temperature. On the other hand, we would expect mechanisms that rely on the presence of cations, such as poisoning, to be less pronounced in fuel cells. These are often introduced in PEMWE by the feed water. Nevertheless, the membrane can still be poisoned by catalyst ions in PEMFC. Bipolar plates show many of the same degradation mechanisms, but Ti is a less used material. The oxidative environment in PEMWE can have a more severe effect on the gaskets. The working pressure is also higher and the materials need to be more resistant to water compared to PEMFC. An overview of the comparison of mechanisms between PEMWE and PEMFC is given in Table SI 4. Overall, the consideration of PEMFC degradation mechanisms can support the analysis of PEMWE degradation. Still, a close look at the exact mechanisms is necessary to enable transfer between the two technologies.

Limitations

The survey among experts provided valuable insights complementing the literature research, as shown by the agreements and discrepancies identified in the previous sections. Nevertheless, research that considers all possible performance-decreasing degradation mechanisms and their respective interactions is not yet widespread, which could limit some of the survey participants' perspectives. Multimodal defect diagnostics are needed in order to close this gap. A quantitative connection between performance decrease and changes observed post-mortem should be included in these investigations. This will generate additional knowledge for the evaluation of severity of degradation mechanisms.

An additional limitation of PEMWE research is the focus on lab-scale measurements and improvements. Regarding size of stacks, contamination levels, as well as lengths and mode of testing, it is essential to scale up to industrially relevant testing conditions for the further development of the field. Unlike currently common test durations (~ 500 to 1000 h), longer operation times may lead to underexamined degradation phenomena becoming relevant after long tests runs and gaining new attention. Short operation times can result in limited observation of degradation mechanisms (e.g. membrane thinning) and general material fatigue as well as critical failure modes or even possibly performance recoveries. The same is true for changing the modes of testing to reflect the variable input electricity of renewable energy sources. Multiple investigations into the effect of a fluctuating input have been carried out in short-term laboratory experiments. However, lack of standardization does still hinder their comparability and a possible transfer to industrial operation. For this reason, further deployment of standardized accelerated stress tests that reflect flexible operation is needed. Nevertheless, stress tests cannot solve the problem of the limited size of stacks in a typical laboratory environment. With larger lateral size of cells, the defects caused by inhomogeneous distributions of water, temperature and pressure will gain additional importance. A higher number of cells in a stack comes with increased challenges to monitor-single cells and large-scale diagnostic methods that can identify regions of degradation are needed. Lastly, the effect of water impurities on the electrolyzer is

an important area, where practically feasible ion-specific limits are needed. In multi-MW-scale electrolyzer plants, the usage of stainless steel pipes is not always avoidable due to security reasons and protective coatings are very costly.

Future Research Directions

Overall, further research is needed, particularly on PTL passivation, cathode side dissolution and catalyst particle loss. For several degradation mechanisms, the overlap with fuel cell research can give new impulses, but the different environments and working conditions need to be carefully considered. As discussed here and in chapter Diagnosis and Measurement of Degradation, the differentiation of degradation mechanisms and their interactions can be challenging and often requires the combination of several microstructural diagnostic methods. An example for this is the migration of catalyst particles into other parts of the electrolyzer after dissolution. While there have been first forays into the localization of “missing” catalyst material, full quantification and assignment to specific mechanisms is still a relevant topic. In order to achieve better understanding, **a multi-modal characterization** beyond solely electrochemical data is necessary, extending to microstructure diagnostics and accurate cause-and-effect analysis.

Another challenge is that less studied degradation mechanisms (i.e. membrane metal poisoning) often have fewer diagnostic methods associated with them. This is a gap in research that should be closed by developing **new measurements procedures and methods** where necessary. This would allow for a more complete impact analysis of different degradation mechanisms and their intercorrelations. In addition, **advanced online-monitoring** needs to be one of the focal points in future research. This could also help in investigating and understanding lateral inhomogeneities, especially in large-scale stacks.

To achieve this, long-term (>1000 h) as well **large-scale** and **industry-informed testing** are necessary to gather realistic information and data. This includes the testing of materials and manufacturing processes that are used in industry, not just on lab-scale.

Lastly, degradation research for PEMWE needs to move towards **standardized tests**: Validated test protocols for accelerated stress testing that enable the reliable comparison of test data, ensuring consistent evaluation of performance parameters and degradation effects under varying operational conditions.

7. Conclusions

This review has given a general overview over PEMWE degradation mechanisms on the cell level, their relevance (frequency and severity) and provided a focus on which diagnostic measurements can be carried out to identify and differentiate them. For the evaluation of the impact of degradation mechanisms and remaining research gaps, a survey among experts was carried out. It is evident that degradation mechanisms such as anode catalyst dissolution and membrane thinning by radicals are considered as important among experts, which is why they are already well researched. Others such as PTL passivation, cathode side catalyst dissolution and catalyst particle loss or layer detachment require further research and may gain more importance in the future. We also emphasize that the interaction and differentiation between mechanisms is a challenge that needs to be addressed. An important point of interest for future degradation studies is the testing in conditions inspired by industrial-scale applications and for longer testing times. While some diagnostic methods for degradation analysis are well-utilized, others such as MFI or light scattering are not used to their potential. At the same time, some degradation mechanisms such as anode and cathode catalyst dissolution are supported by a wide range of diagnostic techniques. Others, i.e. membrane metal poisoning, BPP and PTL corrosion should be supported by the development of further diagnostic tools. In addition, the continued development

of diagnostic methods is of high importance in order to further the differentiation of degradation mechanisms and be able to work on mitigation strategies.

Acknowledgements

The authors gratefully acknowledge the financial support by the German Federal Ministry of Education and Research (BMBF) for the project StacIE (03HY103G) and Schaeffler Technologies AG & Co. KG for support within the project. Parts of experimental analyses have been conducted within projects H2Mare_H2Wind (03HY301D) and FRHY (03HY112E). We additionally acknowledge from Fraunhofer IMWS: Emily Preuschoff for support in creation of Figure 5 and Figure 9, as well as background research on PEMFC; Finn Ostermeyer for support in background research and creation of Figure 4; Anton Mordvinkin and Matthias Pander for carrying out permeation and tensile tests used for Figure 12; and Kathrin Reinhardt and Tobias Albrecht for sample preparation for measurements in Figure 3, Figure 7 and Figure 10.

Conflict of Interest

The authors declare no conflict of interest.

References

[1] International Renewable Energy Agency (IRENA), Ed., "World Energy Transitions Outlook 2024: 1.5°C pathway," 2024.

[2] Q. Feng *et al.,* "A review of proton exchange membrane water electrolysis on degradation mechanisms and mitigation strategies," *Journal of Power Sources*, vol. 366, pp. 33–55, 2017, doi: 10.1016/j.jpowsour.2017.09.006.

[3] F. N. Khatib *et al.,* "Material degradation of components in polymer electrolyte membrane (PEM) electrolytic cell and mitigation mechanisms: A review," *Renewable and Sustainable Energy Reviews*, vol. 111, pp. 1–14, 2019. doi: 10.1016/j.rser.2019.05.007. [Online]. Available: https://reader.elsevier.com/reader/sd/pii/S1364032119303132?token=19A74CB9B979A3E40C62CC22FC7D0515E058C980FF61215CDB50243DDBFF9DB2E580AE4570994EC8474CF241F6AAF149

[4] P. Shirvanian and F. van Berkel, "Novel components in Proton Exchange Membrane (PEM) Water Electrolyzers (PEMWE): Status, challenges and future needs. A mini review," *Electrochemistry Communications*, vol. 114, p. 106704, 2020, doi: 10.1016/j.elecom.2020.106704.

[5] H. Ito, T. Maeda, A. Nakano, and H. Takenaka, "Properties of Nafion membranes under PEM water electrolysis conditions," *International Journal of Hydrogen Energy*, vol. 36, no. 17, pp. 10527–10540, 2011, doi: 10.1016/j.ijhydene.2011.05.127.

[6] A. Kusoglu and A. Z. Weber, "New Insights into Perfluorinated Sulfonic-Acid Ionomers," *Chemical reviews*, early access. doi: 10.1021/acs.chemrev.6b00159.

[7] S. Cherevko, "Stability and dissolution of electrocatalysts: Building the bridge between model and “real world” systems," *Current Opinion in Electrochemistry*, vol. 8, pp. 118–125, 2018, doi: 10.1016/j.coelec.2018.03.034.

[8] C. van Pham, D. Escalera-López, K. Mayrhofer, S. Cherevko, and S. Thiele, "Essentials of High Performance Water Electrolyzers – From Catalyst Layer Materials to Electrode Engineering," *Adv. Energy Mater.*, vol. 11, no. 44, 2021, Art. no. 2101998, doi: 10.1002/aenm.202101998.

[9] K. Ayers, "High efficiency PEM water electrolysis: enabled by advanced catalysts, membranes, and processes," *Current Opinion in Chemical Engineering*, vol. 33, p. 100719, 2021, doi: 10.1016/j.coche.2021.100719.

[10] A. Z. Tomić, I. Pivac, and F. Barbir, "A review of testing procedures for proton exchange membrane electrolyzer degradation," *Journal of Power Sources*, vol. 557, p. 232569, 2023, doi: 10.1016/j.jpowsour.2022.232569.
[11] E. Wallnöfer-Ogris *et al.,* "A review on understanding and identifying degradation mechanisms in PEM water electrolysis cells: Insights for stack application, development, and research," *International Journal of Hydrogen Energy*, vol. 65, pp. 381–397, 2024, doi: 10.1016/j.ijhydene.2024.04.017.
[12] M. Batool, O. Sanumi, and J. Jankovic, "Application of artificial intelligence in the materials science, with a special focus on fuel cells and electrolyzers," *Energy and AI*, vol. 18, p. 100424, 2024, doi: 10.1016/j.egyai.2024.100424.
[13] K. T. Malkow, A. Pilenga, and D. Blagoeva, "EU harmonised terminology for hydrogen generated by electrolysis: JRC validated methods, reference methods and measurements report," Publications Office of the European Union, Luxembourg, 2020, doi: 10.2760/732809.
[14] E. E. Nzaba Madila, A. Makhsoos, M. M. Shanbhag, and B. G. Pollet, "Advancements in electrolyser stack performance: A comprehensive review of Latest technologies and efficiency strategies," *International Journal of Hydrogen Energy*, 2025, doi: 10.1016/j.ijhydene.2025.04.047.
[15] FCH 2 JU, Ed., "Hydrogen Roadmap Europe: A Sustainable Pathway for the European Energy Transition," 2019.
[16] United States Department of Energy (DOE), Ed., "U.S. National Clean Hydrogen Strategy and Roadmap," Jun. 2023.
[17] International Renewable Energy Agency (IRENA), "Green Hydrogen Cost Reduction: Scaling up Electrolysers to meet the 1.5°C Climate Goal," 2020.
[18] Clean Hydrogen Partnership, "Clean Hydrogen Joint UNdertaking: Strategic Research and Innovation Agenda 2021-2027," Feb. 2022. [Online]. Available: https://www.clean-hydrogen.europa.eu/about-us/key-documents/strategic-research-and-innovation-agenda_en
[19] Hydrogen and Fuel Cell Technologies Office. "Technical Targets for Proton Exchange Membrane Electrolysis." Accessed: May 12, 2025. [Online]. Available: https://www.energy.gov/eere/fuelcells/technical-targets-proton-exchange-membrane-electrolysis
[20] M. F. Ahmad Kamaroddin *et al.,* "Membrane-Based Electrolysis for Hydrogen Production: A Review," *Membranes*, early access. doi: 10.3390/membranes11110810.
[21] D. Aili *et al.,* "Phosphoric acid doped membranes based on Nafion®, PBI and their blends – Membrane preparation, characterization and steam electrolysis testing," *International Journal of Hydrogen Energy*, vol. 36, no. 12, pp. 6985–6993, 2011, doi: 10.1016/j.ijhydene.2011.03.058.
[22] A. G. Wright *et al.,* "Hexamethyl-p-terphenyl poly(benzimidazolium): a universal hydroxide-conducting polymer for energy conversion devices," *Energy Environ. Sci.*, vol. 9, no. 6, pp. 2130–2142, 2016, doi: 10.1039/C6EE00656F.
[23] A. Das, K. S. Im, M. M. Kabir, H. K. Shon, and S. Y. Nam, "Polybenzimidazole (PBI)-based membranes for fuel cell, water electrolysis and desalination," *Desalination*, vol. 579, p. 117500, 2024, doi: 10.1016/j.desal.2024.117500.
[24] R. Nolte, K. Ledjeff, M. Bauer, and R. Mülhaupt, "Partially sulfonated poly(arylene ether sulfone) - A versatile proton conducting membrane material for modern energy conversion technologies," *Journal of membrane science*, vol. 83, no. 2, pp. 211–220, 1993, doi: 10.1016/0376-7388(93)85268-2.
[25] G. Wei, L. Xu, C. Huang, and Y. Wang, "SPE water electrolysis with SPEEK/PES blend membrane," *International Journal of Hydrogen Energy*, vol. 35, no. 15, pp. 7778–7783, 2010, doi: 10.1016/j.ijhydene.2010.05.041.

[26] C. A. Linkous, H. R. Anderson, R. W. Kopitzke, and G. L. Nelson, "Development of new proton exchange membrane electrolytes for water electrolysis at higher temperatures," *International Journal of Hydrogen Energy*, vol. 23, no. 7, pp. 525–529, 1998.
[27] I.-Y. Jang, O.-H. Kweon, K.-E. Kim, G.-J. Hwang, S.-B. Moon, and A.-S. Kang, "Application of polysulfone (PSf)– and polyether ether ketone (PEEK)–tungstophosphoric acid (TPA) composite membranes for water electrolysis," *Journal of membrane science*, vol. 322, no. 1, pp. 154–161, 2008, doi: 10.1016/j.memsci.2008.05.028.
[28] C. I. Morfopoulou, A. K. Andreopoulou, M. K. Daletou, S. G. Neophytides, and J. K. Kallitsis, "Cross-linked high temperature polymer electrolytes through oxadiazole bond formation and their applications in HT PEMfuel cells," *J. Mater. Chem. A*, vol. 1, no. 5, pp. 1613–1622, 2013, doi: 10.1039/C2TA00610C.
[29] A. Abdolmaleki, M. Zhiani, M. Maleki, S. Borandeh, and K. Firouz, "Preparation and evaluation of sulfonated polyoxadiazole membrane containing phenol moiety for PEMFC application," *Polymer*, vol. 75, pp. 17–24, 2015, doi: 10.1016/j.polymer.2015.08.021.
[30] D. Gomes, J. Roeder, M. L. Ponce, and S. P. Nunes, "Single-step synthesis of sulfonated polyoxadiazoles and their use as proton conducting membranes," *Journal of Power Sources*, vol. 175, no. 1, pp. 49–59, 2008, doi: 10.1016/j.jpowsour.2007.09.090.
[31] A. Kumar and V. K. Ramani, "Ta Modified TiO 2 Supports Exhibit Exceptional Durability in Polymer Electrolyte Fuel Cells," *ECS Trans.*, vol. 58, no. 1, pp. 1823–1834, 2013, doi: 10.1149/05801.1823ecst.
[32] E. Kuhnert, V. Hacker, and M. Bodner, "A Review of Accelerated Stress Tests for Enhancing MEA Durability in PEM Water Electrolysis Cells," *International Journal of Energy Research*, vol. 2023, pp. 1–23, 2023, doi: 10.1155/2023/3183108.
[33] A. Laconti, H. Liu, C. Mittelsteadt, and R. McDonald, "Polymer Electrolyte Membrane Degradation Mechanisms in Fuel Cells - Findings Over the Past 30 Years and Comparison with Electrolyzers," *ECS Trans.*, vol. 1, no. 8, pp. 199–219, 2006, doi: 10.1149/1.2214554.
[34] S. Stucki, G. G. Scherer, S. Schlagowski, and E. Fischer, "PEM water electrolysers: evidence for membrane failure in 100kW demonstration plants," *Journal of Applied Electrochemistry*, vol. 28, no. 10, pp. 1041–1049, 1998, doi: 10.1023/A:1003477305336.
[35] M. Chandesris, V. Médeau, N. Guillet, S. Chelghoum, D. Thoby, and F. Fouda-Onana, "Membrane degradation in PEM water electrolyzer: Numerical modeling and experimental evidence of the influence of temperature and current density," *International Journal of Hydrogen Energy*, vol. 40, no. 3, pp. 1353–1366, 2015, doi: 10.1016/j.ijhydene.2014.11.111.
[36] S. A. Grigoriev, K. A. Dzhus, D. G. Bessarabov, and P. Millet, "Failure of PEM water electrolysis cells: Case study involving anode dissolution and membrane thinning," *International Journal of Hydrogen Energy*, vol. 39, no. 35, pp. 20440–20446, 2014, doi: 10.1016/j.ijhydene.2014.05.043.
[37] L. Gubler, S. M. Dockheer, and W. H. Koppenol, "Radicals in Fuel Cell Membranes: Mechanisms of Formation and Ionomer Attack," *ECS Trans.*, vol. 41, no. 1, pp. 1431–1439, 2011, doi: 10.1149/1.3635674.
[38] K. H. Wong and E. Kjeang, "Macroscopic In-Situ Modeling of Chemical Membrane Degradation in Polymer Electrolyte Fuel Cells," *J. Electrochem. Soc.*, vol. 161, no. 9, F823-F832, 2014, doi: 10.1149/2.0031409jes.
[39] F. Fouda-Onana, M. Chandesris, V. Médeau, S. Chelghoum, D. Thoby, and N. Guillet, "Investigation on the degradation of MEAs for PEM water electrolysers part I: Effects of testing conditions on MEA performances and membrane properties," *International Journal of Hydrogen Energy*, vol. 41, no. 38, pp. 16627–16636, 2016, doi: 10.1016/j.ijhydene.2016.07.125.
[40] S. H. Frensch *et al.,* "Impact of iron and hydrogen peroxide on membrane degradation for polymer electrolyte membrane water electrolysis: Computational and experimental

investigation on fluoride emission," *Journal of Power Sources*, vol. 420, pp. 54–62, 2019, doi: 10.1016/j.jpowsour.2019.02.076.
[41] A. Voronova, S. Kim, D. Kim, H.-Y. Park, J. H. Jang, and B. Seo, "Systematic degradation analysis in renewable energy-powered proton exchange membrane water electrolysis," *Energy Environ. Sci.*, vol. 16, no. 11, pp. 5170–5184, 2023, doi: 10.1039/D3EE01959D.
[42] J. Xie, D. L. Wood, D. M. Wayne, T. A. Zawodzinski, P. Atanassov, and R. L. Borup, "Durability of PEFCs at High Humidity Conditions," *J. Electrochem. Soc.*, vol. 152, no. 1, A104, 2005, doi: 10.1149/1.1830355.
[43] S. Garbe *et al.,* "Understanding Degradation Effects of Elevated Temperature Operating Conditions in Polymer Electrolyte Water Electrolyzers," *J. Electrochem. Soc.*, vol. 168, no. 4, p. 44515, 2021, doi: 10.1149/1945-7111/abf4ae.
[44] E. Kuhnert, K. Mayer, M. Heidinger, C. Rienessel, V. Hacker, and M. Bodner, "Impact of intermittent operation on photovoltaic-PEM electrolyzer systems: A degradation study based on accelerated stress testing," *International Journal of Hydrogen Energy*, vol. 55, pp. 683–695, 2024, doi: 10.1016/j.ijhydene.2023.11.249.
[45] E. Kuhnert *et al.,* "Fluoride emission rate analysis in proton exchange membrane water electrolyzer cells," *Front. Energy Res.*, vol. 12, 2024, Art. no. 1457310, doi: 10.3389/fenrg.2024.1457310.
[46] A. Sandoval-Amador, A. Egea-Corbacho, D. Engelhardt-Guerrero, D. Muñoz, and M. Zurita-Gotor, "Employment of online conductivity measurements as a diagnostic tool of perfluorosulfonic acid membrane degradation in PEMWE," *International Journal of Hydrogen Energy*, vol. 63, pp. 510–516, 2024, doi: 10.1016/j.ijhydene.2024.03.198.
[47] X.-Z. Yuan *et al.,* "Degradation of a PEM fuel cell stack with Nafion® membranes of different thicknesses. Part II: Ex situ diagnosis," *Journal of Power Sources*, vol. 205, pp. 324–334, 2012, doi: 10.1016/j.jpowsour.2012.01.074.
[48] C. Chen and T. F. Fuller, "The effect of humidity on the degradation of Nafion® membrane," *Polymer Degradation and Stability*, vol. 94, no. 9, pp. 1436–1447, 2009, doi: 10.1016/j.polymdegradstab.2009.05.016.
[49] T. A. Aarhaug, A. M. Svensson, A. Baumann Ofstad, J. G. Hoýdahl Soſli, and H. Couvert, "PEMFC Degradation Assessed by Effluent Analysis from Designed Experiments," *ECS Trans.*, vol. 16, no. 2, pp. 1687–1695, 2008, doi: 10.1149/1.2982009.
[50] S. H. Frensch, F. Fouda-Onana, G. Serre, D. Thoby, S. S. Araya, and S. K. Kær, "Influence of the operation mode on PEM water electrolysis degradation," *International Journal of Hydrogen Energy*, vol. 44, no. 57, pp. 29889–29898, 2019, doi: 10.1016/j.ijhydene.2019.09.169.
[51] H. Tang, S. Peikang, S. P. Jiang, F. Wang, and M. Pan, "A degradation study of Nafion proton exchange membrane of PEM fuel cells," *Journal of Power Sources*, vol. 170, no. 1, pp. 85–92, 2007, doi: 10.1016/j.jpowsour.2007.03.061.
[52] T. Böhm, R. Moroni, M. Breitwieser, S. Thiele, and S. Vierrath, "Spatially Resolved Quantification of Ionomer Degradation in Fuel Cells by Confocal Raman Microscopy," *J. Electrochem. Soc.*, vol. 166, no. 7, F3044-F3051, 2019, doi: 10.1149/2.0051907jes.
[53] C. Lim *et al.,* "Membrane degradation during combined chemical and mechanical accelerated stress testing of polymer electrolyte fuel cells," *Journal of Power Sources*, vol. 257, pp. 102–110, 2014, doi: 10.1016/j.jpowsour.2014.01.106.
[54] L. Ghassemzadeh and S. Holdcroft, "Quantifying the structural changes of perfluorosulfonated acid ionomer upon reaction with hydroxyl radicals," *Journal of the American Chemical Society*, early access. doi: 10.1021/ja4037466.
[55] S. Siracusano, S. Trocino, N. Briguglio, F. Pantò, and A. S. Aricò, "Analysis of performance degradation during steady-state and load-thermal cycles of proton exchange membrane water

electrolysis cells," *Journal of Power Sources*, vol. 468, p. 228390, 2020, doi: 10.1016/j.jpowsour.2020.228390.
[56] A. Voronova, H.-J. Kim, J. H. Jang, H.-Y. Park, and B. Seo, "Effect of low voltage limit on degradation mechanism during high-frequency dynamic load in proton exchange membrane water electrolysis," *Intl J of Energy Research*, 2022, Art. no. er.7953, doi: 10.1002/er.7953.
[57] G. Papakonstantinou, G. Algara-Siller, D. Teschner, T. Vidaković-Koch, R. Schlögl, and K. Sundmacher, "Degradation study of a proton exchange membrane water electrolyzer under dynamic operation conditions," *Applied Energy*, vol. 280, p. 115911, 2020, doi: 10.1016/j.apenergy.2020.115911.
[58] S. A. Grigoriev, D. G. Bessarabov, and V. N. Fateev, "Degradation mechanisms of MEA characteristics during water electrolysis in solid polymer electrolyte cells," *Russ J Electrochem*, vol. 53, no. 3, pp. 318–323, 2017, doi: 10.1134/S1023193517030065.
[59] L. Ghassemzadeh, K.-D. Kreuer, J. Maier, and K. Müller, "Chemical Degradation of Nafion Membranes under Mimic Fuel Cell Conditions as Investigated by Solid-State NMR Spectroscopy," *J. Phys. Chem. C*, vol. 114, no. 34, pp. 14635–14645, 2010, doi: 10.1021/jp102533v.
[60] V. M. Ehlinger, A. R. Crothers, A. Kusoglu, and A. Z. Weber, "Modeling proton-exchange-membrane fuel cell performance/degradation tradeoffs with chemical scavengers," *J. Phys. Energy*, vol. 2, no. 4, p. 44006, 2020, doi: 10.1088/2515-7655/abb194.
[61] Y. Xu *et al.,* "In situ construction of ultra-thin PANI/CeOx layer on proton exchange membrane for enhanced oxidation resistance in PEMFC," *Journal of membrane science*, vol. 689, p. 122167, 2024, doi: 10.1016/j.memsci.2023.122167.
[62] E. Kuhnert, M. Heidinger, D. Sandu, V. Hacker, and M. Bodner, "Analysis of PEM Water Electrolyzer Failure Due to Induced Hydrogen Crossover in Catalyst-Coated PFSA Membranes," *Membranes*, early access. doi: 10.3390/membranes13030348.
[63] S. Sun, Z. Shao, H. Yu, G. Li, and B. Yi, "Investigations on degradation of the long-term proton exchange membrane water electrolysis stack," *Journal of Power Sources*, vol. 267, pp. 515–520, 2014, doi: 10.1016/j.jpowsour.2014.05.117.
[64] P. Millet, "Degradation Processes and Failure Mechanisms in PEM Water Electrolyzers," in *PEM Electrolysis for Hydrogen Production*, D. Bessarabov, H. Wang, H. Li, and N. Zhao, Eds., CRC Press, 2016, pp. 219–240.
[65] C. Arthurs and A. Kusoglu, "Compressive Creep of Polymer Electrolyte Membranes: A Case Study for Electrolyzers," *ACS Appl. Energy Mater.*, vol. 4, no. 4, pp. 3249–3254, 2021, doi: 10.1021/acsaem.0c03024.
[66] F. Lapicque, M. Belhadj, C. Bonnet, J. Pauchet, and Y. Thomas, "A critical review on gas diffusion micro and macroporous layers degradations for improved membrane fuel cell durability," *Journal of Power Sources*, vol. 336, pp. 40–53, 2016, doi: 10.1016/j.jpowsour.2016.10.037.
[67] T. Matsuura, M. Kato, and M. Hori, "Study on metallic bipolar plate for proton exchange membrane fuel cell," *Journal of Power Sources*, vol. 161, no. 1, pp. 74–78, 2006, doi: 10.1016/j.jpowsour.2006.04.064.
[68] J. Kink, M. Ise, B. Bensmann, and R. Hanke-Rauschenbach, "Modeling Mechanical Behavior of Membranes in Proton Exchange Membrane Water Electrolyzers," *J. Electrochem. Soc.*, vol. 170, no. 5, p. 54507, 2023, doi: 10.1149/1945-7111/acd47f.
[69] T. Uchiyama, M. Kato, and T. Yoshida, "Buckling deformation of polymer electrolyte membrane and membrane electrode assembly under humidity cycles," *Journal of Power Sources*, vol. 206, pp. 37–46, 2012, doi: 10.1016/j.jpowsour.2012.01.073.
[70] F. Liu, B. Yi, D. Xing, J. Yu, and H. Zhang, "Nafion/PTFE composite membranes for fuel cell applications," *Journal of membrane science*, vol. 212, 1-2, pp. 213–223, 2003, doi: 10.1016/S0376-7388(02)00503-3.

[71] K. E. Ayers, C. Capuano, and E. B. Anderson, "Recent Advances in Cell Cost and Efficiency for PEM-Based Water Electrolysis," *ECS Trans.*, vol. 41, no. 10, pp. 15–22, 2012, doi: 10.1149/1.3684798.
[72] J. Cargnelli and B. Every, "Recent Advances in PEM Water Electrolsyis," 2013.
[73] M. Obermaier, K. Jozwiak, M. Rauber, A. Bauer, and C. Scheu, "Comparative study of pinhole detection methods for automotive fuel cell degradation analysis," *Journal of Power Sources*, vol. 488, p. 229405, 2021, doi: 10.1016/j.jpowsour.2020.229405.
[74] G. de Moor *et al.,* "Perfluorosulfonic acid membrane degradation in the hydrogen inlet region: A macroscopic approach," *International Journal of Hydrogen Energy*, vol. 41, no. 1, pp. 483–496, 2016, doi: 10.1016/j.ijhydene.2015.10.066.
[75] A. K. Taylor, C. Smith, and K. C. Neyerlin, "Mitigation and diagnosis of pin-hole formation in polymer electrolyte membrane fuel cells," *Journal of Power Sources*, vol. 571, p. 232971, 2023, doi: 10.1016/j.jpowsour.2023.232971.
[76] T. T. Phan, S.-K. Kim, J. Islam, M.-J. Kim, and J.-H. Lee, "Degradation analysis of polymer electrolyte membrane water electrolyzer with different membrane thicknesses," *International Journal of Hydrogen Energy*, vol. 49, pp. 875–885, 2024, doi: 10.1016/j.ijhydene.2023.09.274.
[77] S. Asghari, B. Fouladi, N. Masaeli, and B. F. Imani, "Leak diagnosis of polymer electrolyte membrane fuel cell stacks," *International Journal of Hydrogen Energy*, vol. 39, no. 27, pp. 14980–14992, 2014, doi: 10.1016/j.ijhydene.2014.07.044.
[78] T. V. Reshetenko, G. Bender, K. Bethune, and R. Rocheleau, "Application of a segmented cell setup to detect pinhole and catalyst loading defects in proton exchange membrane fuel cells," *Electrochimica Acta*, vol. 76, pp. 16–25, 2012, doi: 10.1016/j.electacta.2012.04.138.
[79] M. Bodner, C. Hochenauer, and V. Hacker, "Effect of pinhole location on degradation in polymer electrolyte fuel cells," *Journal of Power Sources*, vol. 295, pp. 336–348, 2015, doi: 10.1016/j.jpowsour.2015.07.021.
[80] S. Kreitmeier, G. A. Schuler, A. Wokaun, and F. N. Büchi, "Investigation of membrane degradation in polymer electrolyte fuel cells using local gas permeation analysis," *Journal of Power Sources*, vol. 212, pp. 139–147, 2012, doi: 10.1016/j.jpowsour.2012.03.071.
[81] X. Shi *et al.,* "Effects of the Dynamic Loading Frequency on Performance of the Proton Exchange Membrane Water Electrolysis," *ACS applied materials & interfaces*, early access. doi: 10.1021/acsami.4c13605.
[82] Z. Zhang *et al.,* "Exploring the role of reinforcement in controlling fatigue crack propagation behavior of perfluorosulfonic-acid membranes," *International Journal of Hydrogen Energy*, vol. 43, no. 12, pp. 6379–6389, 2018, doi: 10.1016/j.ijhydene.2018.02.034.
[83] Y. Singh *et al.,* "Ex situ characterization and modelling of fatigue crack propagation in catalyst coated membrane composites for fuel cell applications," *International Journal of Hydrogen Energy*, vol. 44, no. 23, pp. 12057–12072, 2019, doi: 10.1016/j.ijhydene.2019.03.108.
[84] H. Becker, J. Murawski, D. V. Shinde, I. E. L. Stephens, G. Hinds, and G. Smith, "Impact of impurities on water electrolysis: a review," *Sustainable Energy Fuels*, vol. 7, no. 7, pp. 1565–1603, 2023, doi: 10.1039/D2SE01517J.
[85] S. M. Alia *et al.,* "Simulated Start-Stop and the Impact of Catalyst Layer Redox on Degradation and Performance Loss in Low-Temperature Electrolysis," *J. Electrochem. Soc.*, 2024, doi: 10.1149/1945-7111/ad2bea.
[86] T. Okada, Y. Ayato, M. Yuasa, and I. Sekine, "The Effect of Impurity Cations on the Transport Characteristics of Perfluorosulfonated Ionomer Membranes," *The Journal of Physical Chemistry B*, vol. 103, no. 17, pp. 3315–3322, 1999, doi: 10.1021/jp983762d.
[87] K. Hongsirikarn, J. G. Goodwin, S. Greenway, and S. Creager, "Effect of cations (Na+, Ca2+, Fe3+) on the conductivity of a Nafion membrane," *Journal of Power Sources*, vol. 195, no. 21, pp. 7213–7220, 2010, doi: 10.1016/j.jpowsour.2010.05.005.

[88] M. J. Kelly, G. Fafilek, J. O. Besenhard, H. Kronberger, and G. E. Nauer, "Contaminant absorption and conductivity in polymer electrolyte membranes," *Journal of Power Sources*, vol. 145, no. 2, pp. 249–252, 2005, doi: 10.1016/j.jpowsour.2005.01.064.
[89] R. Yoshimura, S. Wai, Y. Ota, K. Nishioka, and Y. Suzuki, "Effects of Artificial River Water on PEM Water Electrolysis Performance," *Catalysts*, vol. 12, no. 9, p. 934, 2022, doi: 10.3390/catal12090934.
[90] P. Shwe Sin, S. Wai, Y. Ota, K. Nishioka, and Y. Suzuki, "Performance recovery of proton exchange membrane electrolyzer degraded by metal cations contamination," *International Journal of Hydrogen Energy*, vol. 53, pp. 86–92, 2024, doi: 10.1016/j.ijhydene.2023.12.049.
[91] E. Padgett *et al.,* "Performance Losses and Current-Driven Recovery from Cation Contaminants in PEM Water Electrolysis," *J. Electrochem. Soc.*, vol. 171, no. 6, p. 64510, 2024, doi: 10.1149/1945-7111/ad576b.
[92] M. J. Kelly, Egger, G. Filek, J. O. Besenhard, H. Kronberger, and G. E. Nauer, "Conductivity of polymer electrolyte membranes by impedance spectroscopy with microelectrodes," *Solid State Ionics*, vol. 176, 25-28, pp. 2111–2114, 2005, doi: 10.1016/j.ssi.2004.07.071.
[93] H. Wang and J. A. Turner, "The influence of metal ions on the conductivity of Nafion 112 in polymer electrolyte membrane fuel cell," *Journal of Power Sources*, vol. 183, no. 2, pp. 576–580, 2008, doi: 10.1016/j.jpowsour.2008.05.077.
[94] L. Zhang, X. Jie, Z.-G. Shao, X. Wang, and B. Yi, "The dynamic-state effects of sodium ion contamination on the solid polymer electrolyte water electrolysis," *Journal of Power Sources*, vol. 241, pp. 341–348, 2013, doi: 10.1016/j.jpowsour.2013.04.049.
[95] H. Liu, F. D. Coms, J. Zhang, H. A. Gasteiger, and A. B. LaConti, "Chemical Degradation: Correlations Between Electrolyzer and Fuel Cell Findings," in *Polymer Electrolyte Fuel Cell Durability*, F. N. Büchi, M. Inaba, and T. J. Schmidt, Eds., New York, NY: Scholars Portal, 2009, pp. 71–118.
[96] A. Tan *et al.,* "The poisoning effects of Ti-ion from porous transport layers on the membrane electrode assembly of proton exchange membrane water electrolyzers," *Chemical Engineering Journal*, vol. 471, p. 144624, 2023, doi: 10.1016/j.cej.2023.144624.
[97] N. Li, S. S. Araya, and S. K. Kær, "Long-term contamination effect of iron ions on cell performance degradation of proton exchange membrane water electrolyser," *Journal of Power Sources*, vol. 434, p. 226755, 2019, doi: 10.1016/j.jpowsour.2019.226755.
[98] A. Rex *et al.,* "Elemental Distribution in Catalyst-Coated Membranes of Proton Exchange Membrane Water Electrolysers Tracked by Synchrotron X-Ray Fluorescence," *Adv Energy and Sustain Res*, 2024, Art. no. 2400048, doi: 10.1002/aesr.202400048.
[99] C.-W. Lin, C.-H. Chien, J. Tan, Y. J. Chao, and J. W. van Zee, "Chemical degradation of five elastomeric seal materials in a simulated and an accelerated PEM fuel cell environment," *Journal of Power Sources*, vol. 196, no. 4, pp. 1955–1966, 2011, doi: 10.1016/j.jpowsour.2010.10.012.
[100] J. Tan, Y. J. Chao, X. Li, and J. W. van Zee, "Degradation of silicone rubber under compression in a simulated PEM fuel cell environment," *Journal of Power Sources*, vol. 172, no. 2, pp. 782–789, 2007, doi: 10.1016/j.jpowsour.2007.05.026.
[101] J. Tan, Y. J. Chao, J. W. van Zee, and W. K. Lee, "Degradation of elastomeric gasket materials in PEM fuel cells," *Materials Science and Engineering: A*, vol. 445-446, pp. 669–675, 2007, doi: 10.1016/j.msea.2006.09.098.
[102] F. Wu, B. Chen, and M. Pan, "Degradation of the Sealing Silicone Rubbers in a Proton Exchange Membrane Fuel Cell at Cold Start Conditions," *International Journal of Electrochemical Science*, vol. 15, no. 4, pp. 3013–3028, 2020, doi: 10.20964/2020.04.54.
[103] H.-Y. Jung and J. W. Kim, "Role of the glass transition temperature of Nafion 117 membrane in the preparation of the membrane electrode assembly in a direct methanol fuel cell (DMFC),"

International Journal of Hydrogen Energy, vol. 37, no. 17, pp. 12580–12585, 2012, doi: 10.1016/j.ijhydene.2012.05.121.

[104] S. H. de Almeida and Y. Kawano, "Thermal Behavior of Nafion Membranes," *J Therm Anal Calorim*, vol. 58, no. 3, pp. 569–577, 1999, doi: 10.1023/A:1010196226309.

[105] L. G. Lage., P. G. Delgado, and Y. Kawano, "Thermal stability and decomposition of nafion® membranes with different cations," *J Therm Anal Calorim*, vol. 75, no. 2, pp. 521–530, 2004, doi: 10.1023/B:JTAN.0000027142.21928.c7.

[106] A. C. Olesen, C. Rømer, and S. K. Kær, "A numerical study of the gas-liquid, two-phase flow maldistribution in the anode of a high pressure PEM water electrolysis cell," *International Journal of Hydrogen Energy*, vol. 41, no. 1, pp. 52–68, 2016, doi: 10.1016/j.ijhydene.2015.09.140.

[107] F. M. Collette, C. Lorentz, G. Gebel, and F. Thominette, "Hygrothermal aging of Nafion®," *Journal of membrane science*, vol. 330, 1-2, pp. 21–29, 2009, doi: 10.1016/j.memsci.2008.11.048.

[108] M. Chandesris, R. Vincent, L. Guetaz, J.-S. Roch, D. Thoby, and M. Quinaud, "Membrane degradation in PEM fuel cells: From experimental results to semi-empirical degradation laws," *International Journal of Hydrogen Energy*, vol. 42, no. 12, pp. 8139–8149, 2017, doi: 10.1016/j.ijhydene.2017.02.116.

[109] S. Shi *et al.,* "Impact of hygrothermal aging on structure/function relationship of perfluorosulfonic-acid membrane," *J. Polym. Sci. Part B: Polym. Phys*, vol. 54, no. 5, pp. 570–581, 2016, doi: 10.1002/polb.23946.

[110] F. M. Collette, F. Thominette, H. Mendil-Jakani, and G. Gebel, "Structure and transport properties of solution-cast Nafion® membranes subjected to hygrothermal aging," *Journal of membrane science*, vol. 435, pp. 242–252, 2013, doi: 10.1016/j.memsci.2013.02.002.

[111] S. Naudy, F. Collette, F. Thominette, G. Gebel, and E. Espuche, "Influence of hygrothermal aging on the gas and water transport properties of Nafion® membranes," *Journal of membrane science*, vol. 451, pp. 293–304, 2014, doi: 10.1016/j.memsci.2013.10.013.

[112] S. M. Clapham, F. D. Coms, T. J. Fuller, and L. Zou, "Degradation of Perfluorosulfonic Acid Membrane Water Permeance via Formation of Sulfonic Acid Anhydrides," *ECS Trans.*, vol. 50, no. 2, pp. 1011–1020, 2013, doi: 10.1149/05002.1011ecst.

[113] G. Gao *et al.,* "Recent advances in Ru/Ir-based electrocatalysts for acidic oxygen evolution reaction," *Applied Catalysis B: Environmental*, vol. 343, p. 123584, 2024, doi: 10.1016/j.apcatb.2023.123584.

[114] W. Zhao, Y. Liu, X. Fu, and W. Wang, "Materials Engineering toward Durable Ru-Based Electrocatalysts for Acidic Oxygen Evolution Reaction," *Renewables*, vol. 1, no. 6, pp. 638–667, 2023, doi: 10.31635/renewables.023.202300038.

[115] S. M. Alia *et al.,* "Catalyst-Specific Accelerated Stress Tests in Proton Exchange Membrane Low-Temperature Electrolysis for Intermittent Operation," *J. Electrochem. Soc.*, vol. 171, no. 2, p. 24505, 2024, doi: 10.1149/1945-7111/ad2735.

[116] S. Geiger *et al.,* "The stability number as a metric for electrocatalyst stability benchmarking," *Nat Catal*, vol. 1, no. 7, pp. 508–515, 2018, doi: 10.1038/s41929-018-0085-6.

[117] V. K. Puthiyapura, S. Pasupathi, H. Su, X. Liu, B. Pollet, and K. Scott, "Investigation of supported IrO2 as electrocatalyst for the oxygen evolution reaction in proton exchange membrane water electrolyser," *International Journal of Hydrogen Energy*, vol. 39, no. 5, pp. 1905–1913, 2014, doi: 10.1016/j.ijhydene.2013.11.056.

[118] X. Wu and K. Scott, "RuO2 supported on Sb-doped SnO2 nanoparticles for polymer electrolyte membrane water electrolysers," *International Journal of Hydrogen Energy*, vol. 36, no. 10, pp. 5806–5810, 2011, doi: 10.1016/j.ijhydene.2010.10.098.

[119] O. Kasian, J.-P. Grote, S. Geiger, S. Cherevko, and K. J. J. Mayrhofer, "The Common Intermediates of Oxygen Evolution and Dissolution Reactions during Water Electrolysis on Iridium," *Angewandte Chemie (International ed. in English)*, early access. doi: 10.1002/anie.201709652.

[120] V. K. Puthiyapura, M. Mamlouk, S. Pasupathi, B. G. Pollet, and K. Scott, "Physical and electrochemical evaluation of ATO supported IrO2 catalyst for proton exchange membrane water electrolyser," *Journal of Power Sources*, vol. 269, pp. 451–460, 2014, doi: 10.1016/j.jpowsour.2014.06.078.

[121] I. Ali Khan, P. Morgen, S. Gyergyek, R. Sharma, and S. Ma Andersen, "Reduced valence state of iridium supported on antimony doped tin oxide as a highly active and robust oxygen evolution reaction electrocatalyst for proton exchange membrane-based electrolysis," *Applied Surface Science*, vol. 646, p. 158924, 2024, doi: 10.1016/j.apsusc.2023.158924.

[122] H.-S. Oh, H. N. Nong, and P. Strasser, "Preparation of Mesoporous Sb-, F-, and In-Doped SnO 2 Bulk Powder with High Surface Area for Use as Catalyst Supports in Electrolytic Cells," *Adv. Funct. Mater.*, vol. 25, no. 7, pp. 1074–1081, 2015, doi: 10.1002/adfm.201401919.

[123] J. K. Lee *et al.,* "Ionomer-free and recyclable porous-transport electrode for high-performing proton-exchange-membrane water electrolysis," *Nat Commun*, early access. doi: 10.1038/s41467-023-40375-x.

[124] X. Lin, J. Z. Y. Seow, and Z. J. Xu, "A brief introduction of electrode fabrication for proton exchange membrane water electrolyzers," *J. Phys. Energy*, vol. 5, no. 3, p. 34003, 2023, doi: 10.1088/2515-7655/acccb1.

[125] D. A. Stevens, M. T. Hicks, G. M. Haugen, and J. R. Dahn, "Ex Situ and In Situ Stability Studies of PEMFC Catalysts," *J. Electrochem. Soc.*, vol. 152, no. 12, A2309, 2005, doi: 10.1149/1.2097361.

[126] J. Speder *et al.,* "Comparative degradation study of carbon supported proton exchange membrane fuel cell electrocatalysts – The influence of the platinum to carbon ratio on the degradation rate," *Journal of Power Sources*, vol. 261, pp. 14–22, 2014, doi: 10.1016/j.jpowsour.2014.03.039.

[127] M. Kroschel, A. Bonakdarpour, J. T. H. Kwan, P. Strasser, and D. P. Wilkinson, "Analysis of oxygen evolving catalyst coated membranes with different current collectors using a new modified rotating disk electrode technique," *Electrochimica Acta*, vol. 317, pp. 722–736, 2019, doi: 10.1016/j.electacta.2019.05.011.

[128] M. Chourashiya, R. Sharma, and S. M. Andersen, "Accurate Determination of Catalyst Loading on Glassy Carbon Disk and Its Impact on Thin Film Rotating Disk Electrode for Oxygen Reduction Reaction," *Analytical chemistry*, early access. doi: 10.1021/acs.analchem.8b02697.

[129] M. Geuß *et al.,* "Quantification of Iridium Dissolution at Water Electrolysis Relevant Conditions Using a Gas Diffusion Electrode Half-Cell Setup," *ACS Catal.*, vol. 14, no. 15, pp. 11819–11831, 2024, doi: 10.1021/acscatal.4c02159.

[130] S. Siracusano, V. Baglio, N. van Dijk, L. Merlo, and A. S. Aricò, "Enhanced performance and durability of low catalyst loading PEM water electrolyser based on a short-side chain perfluorosulfonic ionomer," *Applied Energy*, vol. 192, pp. 477–489, 2017, doi: 10.1016/j.apenergy.2016.09.011.

[131] H. Liu *et al.,* "Optimizing Ionomer Distribution in Anode Catalyst Layer for Stable Proton Exchange Membrane Water Electrolysis," *Advanced materials (Deerfield Beach, Fla.)*, early access. doi: 10.1002/adma.202402780.

[132] O. Kasian *et al.,* "Degradation of iridium oxides via oxygen evolution from the lattice: correlating atomic scale structure with reaction mechanisms," *Energy Environ. Sci.*, vol. 12, no. 12, pp. 3548–3555, 2019, doi: 10.1039/C9EE01872G.

[133] T. Naito, T. Shinagawa, T. Nishimoto, and K. Takanabe, "Recent advances in understanding oxygen evolution reaction mechanisms over iridium oxide," *Inorg. Chem. Front.*, vol. 8, no. 11, pp. 2900–2917, 2021, doi: 10.1039/D0QI01465F.

[134] A. Minguzzi *et al.,* "Observing the oxidation state turnover in heterogeneous iridium-based water oxidation catalysts," *Chem. Sci.*, vol. 5, no. 9, p. 3591, 2014, doi: 10.1039/C4SC00975D.

[135] S. Duran, A. Grimaud, M. Faustini, and J. Peron, "Porosity as a Morphology Marker to Probe the Degradation of IrO 2 Anode Catalyst Layers in Proton Exchange Membrane Water Electrolyzers," *Chem. Mater.*, vol. 35, no. 20, pp. 8590–8598, 2023, doi: 10.1021/acs.chemmater.3c01524.

[136] C. Rozain, E. Mayousse, N. Guillet, and P. Millet, "Influence of iridium oxide loadings on the performance of PEM water electrolysis cells: Part II – Advanced oxygen electrodes," *Applied Catalysis B: Environmental*, vol. 182, pp. 123–131, 2016, doi: 10.1016/j.apcatb.2015.09.011.

[137] C. Da Daiane Ferreira Silva *et al.,* "Oxygen Evolution Reaction Activity and Stability Benchmarks for Supported and Unsupported IrO x Electrocatalysts," *ACS Catal.*, vol. 11, no. 7, pp. 4107–4116, 2021, doi: 10.1021/acscatal.0c04613.

[138] S. Sanjay Karade, R. Sharma, P. Morgen, R. K. Pittkowski, K. M. Ø. Jensen, and S. Ma Andersen, "Intrinsic oxygen evolution reaction activity and stability enhancement of IrOx electrocatalysts by microwave irradiation," *Applied Surface Science*, vol. 682, p. 161758, 2025, doi: 10.1016/j.apsusc.2024.161758.

[139] O. Diaz-Morales *et al.,* "Iridium-based double perovskites for efficient water oxidation in acid media," *Nat Commun*, early access. doi: 10.1038/ncomms12363.

[140] Z. Xie *et al.,* "Honeycomb-Structured IrOx Foam Platelets as the Building Block of Anode Catalyst Layer in PEM Water Electrolyzer," *Angew. Chem. Int. Ed. Engl.*, early access. doi: 10.1002/anie.202415032.

[141] Y. Shi *et al.,* "Tuning the In-Plane Electrical Conductivity and Performance of the Low Ir Anode in a Proton Exchange Membrane Water Electrolyzer," *ACS Sustainable Chem. Eng.*, vol. 12, no. 1, pp. 423–432, 2024, doi: 10.1021/acssuschemeng.3c06209.

[142] H. Yu, L. Bonville, J. Jankovic, and R. Maric, "Microscopic insights on the degradation of a PEM water electrolyzer with ultra-low catalyst loading," *Applied Catalysis B: Environmental*, vol. 260, p. 118194, 2020, doi: 10.1016/j.apcatb.2019.118194.

[143] P. Lettenmeier *et al.,* "Durable Membrane Electrode Assemblies for Proton Exchange Membrane Electrolyzer Systems Operating at High Current Densities," *Electrochimica Acta*, vol. 210, pp. 502–511, 2016, doi: 10.1016/j.electacta.2016.04.164.

[144] M. J. Burch *et al.,* "A novel work-flow to study Ir electrode thinning and dissolution in proton exchange membrane water electrolyzers," *Journal of Power Sources*, vol. 500, p. 229978, 2021, doi: 10.1016/j.jpowsour.2021.229978.

[145] Z. Zeng *et al.,* "Degradation Mechanisms in Advanced MEAs for PEM Water Electrolyzers Fabricated by Reactive Spray Deposition Technology," *J. Electrochem. Soc.*, vol. 169, no. 5, p. 54536, 2022, doi: 10.1149/1945-7111/ac7170.

[146] F. Claudel *et al.,* "Degradation Mechanisms of Oxygen Evolution Reaction Electrocatalysts: A Combined Identical-Location Transmission Electron Microscopy and X-ray Photoelectron Spectroscopy Study," *ACS Catal.*, vol. 9, no. 5, pp. 4688–4698, 2019, doi: 10.1021/acscatal.9b00280.

[147] S. F. Zaccarine *et al.,* "Multi-Scale Multi-Technique Characterization Approach for Analysis of PEM Electrolyzer Catalyst Layer Degradation," *J. Electrochem. Soc.*, vol. 169, no. 6, p. 64502, 2022, doi: 10.1149/1945-7111/ac7258.

[148] P. Lettenmeier, R. Wang, R. Abouatallah, F. Burggraf, A. S. Gago, and K. A. Friedrich, "Coated Stainless Steel Bipolar Plates for Proton Exchange Membrane Electrolyzers," *Journal of The Electrochemical*, vol. 163, no. 11, pp. 3119–3124, 2016, doi: 10.1149/2.0141611jes.

[149] M. Milosevic *et al.,* "In Search of Lost Iridium: Quantification of Anode Catalyst Layer Dissolution in Proton Exchange Membrane Water Electrolyzers," *ACS Energy Lett.*, vol. 8, no. 6, pp. 2682–2688, 2023, doi: 10.1021/acsenergylett.3c00193.

[150] S. M. Alia *et al.,* "Electrolyzer Performance Loss from Accelerated Stress Tests and Corresponding Changes to Catalyst Layers and Interfaces," *J. Electrochem. Soc.*, vol. 169, no. 5, p. 54517, 2022, doi: 10.1149/1945-7111/ac697e.

[151] H. P. Tran *et al.,* "Reactivity and Stability of Reduced Ir-Weight TiO2-Supported Oxygen Evolution Catalysts for Proton Exchange Membrane (PEM) Water Electrolyzer Anodes," *Journal of the American Chemical Society*, early access. doi: 10.1021/jacs.4c07002.

[152] S. M. Alia, S. Stariha, and R. L. Borup, "Electrolyzer Durability at Low Catalyst Loading and with Dynamic Operation," *J. Electrochem. Soc.*, vol. 166, no. 15, F1164-F1172, 2019, doi: 10.1149/2.0231915jes.

[153] S. Cherevko, A. R. Zeradjanin, A. A. Topalov, N. Kulyk, I. Katsounaros, and K. J. J. Mayrhofer, "Dissolution of Noble Metals during Oxygen Evolution in Acidic Media," *ChemCatChem*, vol. 6, no. 8, pp. 2219–2223, 2014, doi: 10.1002/cctc.201402194.

[154] A. P. Dam, T. Franz, G. Papakonstantinou, and K. Sundmacher, "Catalyst dissolution in PEM water electrolysis: Influence of time, current density and Iridium ion transport in single-pass and recirculation water flow modes," *Applied Catalysis B: Environmental*, vol. 365, p. 124946, 2025, doi: 10.1016/j.apcatb.2024.124946.

[155] J. Dodwell *et al.,* "Open-circuit dissolution of platinum from the cathode in polymer electrolyte membrane water electrolysers," *Journal of Power Sources*, vol. 498, p. 229937, 2021, doi: 10.1016/j.jpowsour.2021.229937.

[156] A. Lam *et al.,* "Ex situ study of chloride contamination on carbon supported Pt catalyst," *Journal of Power Sources*, vol. 205, pp. 235–238, 2012, doi: 10.1016/j.jpowsour.2012.01.063.

[157] J. Wang, J. Geng, M. Wang, X. Hu, Z. Shao, and H. Zhang, "Quantification on degradation mechanisms of polymer exchange membrane fuel cell cathode catalyst layers during bus and stationary durability test protocols," *Journal of Power Sources*, vol. 521, p. 230878, 2022, doi: 10.1016/j.jpowsour.2021.230878.

[158] V. Karimi, P. Morgen, S. Gyergyek, R. Sharma, and S. M. Andersen, "An Effective Route to Enhance Pt/C Electrocatalyst Durability through Addition of Ceramic Nanoparticles to Facilitate Pt Redeposition," *ACS applied materials & interfaces*, early access. doi: 10.1021/acsami.4c10430.

[159] P. J. Ferreira *et al.,* "Instability of Pt⁄C Electrocatalysts in Proton Exchange Membrane Fuel Cells," *J. Electrochem. Soc.*, vol. 152, no. 11, A2256, 2005, doi: 10.1149/1.2050347.

[160] A. Zana, J. Speder, M. Roefzaad, L. Altmann, M. Bäumer, and M. Arenz, "Probing Degradation by IL-TEM: The Influence of Stress Test Conditions on the Degradation Mechanism," *J. Electrochem. Soc.*, vol. 160, no. 6, F608-F615, 2013, doi: 10.1149/2.078306jes.

[161] Y. Sugawara, T. Okayasu, A. P. Yadav, A. Nishikata, and T. Tsuru, "Dissolution Mechanism of Platinum in Sulfuric Acid Solution," *J. Electrochem. Soc.*, vol. 159, no. 11, F779-F786, 2012, doi: 10.1149/2.017212jes.

[162] J. Zhang, B. A. Litteer, W. Gu, H. Liu, and H. A. Gasteiger, "Effect of Hydrogen and Oxygen Partial Pressure on Pt Precipitation within the Membrane of PEMFCs," *J. Electrochem. Soc.*, vol. 154, no. 10, B1006, 2007, doi: 10.1149/1.2764240.

[163] N. Li, S. S. Araya, and S. K. Kær, "Investigating low and high load cycling tests as accelerated stress tests for proton exchange membrane water electrolysis," *Electrochimica Acta*, vol. 370, p. 137748, 2021, doi: 10.1016/j.electacta.2021.137748.

[164] S. Maass, F. Finsterwalder, G. Frank, R. Hartmann, and C. Merten, "Carbon support oxidation in PEM fuel cell cathodes," *Journal of Power Sources*, vol. 176, no. 2, pp. 444–451, 2008, doi: 10.1016/j.jpowsour.2007.08.053.

[165] L. Wei and Y. Chen, "Degradation of carbon materials in electrocatalysis," *Current Opinion in Electrochemistry*, vol. 36, p. 101159, 2022, doi: 10.1016/j.coelec.2022.101159.

[166] L. Castanheira, W. O. Silva, F. H. Lima, A. Crisci, L. Dubau, and F. Maillard, "Carbon Corrosion in Proton-Exchange Membrane Fuel Cells: Effect of the Carbon Structure, the Degradation Protocol, and the Gas Atmosphere," *ACS Catal.*, vol. 5, no. 4, pp. 2184–2194, 2015, doi: 10.1021/cs501973j.

[167] M. Hara *et al.,* "Electrochemical and Raman spectroscopic evaluation of Pt/graphitized carbon black catalyst durability for the start/stop operating condition of polymer electrolyte fuel cells," *Electrochimica Acta*, vol. 70, pp. 171–181, 2012, doi: 10.1016/j.electacta.2012.03.043.

[168] N. Li, S. S. Araya, X. Cui, and S. K. Kær, "The effects of cationic impurities on the performance of proton exchange membrane water electrolyzer," *Journal of Power Sources*, vol. 473, p. 228617, 2020, doi: 10.1016/j.jpowsour.2020.228617.

[169] E. Endoh, S. Terazono, H. Widjaja, and Y. Takimoto, "Degradation Study of MEA for PEMFCs under Low Humidity Conditions," *Electrochem. Solid-State Lett.*, vol. 7, no. 7, A209, 2004, doi: 10.1149/1.1739314.

[170] J. D. Fairweather, B. Li, R. Mukundan, J. Fenton, and R. L. Borup, "In Situ and Ex Situ Characterization of Carbon Corrosion in PEMFCs," *ECS Trans.*, vol. 33, no. 1, pp. 433–446, 2010, doi: 10.1149/1.3484542.

[171] C. Wang, M. Ricketts, A. P. Soleymani, J. Jankovic, J. Waldecker, and J. Chen, "Effect of Carbon Support Characteristics on Fuel Cell Durability in Accelerated Stress Testing," *J. Electrochem. Soc.*, vol. 168, no. 4, p. 44507, 2021, doi: 10.1149/1945-7111/abf265.

[172] M. Kitazawa, A. Y. Nosaka, and Y. Nosaka, "Radical formation in polymer electrolyte fuel cell components as studied by ESR spectroscopy," *J Appl Electrochem*, vol. 38, no. 4, pp. 491–496, 2008, doi: 10.1007/s10800-007-9464-4.

[173] K. Sasaki, M. Shao, and R. Adzic, "Dissolution and Stabilization of Platinum in Oxygen Cathodes," in *Polymer Electrolyte Fuel Cell Durability*, F. N. Büchi, M. Inaba, and T. J. Schmidt, Eds., New York, NY: Scholars Portal, 2009, pp. 7–27.

[174] S. Yuan *et al.,* "Bubble evolution and transport in PEM water electrolysis: Mechanism, impact, and management," *Progress in Energy and Combustion Science*, vol. 96, p. 101075, 2023, doi: 10.1016/j.pecs.2023.101075.

[175] D. Kulkarni *et al.,* "Influence of Microporous Layers on Interfacial Properties, Oxygen Flow Distribution, and Durability of Proton Exchange Membrane Water Electrolyzers," *ACS applied materials & interfaces*, early access. doi: 10.1021/acsami.3c06899.

[176] J. Liu *et al.,* "Efficient and Stable Proton Exchange Membrane Water Electrolysis Enabled by Stress Optimization," *ACS central science*, early access. doi: 10.1021/acscentsci.4c00037.

[177] U. Panchenko, T. Arlt, I. Manke, M. Müller, D. Stolten, and W. Lehnert, "Synchrotron Radiography for a Proton Exchange Membrane (PEM) Electrolyzer," *Fuel cells*, vol. 20, no. 3, pp. 300–306, 2020, doi: 10.1002/fuce.201900055.

[178] E. Leonard *et al.,* "Operando X-ray tomography and sub-second radiography for characterizing transport in polymer electrolyte membrane electrolyzer," *Electrochimica Acta*, vol. 276, pp. 424–433, 2018, doi: 10.1016/j.electacta.2018.04.144.

[179] C. Spöri, J. T. H. Kwan, A. Bonakdarpour, D. P. Wilkinson, and P. Strasser, "The Stability Challenges of Oxygen Evolving Catalysts: Towards a Common Fundamental Understanding and Mitigation of Catalyst Degradation," *Angewandte Chemie (International ed. in English)*, early access. doi: 10.1002/anie.201608601.

[180] P. Paciok, M. Carmo, W. Lüke, M. Heggen, and D. Stolten, "Investigation of Pt/C Catalysts Using Identical Location Transmission Electron Microscopy Under PEM Electrolysis Conditions," *Meet. Abstr.*, vol. MA2016-02, no. 38, p. 2505, 2016, doi: 10.1149/MA2016-02/38/2505.

[181] S. Zhao, A. Stocks, B. Rasimick, K. More, and H. Xu, "Highly Active, Durable Dispersed Iridium Nanocatalysts for PEM Water Electrolyzers," *J. Electrochem. Soc.*, vol. 165, no. 2, F82-F89, 2018, doi: 10.1149/2.0981802jes.

[182] P. Paciok, M. Schalenbach, M. Carmo, and D. Stolten, "On the mobility of carbon-supported platinum nanoparticles towards unveiling cathode degradation in water electrolysis," *Journal of Power Sources*, vol. 365, pp. 53–60, 2017, doi: 10.1016/j.jpowsour.2017.07.033.

[183] C. Rakousky *et al.,* "Polymer electrolyte membrane water electrolysis: Restraining degradation in the presence of fluctuating power," *Journal of Power Sources*, vol. 342, pp. 38–47, 2017, doi: 10.1016/j.jpowsour.2016.11.118.

[184] C. Rakousky, U. Reimer, K. Wippermann, M. Carmo, W. Lueke, and D. Stolten, "An analysis of degradation phenomena in polymer electrolyte membrane water electrolysis," *Journal of Power Sources*, vol. 326, pp. 120–128, 2016, doi: 10.1016/j.jpowsour.2016.06.082.

[185] E. Leonard *et al.,* "Interfacial analysis of a PEM electrolyzer using X-ray computed tomography," *Sustainable Energy Fuels*, vol. 4, no. 2, pp. 921–931, 2020, doi: 10.1039/C9SE00364A.

[186] R. L. Borup, J. R. Davey, F. H. Garzon, D. L. Wood, and M. A. Inbody, "PEM fuel cell electrocatalyst durability measurements," *Journal of Power Sources*, vol. 163, no. 1, pp. 76–81, 2006, doi: 10.1016/j.jpowsour.2006.03.009.

[187] M. Stähler, A. Burdzik, I. Friedrich, A. Everwand, and F. Scheepers, "Oxygen flow rate measurement as a whistleblower for degradation effects in PEM water electrolysis," *International Journal of Hydrogen Energy*, vol. 78, pp. 682–687, 2024, doi: 10.1016/j.ijhydene.2024.06.334.

[188] C. Klose *et al.,* "Membrane Interlayer with Pt Recombination Particles for Reduction of the Anodic Hydrogen Content in PEM Water Electrolysis," *J. Electrochem. Soc.*, vol. 165, no. 16, F1271-F1277, 2018, doi: 10.1149/2.1241814jes.

[189] O. Panchenko *et al.,* "Non-destructive In-Operando Investigation of Catalyst Layer Degradation for Water Electrolyzers using Synchrotron Radiography," *Materials Today Energy*, no. 16, p. 100394, 2020, doi: 10.1016/j.mtener.2020.100394.

[190] M. K. Debe *et al.,* "Initial Performance and Durability of Ultra-Low Loaded NSTF Electrodes for PEM Electrolyzers," *J. Electrochem. Soc.*, vol. 159, no. 6, K165-K176, 2012, doi: 10.1149/2.065206jes.

[191] A. Weiß, A. Siebel, M. Bernt, T.-H. Shen, V. Tileli, and H. A. Gasteiger, "Impact of Intermittent Operation on Lifetime and Performance of a PEM Water Electrolyzer," *J. Electrochem. Soc.*, vol. 166, no. 8, F487-F497, 2019, doi: 10.1149/2.0421908jes.

[192] Y. Cai *et al.,* "Electrode Edge Cobalt Cation Migration in an Operating Fuel Cell: An In Situ Micro-X-ray Fluorescence Study," *J. Electrochem. Soc.*, vol. 165, no. 6, F3132-F3138, 2018, doi: 10.1149/2.0201806jes.

[193] J.-P. B. Haraldsted *et al.,* "Trace anodic migration of iridium and titanium ions and subsequent cathodic selectivity degradation in acid electrolysis systems," *Materials Today Energy*, vol. 14, p. 100352, 2019, doi: 10.1016/j.mtener.2019.100352.

[194] R. Sharma, P. Morgen, D. Makovec, S. Gyergyek, and S. M. Andersen, "Enhanced electrochemical dissolution of Iridium oxide in acidic electrolytes through presence of metal ions: shortened lifetime and hope for recovery," *RSC Sustain.*, 2024, doi: 10.1039/D4SU00257A.

[195] X. Wang, L. Zhang, G. Li, G. Zhang, Z.-G. Shao, and B. Yi, "The influence of Ferric ion contamination on the solid polymer electrolyte water electrolysis performance," *Electrochimica Acta*, vol. 158, pp. 253–257, 2015, doi: 10.1016/j.electacta.2015.01.140.

[196] M. Zlobinski, "Investigation of Water and Gas Distribution in Proton Exchange Membrane Water Electrolyzer," Dissertation, ETH Zurich, 2021.

[197] M. Zlobinski, U. Babic, M. Fikry, L. Gubler, T. J. Schmidt, and P. Boillat, "Dynamic Neutron Imaging and Modeling of Cationic Impurities in Polymer Electrolyte Water Electrolyzer," *J. Electrochem. Soc.*, vol. 167, no. 14, p. 144509, 2020, doi: 10.1149/1945-7111/abc83b.

[198] C. Liu *et al.,* "Degradation Effects at the Porous Transport Layer/Catalyst Layer Interface in Polymer Electrolyte Membrane Water Electrolyzer," *J. Electrochem. Soc.*, vol. 170, no. 3, p. 34508, 2023, doi: 10.1149/1945-7111/acc1a5.

[199] H. Liu *et al.,* "Constructing Robust 3D Ionomer Networks in the Catalyst Layer to Achieve Stable Water Electrolysis for Green Hydrogen Production," *ACS applied materials & interfaces*, early access. doi: 10.1021/acsami.4c03318.

[200] M. Stähler, A. Stähler, F. Scheepers, M. Carmo, W. Lehnert, and D. Stolten, "Impact of porous transport layer compression on hydrogen permeation in PEM water electrolysis," *International Journal of Hydrogen Energy*, vol. 45, no. 7, pp. 4008–4014, 2020, doi: 10.1016/j.ijhydene.2019.12.016.

[201] I. Nitta, T. Hottinen, O. Himanen, and M. Mikkola, "Inhomogeneous compression of PEMFC gas diffusion layer," *Journal of Power Sources*, vol. 171, no. 1, pp. 26–36, 2007, doi: 10.1016/j.jpowsour.2006.11.018.

[202] I. Nitta, O. Himanen, and M. Mikkola, "Thermal Conductivity and Contact Resistance of Compressed Gas Diffusion Layer of PEM Fuel Cell," *Fuel cells*, vol. 8, no. 2, pp. 111–119, 2008, doi: 10.1002/fuce.200700054.

[203] J. H. Chun, D. H. Jo, S. G. Kim, S. H. Park, C. H. Lee, and S. H. Kim, "Improvement of the mechanical durability of micro porous layer in a proton exchange membrane fuel cell by elimination of surface cracks," *Renewable Energy*, vol. 48, pp. 35–41, 2012, doi: 10.1016/j.renene.2012.04.011.

[204] V. Radhakrishnan and P. Haridoss, "Effect of cyclic compression on structure and properties of a Gas Diffusion Layer used in PEM fuel cells," *International Journal of Hydrogen Energy*, vol. 35, no. 20, pp. 11107–11118, 2010, doi: 10.1016/j.ijhydene.2010.07.009.

[205] E. A. Wargo, T. Kotaka, Y. Tabuchi, and E. C. Kumbur, "Comparison of focused ion beam versus nano-scale X-ray computed tomography for resolving 3-D microstructures of porous fuel cell materials," *Journal of Power Sources*, vol. 241, pp. 608–618, 2013, doi: 10.1016/j.jpowsour.2013.04.153.

[206] S. Escribano, J.-F. Blachot, J. Ethève, A. Morin, and R. Mosdale, "Characterization of PEMFCs gas diffusion layers properties," *Journal of Power Sources*, vol. 156, no. 1, pp. 8–13, 2006, doi: 10.1016/j.jpowsour.2005.08.013.

[207] Y. Pan, H. Wang, and N. P. Brandon, "Gas diffusion layer degradation in proton exchange membrane fuel cells: Mechanisms, characterization techniques and modelling approaches," *Journal of Power Sources*, vol. 513, p. 230560, 2021, doi: 10.1016/j.jpowsour.2021.230560.

[208] D. Qiu, H. Janßen, L. Peng, P. Irmscher, X. Lai, and W. Lehnert, "Electrical resistance and microstructure of typical gas diffusion layers for proton exchange membrane fuel cell under compression," *Applied Energy*, vol. 231, pp. 127–137, 2018, doi: 10.1016/j.apenergy.2018.09.117.

[209] D. Spernjak, J. Fairweather, R. Mukundan, T. Rockward, and R. L. Borup, "Influence of the microporous layer on carbon corrosion in the catalyst layer of a polymer electrolyte membrane fuel cell," *Journal of Power Sources*, vol. 214, pp. 386–398, 2012, doi: 10.1016/j.jpowsour.2012.04.086.

[210] H. Liu *et al.,* "Accelerated Degradation of Polymer Electrolyte Membrane Fuel Cell Gas Diffusion Layers," *J. Electrochem. Soc.*, vol. 164, no. 7, F695-F703, 2017, doi: 10.1149/2.0071707jes.

[211] J. Chlistunoff, J. R. Davey, K. C. Rau, R. Mukundan, and R. L. Borup, "PEMFC Gas Diffusion Media Degradation Determined by Acid-Base Titrations," *ECS Trans.*, vol. 50, no. 2, pp. 521–529, 2013, doi: 10.1149/05002.0521ecst.

[212] Z. Kang *et al.,* "Developing titanium micro/nano porous layers on planar thin/tunable LGDLs for high-efficiency hydrogen production," *International Journal of Hydrogen Energy*, vol. 43, no. 31, pp. 14618–14628, 2018, doi: 10.1016/j.ijhydene.2018.05.139.

[213] J. Mo *et al.,* "Study on corrosion migrations within catalyst-coated membranes of proton exchange membrane electrolyzer cells," *International Journal of Hydrogen Energy*, vol. 42, no. 44, pp. 27343–27349, 2017, doi: 10.1016/j.ijhydene.2017.09.020.

[214] H. Ito *et al.,* "Experimental study on porous current collectors of PEM electrolyzers," *International Journal of Hydrogen Energy*, vol. 37, no. 9, pp. 7418–7428, 2012, doi: 10.1016/j.ijhydene.2012.01.095.

[215] E. Borgardt *et al.,* "Mechanical characterization and durability of sintered porous transport layers for polymer electrolyte membrane electrolysis," *Journal of Power Sources*, vol. 374, pp. 84–91, 2018, doi: 10.1016/j.jpowsour.2017.11.027.

[216] C. M. Hwang *et al.,* "Effect of titanium powder loading in gas diffusion layer of a polymer electrolyte unitized reversible fuel cell," *Journal of Power Sources*, vol. 202, pp. 108–113, 2012, doi: 10.1016/j.jpowsour.2011.11.041.

[217] J. Mo, S. M. Steen, F.-Y. Zhang, T. J. Toops, M. P. Brady, and J. B. Green, "Electrochemical investigation of stainless steel corrosion in a proton exchange membrane electrolyzer cell," *International Journal of Hydrogen Energy*, vol. 40, no. 36, pp. 12506–12511, 2015, doi: 10.1016/j.ijhydene.2015.07.061.

[218] Z. Kang *et al.,* "Thin film surface modifications of thin/tunable liquid/gas diffusion layers for high-efficiency proton exchange membrane electrolyzer cells," *Applied Energy*, vol. 206, pp. 983–990, 2017, doi: 10.1016/j.apenergy.2017.09.004.

[219] J. Wind, R. Späh, W. Kaiser, and G. Böhm, "Metallic bipolar plates for PEM fuel cells," *Journal of Power Sources*, vol. 105, no. 2, pp. 256–260, 2002, doi: 10.1016/S0378-7753(01)00950-8.

[220] C. Liu *et al.,* "Performance enhancement of PEM electrolyzers through iridium-coated titanium porous transport layers," *Electrochemistry Communications*, vol. 97, pp. 96–99, 2018, doi: 10.1016/j.elecom.2018.10.021.

[221] C. Liu *et al.,* "Exploring the Interface of Skin-Layered Titanium Fibers for Electrochemical Water Splitting," *Adv. Energy Mater.*, vol. 11, no. 8, p. 2002926, 2021, doi: 10.1002/aenm.202002926.

[222] R. Günzel, S. Mändl, E. Richter, A. Liu, B. Y. Tang, and P. K. Chu, "Corrosion protection of titanium by deposition of niobium thin films," *Surface and Coatings Technology*, vol. 116-119, pp. 1107–1110, 1999, doi: 10.1016/S0257-8972(99)00321-7.

[223] C.-C. Sung and C.-Y. Liu, "A novel micro protective layer applied on a simplified PEM water electrolyser," *International Journal of Hydrogen Energy*, vol. 38, no. 24, pp. 10063–10067, 2013, doi: 10.1016/j.ijhydene.2013.06.034.

[224] M. Kıstı, S. Uysal, and M. F. Kaya, "Development of Pt coated SS316 mesh gas diffusion electrodes for a PEM water electrolyzer anode," *Fuel*, vol. 324, p. 124775, 2022, doi: 10.1016/j.fuel.2022.124775.

[225] S. Stiber *et al.,* "A high-performance, durable and low-cost proton exchange membrane electrolyser with stainless steel components," *Energy Environ. Sci.*, vol. 15, no. 1, pp. 109–122, 2022, doi: 10.1039/D1EE02112E.

[226] H. Becker *et al.,* "Assessing potential profiles in water electrolysers to minimise titanium use," *Energy Environ. Sci.*, vol. 15, no. 6, pp. 2508–2518, 2022, doi: 10.1039/d2ee00876a.

[227] S. M. Steen, J. Mo, Z. Kang, G. Yang, and F.-Y. Zhang, "Investigation of titanium liquid/gas diffusion layers in proton exchange membrane electrolyzer cells," *International Journal of Green Energy*, vol. 14, no. 2, pp. 162–170, 2017, doi: 10.1080/15435075.2016.1253582.

[228] S. A. Grigoriev, P. Millet, S. A. Volobuev, and V. N. Fateev, "Optimization of porous current collectors for PEM water electrolysers," *International Journal of Hydrogen Energy*, vol. 34, no. 11, pp. 4968–4973, 2009, doi: 10.1016/j.ijhydene.2008.11.056.

[229] Z. Kang *et al.,* "Investigation of thin/well-tunable liquid/gas diffusion layers exhibiting superior multifunctional performance in low-temperature electrolytic water splitting," *Energy Environ. Sci.*, vol. 10, no. 1, pp. 166–175, 2017, doi: 10.1039/C6EE02368A.

[230] J. Mo, R. R. Dehoff, W. H. Peter, T. J. Toops, J. B. Green, and F.-Y. Zhang, "Additive manufacturing of liquid/gas diffusion layers for low-cost and high-efficiency hydrogen production," *International Journal of Hydrogen Energy*, vol. 41, no. 4, pp. 3128–3135, 2016, doi: 10.1016/j.ijhydene.2015.12.111.

[231] Y. J. Park *et al.,* "Electrodeposition of High-Surface-Area IrO2 Films on Ti Felt as an Efficient Catalyst for the Oxygen Evolution Reaction," *Frontiers in chemistry*, early access. doi: 10.3389/fchem.2020.593272.

[232] P. Lettenmeier *et al.,* "Comprehensive investigation of novel pore-graded gas diffusion layers for high-performance and cost-effective proton exchange membrane electrolyzers," *Energy Environ. Sci.*, vol. 10, no. 12, pp. 2521–2533, 2017, doi: 10.1039/C7EE01240C.

[233] G. Dotelli, L. Omati, P. Gallo Stampino, P. Grassini, and D. Brivio, "Investigation of gas diffusion layer compression by electrochemical impedance spectroscopy on running polymer electrolyte membrane fuel cells," *Journal of Power Sources*, vol. 196, no. 21, pp. 8955–8966, 2011, doi: 10.1016/j.jpowsour.2011.01.078.

[234] L. Bertuccioli, A. Chan, D. Hart, F. Lehner, B. Madden, and E. Standen, "Development of water electrolysis in the EU: Final Report," 2014.

[235] K. E. Ayers *et al.,* "Research advances towards low cost, high efficiency PEM electrolysis," *ECS Trans.*, vol. 33, no. 1, p. 3, 2010.

[236] H. Zhang *et al.,* "Performance of Ti–Ag-deposited titanium bipolar plates in simulated unitized regenerative fuel cell (URFC) environment," *International Journal of Hydrogen Energy*, vol. 36, no. 9, pp. 5695–5701, 2011, doi: 10.1016/j.ijhydene.2011.01.154.

[237] M. Carmo, D. L. Fritz, J. Mergel, and D. Stolten, "A comprehensive review on PEM water electrolysis," *International Journal of Hydrogen Energy*, vol. 38, no. 12, pp. 4901–4934, 2013, doi: 10.1016/j.ijhydene.2013.01.151.

[238] M. Langemann, D. L. Fritz, M. Müller, and D. Stolten, "Validation and characterization of suitable materials for bipolar plates in PEM water electrolysis," *International Journal of Hydrogen Energy*, vol. 40, no. 35, pp. 11385–11391, 2015, doi: 10.1016/j.ijhydene.2015.04.155.

[239] A. V. Nikiforov, I. M. Petrushina, E. Christensen, A. L. Tomás-García, and N. J. Bjerrum, "Corrosion behaviour of construction materials for high temperature steam electrolysers," *International Journal of Hydrogen Energy*, vol. 36, no. 1, pp. 111–119, 2011, doi: 10.1016/j.ijhydene.2010.09.023.

[240] T. Liu, Y. Tao, Y. Wang, M. Hu, Z. Zhang, and J. Shao, "Towards cost-effective and durable bipolar plates for proton exchange membrane electrolyzers: A review," *Fuel*, vol. 368, p. 131610, 2024, doi: 10.1016/j.fuel.2024.131610.

[241] A. S. Gago *et al.,* "Protective coatings on stainless steel bipolar plates for proton exchange membrane (PEM) electrolysers," *Journal of Power Sources*, vol. 307, pp. 815–825, 2016, doi: 10.1016/j.jpowsour.2015.12.071.

[242] L. Fiedler *et al.,* "Stability of Bipolar Plate Materials for Proton-Exchange Membrane Water Electrolyzers: Dissolution of Titanium and Stainless Steel in DI Water and Highly Diluted Acid," *ChemElectroChem*, vol. 10, no. 20, 2023, Art. no. e202300373, doi: 10.1002/celc.202300373.

[243] N. de las Heras, E. P. L. Roberts, R. Langton, and D. R. Hodgson, "A review of metal separator plate materials suitable for automotive PEMfuel cells," *Energy Environ. Sci.*, vol. 2, no. 2, pp. 206–214, 2009, doi: 10.1039/B813231N.

[244] G. Yang *et al.,* "Bipolar plate development with additive manufacturing and protective coating for durable and high-efficiency hydrogen production," *Journal of Power Sources*, vol. 396, pp. 590–598, 2018, doi: 10.1016/j.jpowsour.2018.06.078.

[245] H.-Y. Jung, S.-Y. Huang, P. Ganesan, and B. N. Popov, "Performance of gold-coated titanium bipolar plates in unitized regenerative fuel cell operation," *Journal of Power Sources*, vol. 194, no. 2, pp. 972–975, 2009, doi: 10.1016/j.jpowsour.2009.06.030.

[246] T. J. Toops *et al.,* "Evaluation of nitrided titanium separator plates for proton exchange membrane electrolyzer cells," *Journal of Power Sources*, vol. 272, pp. 954–960, 2014, doi: 10.1016/j.jpowsour.2014.09.016.

[247] T. Nishikiori, T. Nohira, and Y. Ito, "Electrochemical evaluation of high temperature hydrogen impermeability of TiN films and its dependence on film thickness," *Thin Solid Films*, vol. 408, 1-2, pp. 148–154, 2002, doi: 10.1016/S0040-6090(02)00053-6.

[248] A. S. Gago, A. S. Ansar, P. Gazdzicki, N. Wagner, J. Arnold, and K. A. Friedrich, "Low Cost Bipolar Plates for Large Scale PEM Electrolyzers," *ECS Trans.*, vol. 64, no. 3, pp. 1039–1048, 2014, doi: 10.1149/06403.1039ecst.

[249] M. Zhang, L. Hu, G. Lin, and Z. Shao, "Honeycomb-like nanocomposite Ti-Ag-N films prepared by pulsed bias arc ion plating on titanium as bipolar plates for unitized regenerative fuel cells," *Journal of Power Sources*, vol. 198, pp. 196–202, 2012, doi: 10.1016/j.jpowsour.2011.10.022.

[250] J.-T. Wang, W.-W. Wang, C. Wang, and Z.-Q. Mao, "Corrosion behavior of three bipolar plate materials in simulated SPE water electrolysis environment," *International Journal of Hydrogen Energy*, vol. 37, no. 17, pp. 12069–12073, 2012, doi: 10.1016/j.ijhydene.2012.04.146.

[251] K. W. Ahmed, M. J. Jang, M. G. Park, Z. Chen, and M. Fowler, "Effect of Components and Operating Conditions on the Performance of PEM Electrolyzers: A Review," *Electrochem*, vol. 3, no. 4, pp. 581–612, 2022, doi: 10.3390/electrochem3040040.

[252] D. G. Bessarabov, H. Wang, H. Li, and N. Zhao, Eds. *PEM electrolysis for hydrogen production: Principles and applications*. Boca Raton Florida: CRC Press, 2016.

[253] P. Millet, "Design and performance of a solid polymer electrolyte water electrolyzer," *International Journal of Hydrogen Energy*, vol. 21, no. 2, pp. 87–93, 1996, doi: 10.1016/0360-3199(95)00005-4.

[254] S.-H. Wang, J. Peng, W.-B. Lui, and J.-S. Zhang, "Performance of the gold-plated titanium bipolar plates for the light weight PEM fuel cells," *Journal of Power Sources*, vol. 162, no. 1, pp. 486–491, 2006, doi: 10.1016/j.jpowsour.2006.06.084.

[255] M.-T. Lin, C.-H. Wan, and W. Wu, "Comparison of corrosion behaviors between SS304 and Ti substrate coated with (Ti,Zr)N thin films as Metal bipolar plate for unitized regenerative fuel cell," *Thin Solid Films*, vol. 544, pp. 162–169, 2013, doi: 10.1016/j.tsf.2013.03.130.

[256] P. Lettenmeier *et al.,* "Low-Cost and Durable Bipolar Plates for Proton Exchange Membrane Electrolyzers," *Scientific reports*, early access. doi: 10.1038/srep44035.

[257] T. Reier *et al.,* "Electrocatalytic Oxygen Evolution on Iridium Oxide: Uncovering Catalyst-Substrate Interactions and Active Iridium Oxide Species," *J. Electrochem. Soc.*, vol. 161, no. 9, F876-F882, 2014, doi: 10.1149/2.0411409jes.

[258] T. Bystron *et al.,* "Enhancing PEM water electrolysis efficiency by reducing the extent of Ti gas diffusion layer passivation," *J Appl Electrochem*, vol. 48, no. 6, pp. 713–723, 2018, doi: 10.1007/s10800-018-1174-6.

[259] N. F. Daudt, A. D. Schneider, E. R. Arnemann, C. J. Scheuer, L. S. Dorneles, and L. F. Schelp, "Fabrication of NbN-Coated Porous Titanium Sheets for PEM Electrolyzers," *J. of Materi Eng and Perform*, vol. 29, no. 8, pp. 5174–5183, 2020, doi: 10.1007/s11665-020-05026-y.

[260] X. Min *et al.,* "High performance and cost-effective supported IrOx catalyst for proton exchange membrane water electrolysis," *Electrochimica Acta*, vol. 385, p. 138391, 2021, doi: 10.1016/j.electacta.2021.138391.

[261] Y. Liu *et al.,* "Modifying Ti-Based Gas Diffusion Layer Passivation for Polymer Electrolyte Membrane Water Electrolysis via Electrochemical Nitridation," *ACS applied materials & interfaces*, vol. 14, no. 13, pp. 15728–15735, 2022, doi: 10.1021/acsami.1c22639.

[262] S. Lædre, O. E. Kongstein, A. Oedegaard, H. Karoliussen, and F. Seland, "Materials for Proton Exchange Membrane water electrolyzer bipolar plates," *International Journal of Hydrogen Energy*, vol. 42, no. 5, pp. 2713–2723, 2017, doi: 10.1016/j.ijhydene.2016.11.106.

[263] N. Rojas *et al.,* "Coated stainless steels evaluation for bipolar plates in PEM water electrolysis conditions," *International Journal of Hydrogen Energy*, vol. 46, no. 51, pp. 25929–25943, 2021. doi: 10.1016/j.ijhydene.2021.03.100. [Online]. Available: https://www.sciencedirect.com/science/article/pii/S0360319921010119

[264] A. O. Erdem, P. Stannek, and M. Grundler, "Development of Continuously Produced Thin-Walled Graphite-Polymer Bipolar Plates for Fuel Cells," in *2023 4th International Conference on Clean and Green Energy Engineering (CGEE)*, Ankara, Turkiye, 2023, pp. 85–89, doi: 10.1109/CGEE59468.2023.10351999.

[265] Z. B. Wang, H. X. Hu, C. B. Liu, and Y. G. Zheng, "The effect of fluoride ions on the corrosion behavior of pure titanium in 0.05M sulfuric acid," *Electrochimica Acta*, vol. 135, pp. 526–535, 2014, doi: 10.1016/j.electacta.2014.05.055.

[266] D. C. Bittinat, "Infrared Thermographic Defect Detection In Fuel Cell Gas Diffusion Electrodes,"

[267] D.-S. Kong and Y.-Y. Feng, "Electrochemical Anodic Dissolution Kinetics of Titanium in Fluoride-Containing Perchloric Acid Solutions at Open-Circuit Potentials," *J. Electrochem. Soc.*, vol. 156, no. 9, C283, 2009, doi: 10.1149/1.3153148.

[268] J. Wu *et al.,* "A review of PEM fuel cell durability: Degradation mechanisms and mitigation strategies," *Journal of Power Sources*, vol. 184, no. 1, pp. 104–119, 2008, doi: 10.1016/j.jpowsour.2008.06.006.

[269] N. Li, S. S. Araya, and S. K. Kær, "The effect of Fe3+ contamination in feed water on proton exchange membrane electrolyzer performance," *International Journal of Hydrogen Energy*, vol. 44, no. 26, pp. 12952–12957, 2019, doi: 10.1016/j.ijhydene.2019.04.015.

[270] H. Wang, "Stainless steel as bipolar plate material for polymer electrolyte membrane fuel cells," *Journal of Power Sources*, vol. 115, no. 2, pp. 243–251, 2003, doi: 10.1016/S0378-7753(03)00023-5.

[271] R. A. Antunes, M. C. L. Oliveira, G. Ett, and V. Ett, "Corrosion of metal bipolar plates for PEM fuel cells: A review," *International Journal of Hydrogen Energy*, vol. 35, no. 8, pp. 3632–3647, 2010, doi: 10.1016/j.ijhydene.2010.01.059.

[272] A. Miyazawa, E. Tada, and A. Nishikata, "Influence of corrosion of SS316L bipolar plate on PEFC performance," *Journal of Power Sources*, vol. 231, pp. 226–233, 2013, doi: 10.1016/j.jpowsour.2012.12.088.

[273] H.-Y. Jung, S.-Y. Huang, and B. N. Popov, "High-durability titanium bipolar plate modified by electrochemical deposition of platinum for unitized regenerative fuel cell (URFC)," *Journal of Power Sources*, vol. 195, no. 7, pp. 1950–1956, 2010, doi: 10.1016/j.jpowsour.2009.10.002.

[274] M.-T. Lin, C.-H. Wan, and W. Wu, "Enhanced Corrosion Resistance of SS304 Stainless Steel and Titanium Coated with Alternate Layers of TiN and ZrN in a Simulated O2-rich Environment of a Unitized Regenerative Fuel Cell," *1452-3981*, vol. 9, no. 12, pp. 7832–7845, 2014, doi: 10.1016/S1452-3981(23)11009-1.

[275] *Titanium coatings deposited by thermal spraying for bipolar plates of PEM electrolysers*, 2013.

[276] S. Stiber *et al.,* "Long-Term Operation of Nb-Coated Stainless Steel Bipolar Plates for Proton Exchange Membrane Water Electrolyzers," *Adv Energy and Sustain Res*, vol. 3, no. 8, 2022, Art. no. 2200024, doi: 10.1002/aesr.202200024.

[277] L. Fiedler *et al.,* "Stainless steel 316L as bipolar plate material in proton exchange membrane water electrolyzer: The influence of potential and temperature on dissolution stability," *Materials Today Sustainability*, vol. 31, p. 101155, 2025, doi: 10.1016/j.mtsust.2025.101155.

[278] L. H. Prado, S. Virtanen, N. Weineck, A. Ghicov, and F. Kessler, "How to perform corrosion experiments for proton exchange membrane water electrolysis bipolar plates," *Journal of Power Sources*, vol. 613, p. 234815, 2024, doi: 10.1016/j.jpowsour.2024.234815.

[279] C. Briant, Z. Wang, and N. Chollocoop, "Hydrogen embrittlement of commercial purity titanium," *Corrosion Science*, vol. 44, no. 8, pp. 1875–1888, 2002, doi: 10.1016/S0010-938X(01)00159-7.

[280] M. Hamdan, "PEM Electrolyzer Incorporating an Advanced Low-Cost Membrane," Virginia Polytechnic Institute and University, 2013, doi: 10.2172/1091385.

[281] K. Videm, S. Lamolle, M. Monjo, J. E. Ellingsen, S. P. Lyngstadaas, and H. J. Haugen, "Hydride formation on titanium surfaces by cathodic polarization," *Applied Surface Science*, vol. 255, no. 5, pp. 3011–3015, 2008, doi: 10.1016/j.apsusc.2008.08.090.

[282] S. Yen, "Retardation effects of thermally grown oxide films on the hydrogen embrittlement of commercial pure titanium," *Corrosion Science*, vol. 41, no. 10, pp. 2031–2051, 1999, doi: 10.1016/S0010-938X(99)00022-0.

[283] American Bureau of Shipping (ABS), Ed., "Sustainability Whitepaper - Hydrogen as Marine Fuel," Jun. 2021.

[284] G. Bickel, L. Green, M. James, T. Lamarche, P. Leeson, and H. Michel, "The determination of hydrogen and deuterium in Zr–2.5Nb material by hot vacuum extraction mass spectrometry," *Journal of Nuclear Materials*, vol. 306, no. 1, pp. 21–29, 2002, doi: 10.1016/S0022-3115(02)01230-8.

[285] M. Schulze, T. Knöri, A. Schneider, and E. Gülzow, "Degradation of sealings for PEFC test cells during fuel cell operation," *Journal of Power Sources*, vol. 127, 1-2, pp. 222–229, 2004, doi: 10.1016/j.jpowsour.2003.09.017.

[286] D. A. Dillard *et al.,* "Seals and Sealants in PEM Fuel Cell Environments: Materials, Design, and Durability Challenges," 2004, doi: 10.1115/FUELCELL2004-2520.

[287] R. Moreno Soriano, N. Rojas, E. Nieto, R. de Guadalupe González-Huerta, and J. M. Sandoval-Pineda, "Influence of the gasket materials on the clamping pressure distribution in a PEM water electrolyzer: Bolt torques and operation mode in pre-conditioning," *International Journal of Hydrogen Energy*, vol. 46, no. 51, pp. 25944–25953, 2021, doi: 10.1016/j.ijhydene.2021.03.076.

[288] U. Basuli *et al.,* "Properties and degradation of the gasket component of a proton exchange membrane fuel cell--a review," *Journal of nanoscience and nanotechnology*, vol. 12, no. 10, pp. 7641–7657, 2012, doi: 10.1166/jnn.2012.6627.

[289] J. Tan, Y. J. Chao, M. Yang, C. T. Williams, and J. W. van Zee, "Degradation Characteristics of Elastomeric Gasket Materials in a Simulated PEM Fuel Cell Environment," *J. of Materi Eng and Perform*, vol. 17, no. 6, pp. 785–792, 2008, doi: 10.1007/s11665-008-9233-5.

[290] J. Tan, Y. J. Chao, M. Yang, W.-K. Lee, and J. W. van Zee, "Chemical and mechanical stability of a Silicone gasket material exposed to PEM fuel cell environment," *International Journal of Hydrogen Energy*, vol. 36, no. 2, pp. 1846–1852, 2011, doi: 10.1016/j.ijhydene.2009.12.048.

[291] G. Bender *et al.,* "Initial approaches in benchmarking and round robin testing for proton exchange membrane water electrolyzers," *International Journal of Hydrogen Energy*, vol. 44, no. 18, pp. 9174–9187, 2019, doi: 10.1016/j.ijhydene.2019.02.074.

[292] S. Bhargava, K. A. O'Leary, T. C. Jackson, and B. Lakshmanan, "Durability Testing og Silicone Materials for Proton Exchange Membrane Fuel Cell Use," *Rubber Chemistry and Technology*, vol. 86, no. 1, pp. 28–37, 2013, doi: 10.5254/rct.13.88931.

[293] S. Barwe, B. Mei, J. Masa, W. Schuhmann, and E. Ventosa, "Overcoming cathode poisoning from electrolyte impurities in alkaline electrolysis by means of self-healing electrocatalyst films," *Nano Energy*, vol. 53, pp. 763–768, 2018, doi: 10.1016/j.nanoen.2018.09.045.

[294] E. Wallnöfer-Ogris, F. Poimer, R. Köll, M.-G. Macherhammer, and A. Trattner, "Main degradation mechanisms of polymer electrolyte membrane fuel cell stacks – Mechanisms, influencing factors, consequences, and mitigation strategies," *International Journal of Hydrogen Energy*, vol. 50, pp. 1159–1182, 2024, doi: 10.1016/j.ijhydene.2023.06.215.

[295] L. Dubau *et al.,* "A review of PEM fuel cell durability: materials degradation, local heterogeneities of aging and possible mitigation strategies," *WIREs Energy Environ.*, vol. 3, no. 6, pp. 540–560, 2014, doi: 10.1002/wene.113.

[296] M. Jouin, R. Gouriveau, D. Hissel, M.-C. Péra, and N. Zerhouni, "Degradations analysis and aging modeling for health assessment and prognostics of PEMFC," *Reliability Engineering & System Safety*, vol. 148, pp. 78–95, 2016, doi: 10.1016/j.ress.2015.12.003.

[297] F. A. de Bruijn, V. A. T. Dam, and G. J. M. Janssen, "Review: Durability and Degradation Issues of PEM Fuel Cell Components," *Fuel cells*, vol. 8, no. 1, pp. 3–22, 2008, doi: 10.1002/fuce.200700053.

Supplemental Information

Table SI 1: Degradation mechanisms and their description as given in the survey.

Degradation Mechanism	**Description**
Anode catalyst dissolution	Chemical dissolution of anode side catalyst such as Iridium
Cathode catalyst dissolution	Chemical dissolution of cathode side catalysts such as Platinum
Cathode catalyst passivation	Passivation of cathode side catalysts such as Platinum via reaction with oxygen or hydroxyl radicals
Catalyst particle loss, layer detachment	(Mechanical) Removal of catalyst as metallic particles
Catalyst particle agglomeration	Agglomeration of catalyst particles into bigger congregates with lower surface area
Catalyst migration	Migration of catalyst ions through the membrane
Cation-induced catalyst poisoning	Degradation of catalysts due to cationic impurities, that accumulate and block active sites
Ionomer loss and rearrangement	Dissolution of ionomer, i.e. due to radical attack and loss of contact to the catalyst layer due to rearrangement
Membrane mechanical degradation	Mechanical damage to the membrane by puncture, tearing, cracking, mechanical stresses and pressure
Membrane thinning via radical attack	Decrease in membrane thickness due to attack of radical species, i.e. hydroxyl radicals
Membrane metal poisoning	Occupation of ion exchange sites in the membrane by foreign cations and precipitation of catalyst particles in the membrane
Membrane thermal degradation	Thinning of the membrane due to increased temperature and local hotspots
Bipolar plate: hydrogen embrittlement	Mechanical Failure of Bipolar Plates from hydrogen gas absorption
Bipolar plate: passivation	Increasing contact resistance from the formation of a passivation layer on Bipolar Plates
Bipolar plate: corrosion	Corrosion of bipolar plates or coatings from i.e. fluoride ions causing an increase in contact resistance between BPP and current collector.

Bipolar plate: mechanical degradation	Mechanical degradation of BPPs, e.g. deformation, formation of cracks etc.
PTL: corrosion	Degradation of the anode-side PTL from corrosion
PTL: passivation	Degradation of the anode-side PTL from passivation
PTL: hydrogen embrittlement	Degradation of the anode-side PTL from hydrogen embrittlement
PTL: mechanical degradation	Mechanical degradation on anode-side PTL from high local pressures or temperatures
GDL: chemical degradation	Dissolution of cathode-side carbon GDL
GDL: mechanical degradation	Degradation of cathode-side carbon GDL due to high pressures and localized mechanical stress

Table SI 2: Additional information on all measurement methods, including measurement principle, measured value, in-operando capability and lateral resolution.

	Name	**Measurement Principle**	**Measured value**	**in-operando possible?**	**lateral resolution**
Electrical	Conductivity measurements (e.g. 4-point and 2-point measurements)	Current running between defined points	Electric conductivity	Partially	µm
	ECT	Locally induced current from alternating magnetic field	Sheet resistance	No	µm
Microscopy	Light microscopy	Reflected light	Surface morphology	No	µm
	SEM (/EDX)	Backscattered and secondary electrons from surface + characteristic x-rays emitted from atoms after stimulation by electrons	Surface features, elemental distribution, morphology	No	nm
	(S)TEM (/EDX)	Transmitted electrons through thin sample + characteristic x-rays emitted from atoms after stimulation by electrons	Small physical features, elemental distribution, microstructure, morphology	No	Å
	Radiography/CT	Transmitted x-rays through a sample	Physical features throughout the sample	No	µm

	AFM and associated methods	Surface changes by height, conductivity, or chemical information	Surface features and composition	No	µm
Scattering	XRD	Diffracted x-rays (inter-atomic distances)	Crystal structure, crystallinity, composition of crystalline material, phase analysis	Only with synchrotron radiation	mm
	SAXS	Diffracted x-rays (inter-particle distances)	Pore sizes, particle sizes, ion channel features	Only with synchrotron radiation	mm
	Electron scattering	Diffracted electrons	Crystal structure, crystallinity, composition of crystalline material, (phase analysis)	No	nm
	Neutron scattering	Diffracted neutrons	Crystal structure, crystallinity, composition of crystalline material, phase analysis	With special cell setup	mm
	Light scattering and interference	Scattered light, often with interference for height/thickness information	Surface features	No	µm
Spectroscopy	EPMA	Characteristic x-rays emitted from atoms after stimulation by electrons, wave-length dispersive	Elemental composition	No	µm
	XPS (and extended methods)	Photoelectrons after stimulation by x-rays	Elemental surface composition and chemical bonds	No	µm
	XRF	Fluorescent x-rays after stimulation by x-rays	Elemental composition	No	µm
	XAS/XANES	X-rays absorbed	Elemental composition and oxidation states	Only with synchrotron radiation	µm
	ICP-MS (or -OES)	Characteristic mass or emission of elements brough out of solution	Elemental composition	Yes, on effluent water	N/A
	ToF-SIMS	Characteristic mass of ions under sputtering	Elemental composition	No	µm

	LIBS	Characteristic light emission of breakdown products	Elemental composition	No	mm
	Uv-Vis	Absorbed or reflected light in defined spectral range	Absorption features	No	mm
	FTIR	Absorbed or reflected light in defined spectral range	Chemical bonds	With special cell setup	mm
	Raman	Inelastically scattered photons	Chemical bonds	With special cell setup	mm
	NMR	Relaxation time of magnetic moments after stimulation with magnetic field	Chemical bonds	On water	N/A
	GCMS	Characteristic mass after separation	Components	No	N/A
	ESR	Spin transitions of unpaired electrons in a magnetic field	Magnetic defects	With special cell setup	N/A
	EELS (with TEM)	Energy-loss of inelastically scattered electrons	Elemental composition and oxidation states	No	Sub-nm
	Thermography methods (e.g. LIT)	Lateral distribution of temperature measured from higher IR light emission	Heating under different stimuli	No	mm
Thermal	TGA or DSC	Mass changes or changes in heat flow during heating and cooling	Decomposition temperatures and weight loss, enthalpy changes	No	mm
	Thermal conductivity	Thermal conductivity between two points	Thermal conductivity	No	mm
Mechanical	Bending measurements	Resistance to bending	Stiffness, breakage point	No	mm
	Hardness tests	Resistance to probe	Hardness	No	mm
	Micro- and nanoindentation	Resistance to probe	Local Hardness and E-Modulus	No	µm/nm
	Tensile test	Resistance to elongation	E-Modulus, elongation at break, stress-strain behavior	No	mm
	Dynamic mechanical testing	Resistance to changing mechanical loads	Mechanical properties under changing load	No	mm
M	MFI	Magnetic field induced by current	Current density changes	yes	mm

	Non-reactive gas crossover	Amount of gas crossing through a sample	Holes and cracks (presence and size)	No	mm
	Hydrogen crossover	Amount of gas crossing through a sample	Holes and cracks (presence and size)	Yes	mm
	Permeation test	Permeability of gas (e.g. He) through a sample	Gas transmission rate, permeation, solubility and diffusion coefficient	No	
	Pressure drop	Ability to withstand certain pressure	Holes and cracks (presence)	Yes	Whole cell
	Bubble test	Bubbling of liquid through holes	Holes and cracks (presence)	No	Whole membrane
	Porosity measurements	Pressure needed to force probe molecules into sample pores	Porosity, pore size distribution	No	Sample size
	Prompt gamma ray and neutron activation analysis	Characteristic gamma rays after stimulation by neutrons	Elemental analysis	No	mm
	Mass measurements	Mass	Mass changes	No	Whole cell
	Ion-selective electrodes	Electrical current induced by certain ions	Ion concentration	Yes, on effluent water	N/A
	Ion chromatography	Characteristic retention time of ions	Ion concentration	Yes, on effluent water	N/A
	Hot vacuum extraction	Heated sample in vacuum, gas transfer to mass spectrometer inlet for analysis	Amount of hydrogen in the sample	No	N/A
	Contact angle measurement	Angle between surface and probe liquid	Contact angle, hydrophobicity	No	mm

Table SI 3: Capability of each measurement method for diagnosing degradation mechanisms. Nomenclature: "+" method can be found in literature; "(+)" not found in literature, but theoretically suited; "++" and "(++)" especially suited for the degradation mechanism.

	Catalyst	**Membrane**	**Porous Transport Layers**	**Bipolar Plates**	**Gasket**

	Anode cat. dissolution	Cathode cat. dissolution	Carbon support dissolution	Cathode cat. passivation	Catalyst particle loss/layer detachment	Catalyst particle agglomeration	Catalyst migration	Catalyst cationic poisoning	Ionomer loss/ rearrangement	Membrane mechanical degradation	Membrane thinning via radical attack	Membrane metal poisoning	Membrane (hygro)thermal degradation	PTL passivation	PTL hydrogen embrittlement	PTL corrosion	GDL dissolution	GDL mechanical degradation	PTL mechanical degradation	BPP hydrogen embrittlement	BPP passivation	BPP corrosion	BPP mechanical degradation	Gasket mechanical degradation	Gasket chemical degradation
Conductivity measurements	(+)	(+)		(+)	(+)		(+)	(+)			(+)	(+)		++	(++)	+		+		(++)	++	+			
ECT	(+)	(+)		(+)	(+)		(+)	(+)				(+)			(+)	(+)		(++)	(+)	(+)		(+)	(+)		
Light microscopy					(++)					+	(+)				+			+	+	+			+	+	
SEM (/EDX)	++	++	(+)		++		++	+	++	+	++	+		+	+	++	(+)	++	++	+	+	++	++	+	(+)
TEM (/EDX)	++	++	+	(+)	+	++	++	+	++		+	(+)		(++)	(+)	(++)	+			(+)	(++)	(++)	+		
Radiography/CT	(+)	(+)			++	+	(+)	(+)	(+)	+	(+)	(+)						+	(++)				(++)		
AFM	+	(+)		(+)	(+)		(+)		++					+		+					+	+			
XRD	+	(+)			(+)	+								+	(+)	+				(+)	+	+			
SAXS						++	(+)		(+)																
Neutron scattering						(+)	(+)	+				(+)													
Electron scattering	+	+														(++)						(++)			
Light scattering and interference	(+)	(+)			(+)					(+)	(++)				(+)	(+)		(++)		(+)		(+)		(+)	
EPMA	(+)	+					(+)	+				+													
XPS (and extended methods)	+	(+)	(++)	+		+	(+)	(+)	+			+	(+)	++		+	(++)			+	++	+			+
XRF	++	++			+		+							+							+				
XAS/XANES	+			(+)																					
ICP-MS (or -OES)	++	++						(+)	(+)		+	++				(++)						(++)			+

ToF-SIMS							++	++				++			(++)					(++)					(+)
LIBS	(++)	(++)			(+)							(+)														
Uv-Vis											+															
FTIR	(+)	(+)	++				(+)	(+)				(+)	+				++									++
Raman			++				(+)	(+)			+	(+)	(+)				++									(+)
NMR											++		++													
GC (-MS)															+											+
ESR			+														+			+						
EELS	(+)	(+)	(+)	(+)										(+)		(+)					(+)	(+)				
Thermography methods	(+)	(+)		(+)	(+)		(+)	(+)		++		(++)														
TGA or DSC	(++)	(++)																								+
Thermal conductivity																		+	+				+			
Bending measurements															(+)	(+)		+	(+)	(+)		(+)	(+)	(+)		
Hardness tests															(++)	(+)			(+)	(++)		(+)	(+)	(+)		
Micro- and nanoindentation															(++)	(+)			(+)	(++)		(+)	(+)	+		
Tensile test																							(+)	+		
Dynamic mechanical testing															(+)	(+)		+	(+)	(+)		(+)	(+)	+		
MFI	(+)	(+)			(+)		(+)			(+)				(+)		(+)		(+)	(+)		(+)	(+)	(+)			
Non-reactive gas crossover										+								+								
Hydrogen crossover										+																
Permeation test										(+)	(+)													+		
Pressure drop										+													(+)			
Bubble test										+																
Porosity measurements																		+								
Gamma ray + neutron activation analysis							+																			
Mass measurements	(+)	+			(+)										+			+	+	+						(+)

Ion-selective electrodes	(+)	(+)									+														
Ion chromatography	(+)	(+)									+														
Hot vacuum extraction															+					+					
Contact angle measurement									(+)					(++)				+			(++)				

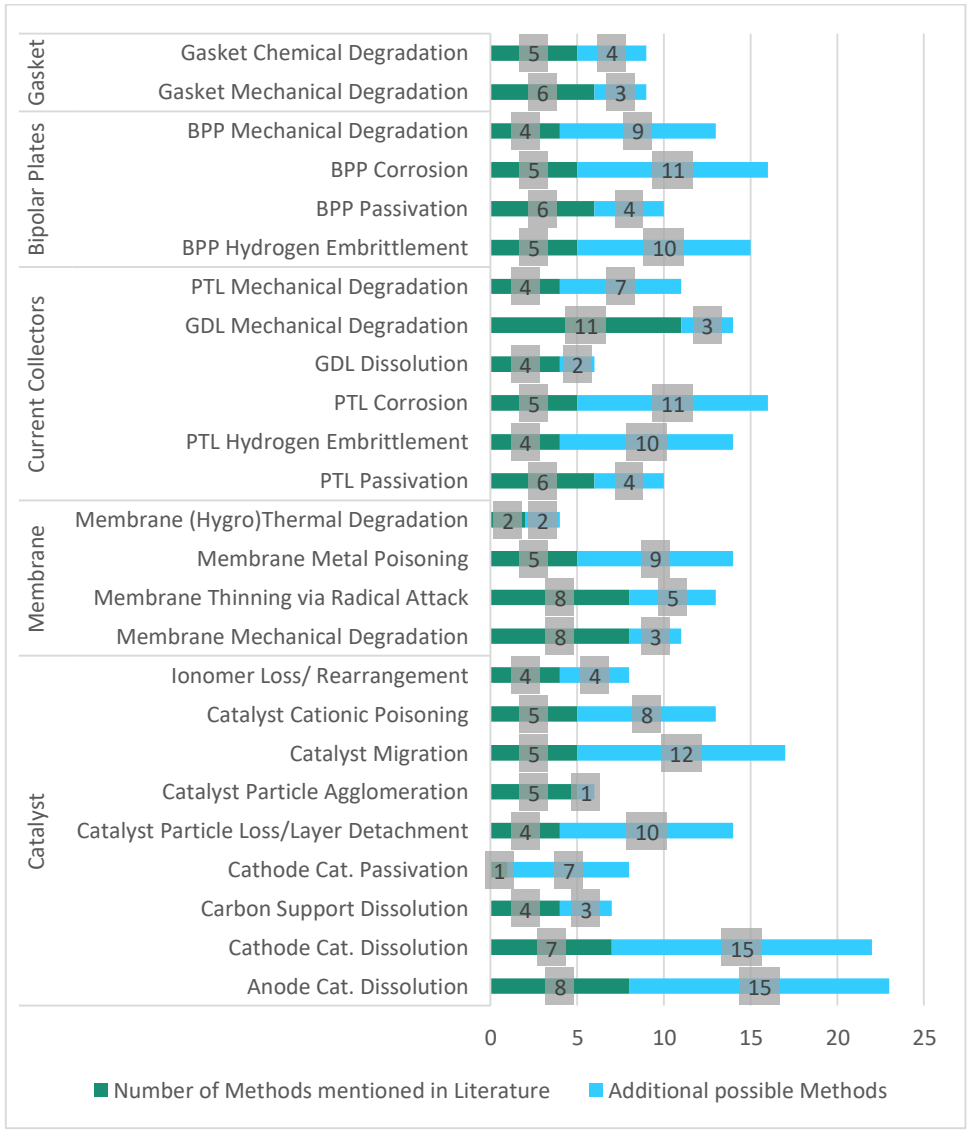


Figure SI 1: Number of measurement methods available known to us for each degradation mechanism.

Table SI 4: Comparison of PEMWE and PEMFC degradation mechanisms.

Component	Electrolyzer Mechanisms	Fuel Cell Mechanisms	More Pronounced
Membrane	Thinning by radicals	Thinning by radicals	
	Mechanical	Mechanical	FC
	Metal poisoning	Metal poisoning	WE
		Thermal degradation	
	Hygrothermal degradation	Hygrothermal degradation	FC
Catalyst Layers	Anode dissolution		
	Cathode dissolution	Pt dissolution	FC
	Cathode passivation	Pt passivation	FC
	Carbon support dissolution	Carbon support dissolution	FC
	Particle loss/detachment	Particle loss/detachment	
	NP agglomeration	NP agglomeration	
	Migration	Migration	
	Cationic poisoning	Cationic poisoning	WE
		Poisoning by gas	
	Ionomer rearrangement	Ionomer rearrangement	
GDL	Dissolution	Dissolution	
		Hydrophobisation	
	Mechanical degradation	Mechanical degradation	
PTL	Corrosion		
	Passivation		
	Embrittlement		
	Mechanical degradation		
BPP	Embrittlement	Embrittlement	WE
	Passivation	Passivation	
	Corrosion	Corrosion	
	Mechanical degradation	Mechanical degradation	
Gasket	Mechanical degradation	Mechanical degradation	WE
	Chemical degradation	Chemical degradation	WE